THE PROTECTION OF ULTRAVIOLET SENSITIVE MOLECULES THROUGH POLYMERIC ENCAPSULATION AND PROXIMITY

by

KRISTIN GILIDA STEELEY

A dissertation submitted to the

Graduate School – New Brunswick

Rutgers, The State University of New Jersey

In partial fulfillment of the requirements

For the degree of

Doctor of Philosophy

Graduate Program in Chemical and Biochemical Engineering

Written under the direction of

Professor Nina C. Shapley

And approved by

_____

_____

_____

_____

New Brunswick, New Jersey

January 2014

ABSTRACT OF THE DISSERTATION

The Protection of Ultraviolet Sensitive Molecules through Polymeric Encapsulation and Proximity

By KRISTIN GILIDA STEELEY

Dissertation Director:

Professor Nina C. Shapley

Exposure to ultraviolet (UV) radiation causes many materials to undergo chemical reactions leading to degradation. While the negative impact of UV radiation on human skin remains in the spotlight, many commercial products have also proven to be photosensitive, leading to the desire to protect molecules from photodegradation. The most common method of UV protection is to add protective materials such as UV absorbers or antioxidants to a formulation. Encapsulation of a photosensitive molecule is also a proven method of photoprotection. In this work, novel UV protective systems were created by encapsulating a photosensitive molecule, beta-carotene, in various polymer particle geometries with protectant molecules. The goal of this dissertation was to use such systems to examine the effect of proximity between photosensitive and UV protecting molecules.

Uniform particles were initially created in order to quantify the effect of encapsulation and to study the result of encapsulating beta-carotene with UV absorbers (oxybenzone, avobenzone, and octyl-4-methoxycinnamate (OMC)) and an antioxidant

(vitamin E) in a polymer matrix. Particles were synthesized by the solvent evaporation method. UV protection was found to be dependent on the protectant added and the concentration of the protectant, except in the case of OMC. The most effective particle formulation contained both oxybenzone and vitamin E.

Experimental designs were created to discover the proper composition and procedure for synthesizing various core-shell particle geometries. These core-shell particles were used to study the effect of proximity on UV protection. The core-shell particles themselves offered more protection than the uniform particles, and in most cases the addition of a protectant increased UV protection. Splitting the protectant concentration between the core and shell did not have a significant effect in most cases. The optimal formulation consisted of a suspension of polymer particles containing vitamin E and beta-carotene in the particle core and a UV absorber in the particle shell. Other particle characteristics were studied, including particle size and shell thickness, and were found to have minimal effect. The core-shell particles provide a new protective system for photosensitive molecules as well as a method of studying the effect of proximity on UV protection.

Acknowledgements

I have received guidance and support from many people during my time as a graduate student, and they have my sincerest gratitude for all of their help. First I would like to thank my advisor, Prof. Nina C. Shapley, for helping to guide my research and offering support through challenges and roadblocks. I also thank my collaborators: Ahubhav Tripathi and Kenneth Morabito from Brown University, and Dapeng Li, Paul Calvert, and Charlene Mello from University of Massachusetts Dartmouth for providing valuable suggestions and insight. I would like to thank fellow graduate students for their assistance and encouragement: Jen Winkler, Sara Koynov, Eric Jayjock, Frank Romanski, Kapil Deshpande, and Kun Yu. Many undergraduate students also deserve gratitude for their contributions to this work: Chelsea Stanton, Brett Kuestermeyer, Samie Leigh, Sharif Farghaly, and Vetri Velan.

I especially would like to thank my parents, Richard and Deborah, for pointing me in the direction of chemical engineering and for being supportive through my entire academic journey. And finally I must thank my husband, Steven, for being an unending source of support and motivation.

Publications

Parts of this work are awaiting publication and must be acknowledged:

Chapter 2 has been accepted for publication:

Steeley, K. G., Kuestermeyer, K., Stanton, C., Yu, J., Morabito, K., Li, D., Mello, C., Calvert, P., Tripathi, A., Shapley, N. C. Uniform polymer particles formulated with ultraviolet protective materials for the protection of UV sensitive molecules. Dyes and Pigments, 2013.

Chapter 3 is in preparation for submission:

Steeley, K. G., Leigh, S., Shapley, N. C. Core-shell particle geometries by the solvent evaporation method.

Table of Contents

List of Tables

List of Figures

Chapter 1 Introduction

1.1 Motivation

Techniques to prevent photooxidation and protect photosensitive substances are in high demand due to the many industries that are affected by photodegradation from exposure to ultraviolet (UV) radiation. The cosmetic, paint, textile, pharmaceutical, and automotive industries all battle with the degradation of their products when exposed to UV radiation. Current methods of UV protection include opaque packaging of a product or the addition of UV absorbers or physical blockers to the product formulation. While these methods do increase the photostability of products, protection is usually either not complete or diminishes over time. As a result, novel methods of protecting UV sensitive materials are in continuous demand to decrease product degradation due to exposure to ultraviolet radiation.

Ultraviolet radiation is composed of all wavelengths of light 400 nm and below. UV can be further split into three categories: UVA (400-315 nm), UVB (315-280 nm), and UVC (<280nm). UVC has the shortest wavelength and the highest energy, and is therefore the most destructive. Fortunately all UVC radiation is absorbed by the atmosphere before it ever reaches Earth's surface, so protective measures for UVC do not need to be taken. UVA and UVB are absorbed in the atmosphere as well, but not completely. Of the UV that does reach the surface of the Earth, 5% is UVB and 95% is UVA. Even though very little UVB makes it to Earth, UVB is higher energy than UVA,

making it a threat even in small doses. Therefore methods of protection mainly focus on protecting over the UVA and UVB wavelengths.

Humans have noticed adverse effects from large doses of sunlight before recorded history; as is evidenced in the clothing choices of people living in a climate that exposed them to harsh amounts of sunlight. Flowing clothing, veils, canopies, and umbrellas were all early methods of protection from the dangers accompanying sunlight exposure. In 1820 Sir Everard Home proved that erythema is not a product of the heat felt from the sun, therefore it must be from exposure to the light. He did this by exposing both of his hands to sunlight, one bare and the other covered in a black cloth. Even though the temperature under the black cloth was higher than ambient, it was the bare hand that was burned. By the late nineteenth century Widmark proved that the specific wavelengths of light that cause erythema are UV radiation. He took advantage of the characteristic of quartz to transmit UV, and that of glass to filter UV, to determine that UV exposure was the reason behind sunburn. Soon after Widmark published his work, research into potential sunscreen materials was well underway.[1]

Almost two centuries after Home's discovery, much more is known about the damaging effects of exposure of human skin to UV radiation. Not only does UV cause the discomfort of erythema, but it has also been found to increase the risk of skin cancer, which can be seen by the rise in the incidence of nonmelanoma skin cancer in the last 15 years.[2] Before UV can do damage to the skin it must exhaust the body's defenses, which it does by reducing the concentration of antioxidants in the skin through photodegradation.[3] Skin cancer develops when the DNA of the skin is damaged.[4] UVB directly reacts with DNA[5, 6] while UVA indirectly causes damage by creating

oxygen radicals that react with DNA.[6, 7] UVB is notorious for causing erythema and skin cancer, while UVA causes tanning and photoaging.[6] UV exposure is also known to cause damage to the eyes such as photokeratoconjunctivitis or photoretinitis[8-10].

Due to the increase in cases of skin cancer, the sunscreen industry has grown considerably. Modern sunscreens are usually composed either of UV absorbers, physical blockers, or a combination of both. UV absorbers absorb the light before it reaches the skin. Common UV absorbers in sunscreens are oxybenzone and avobenzone. Physical blockers are nano- or microparticles that reflect the damaging light. Many physical blockers such as titanium dioxide and zinc oxide also function as UV absorbers. The United States Food and Drug Administration (FDA) regulates the manufacture and packaging of sunscreens. The FDA has a list of allowed active sunscreen ingredients. While additional sunscreens have been approved throughout Europe, they cannot be used in the United States without first going through the approval process with the FDA. According to the latest FDA guidelines, as of June 2012 any sunscreen boasting an SPF higher than 50 must be labeled as simply “50+” and additional testing in the UVA region will be required before any sunscreen can be considered “broad spectrum” (offering UVA and UVB protection).

Novel methods of protecting skin from UV radiation are continuing to be developed. For example, it is now possible to alter fabric used to make clothing in order to make it more protective. A natural dye can be used that absorbs UV[11] or UV absorbers can be added to the fabric.[12, 13] New ways to formulate sunscreens have also been proposed. The inclusion of an antioxidant to a sunscreen formulation can increase protection, either by combining an antioxidant with a sunscreen to utilize both protection

mechanisms,[14] or by encapsulating the antioxidant in solid lipid nanoparticles to harness both the antioxidant and physical blocker effects.[15] Another option would be to formulate a sunscreen whose active ingredient is actually a precursor to a UV absorber, that way protection increases as UV exposure increases.[16]

Biological tissue isn't unique in its sensitivity to UV radiation. Many industrial products such as dyes, paints, and pharmaceuticals also suffer from photosensitivity. The approaches to protecting these products are very similar to those used to protect human skin: the addition of UV absorbers or physical blockers. Methods to protect more efficiently and with environmentally friendly additives are continuing to be developed.

Natural dyes are known for their photosensitivity, which is part of the reason they were almost completely replaced by synthetic dyes in the early twentieth century. As concern for the environment grows, increasing the light fastness of natural dyes is an attractive option since they are biodegradable and environmentally friendly.[17] The addition of UV absorbers and antioxidants to dyed fabric has been shown to increase light fastness,[18] and natural dyes are being discovered that have better light fastness properties than their predecessors.[19]

Developers of automotive paints also harbor concern about UV damage as it contributes to the weathering effects that a vehicle experiences when outside. Specifically, the polymer component of automotive coatings is UV sensitive. Weathering tests normally last at least 5 years. In addition, paint coatings are often very complex, consisting of many different layers, making them difficult to analyze. In response, many new methods of analyzing automotive coatings have been studied, including time-of-flight secondary ion mass spectrometry,[20] UV microspectroscopy,[21] adding a filter to

an ultraviolet/visible spectrophotometer,[22] and realizing which components of a test can be accelerated without affecting the results.[23] Increased resistance to weathering has been achieved by adding aminopropyltrimethoxy silane treated titanium dioxide nanoparticles to automotive coatings.[24]

Many active pharmaceutical ingredients are sensitive to UV radiation due to functional groups in their structure, such as carbon-carbon double bonds and carbonyl groups.[25] Dihydropyridine calcium channel blockers, medications used to control high blood pressure, are notorious for their sensitivity to UV radiation.[26] Protecting a photosensitive pharmaceutical product is important because in addition to decreased potency when a drug is exposed to UV during storage, phototoxic effects of a drug can be witnessed after someone ingests the drug and is subjected to UV radiation.[27] Even some excipients, the ingredients in a formulation that are not the active ingredient, can be photosensitive. For example, a polymer added to extended release tablets can degrade when exposed to UV, increasing the release rate of the drug.[28] The manufacturing process of a pharmaceutical dosage form can also affect its photostability.[29]

The potential for adverse effects from accidental exposure of photosensitive pharmaceuticals to UV radiation has caused a stir among regulatory bodies, including the FDA. The FDA has issued a Guidance for Industry: Photosafety Testing, and the International Conference on Harmonisation of Technical Requirements for Registration of Pharmaceuticals for Human Use (ICH) published guidelines on how to manufacture, store, and distribute photosensitive pharmaceutical products.[27] The first step in protecting photosensitive drugs is to identify them as photosensitive. While both sets of guidelines provide some testing methods, many more are outlined in the literature such as

use of a cumulative illuminometer,[30] molar extinction coefficients,[31] and determining reactive oxygen species after illumination.[32, 33] Current methods of protecting pharmaceuticals from UV include storing them in containers that filter or block UV radiation such as colored glass or plastic, or secondary packaging such as an opaque sleeve or carton.[34] It has also been shown that tablet coatings can provide protection.[35]

While erythema and skin cancer are the most obvious negative affects of UV radiation, there are many other materials that suffer degradation due to exposure to UV radiation. Current methods of protection generally involve either shielding the product from light completely, or adding UV absorbers or physical blockers to the formulation. With the vast amount of UV sensitive materials on the market, novel protection techniques are continuing to be explored. This work utilizes an approach combining UV absorbers, antioxidants, and the scattering properties of encapsulation in a particle and at interfaces.

1.2 Mechanisms of UV protection

1.2.1 Barriers

The simplest method of protecting a material from exposure to UV radiation is to protect the material using a barrier. The idea of a barrier, displayed in figure 1.1a, is to cover a material with something practically impenetrable by light, either because the material absorbs light, reflects it, or both. Humans are protected by using umbrellas, hats,

sunglasses, and clothing. There have even been modifications made to clothing to make it a more effective barrier to UV radiation.[12, 13] Cars are protected when stored in garages, and pharmaceuticals can be protected by storing in cardboard or aluminum secondary packaging.[34, 36]

1.2.2 Physical blockers

Physical blockers, also known as inorganic agents, protect by scattering the UV radiation therefore preventing it from reaching the photosensitive material, as shown in figure 1.1b. Widely used physical blockers include titanium dioxide and zinc oxide. Physical blockers are used as a means of UV protection in sunscreens,[37, 38] automotive coatings,[24] and fabrics.[39]

Particles used as physical blockers scatter light via Rayleigh scattering. The size of the particle dictates the wavelengths of light that are scattered; larger particles are used as pigments because they scatter visible light, while UV is scattered by particles that are 20 to 100 nm in diameter.[40] As a general rule, a particle scatters most efficiently when the diameter is half of the wavelength of light that is desired to be scattered.[41] Physical blockers most effectively protect by forming a film of particles on the surface of the material needing protection, ensuring that minimal UV passes between the particles. Additional factors that determine whether or not a physical blocker will provide effective protection are it's refractive index, dispersion within the film chosen as a delivery media, and the thickness of that film.[37]

1.2.3 UV absorbers

UV absorbers, also known as organic agents, are named such because they absorb UV radiation before it can reach the material being protected, as depicted in figure 1.1c. The majority of UV absorbers, such as oxybenzone and avobenzone, contain either an aromatic ring or a chain of carbon-carbon double bonds which allow delocalization of the excited electron. After being absorbed, the photon is released at a lower energy.

The Beer-Lambert law has shown that at a given concentration, a substance can absorb a set amount of a wavelength of light.[40] When a photon of light, such as UV radiation, is absorbed by a molecule, one of the molecule's electrons becomes excited. The electron is usually at the ground state before absorbing the photon, and typically transitions to the singlet excited state. From the singlet excited state, the electron can undergo three types of transitions. The electron can emit excess energy radiatively and relax to the ground state by emitting fluorescence, it can transition to the ground state nonradiatively and give off heat through internal conversion, or it can transition to the excited triplet state via intersystem crossing. From the triplet excited state two transitions to the ground state are possible: a radiative transition via phosphorescence or heat can be given off through intersystem crossing. Both the radiative (giving off light via fluorescence or phosphorescence) and nonradiative (emitting heat by internal conversion or intersystem crossing) transitions leave the molecule intact and able to absorb again. The last method of energy dissipation is through chemical reaction, where a molecule uses the excess energy to react with itself or another molecule. Chemical reaction is

usually undesirable because the molecule can no longer be used for protection and it has the capability of reacting with a molecule that it is supposed to protect.

1.2.4 Antioxidants

Unlike physical blockers and UV absorbers, antioxidants do not prevent UV radiation from reaching the UV sensitive molecule. As shown in figure 1.1d, the antioxidant interferes with the excited molecule, taking its excess energy and allowing it to return to the ground state. Because antioxidants distribute the excited electron throughout their molecular structure by resonance, it is not as reactive as another molecule with an excited electron. Antioxidants are the body's main defense against UV radiation.[42]

Excitation is the beginning of a chain of reactions that a molecule goes through when interacting with UV radiation. In general, this chain of reactions includes an initiation step in which the molecule absorbs UV radiation and becomes excited, propagation steps in which the initial radical is used to create other species of radicals, and a termination step in which the radicals of interest undergo a reaction to return them to a ground state. Unfortunately when it comes to UV protection, in many cases the products of the termination step are different molecules than the ones that absorbed UV radiation in the initiation step.[43]

There are two types of antioxidants that work by interfering with different parts of the aforementioned chain of reactions. Preventative antioxidants, also known as excited state quenchers, reduce the frequency of the initiation reaction by disabling molecules

such as metal ions or hyperoxides that may catalyze the production of radicals. Chain-breaking antioxidants, also known as radical trapping antioxidants, react with free radicals to create stable products and hinder the propagation reactions. Chain-breaking antioxidants usually neutralize radicals by donating a hydrogen atom, which gives them a negative charge that their structure allows them to stabilize by resonance.[44, 45]

1.2.5 Combinations

Individual protection mechanisms can provide substantial protection from UV radiation, but protection can be increased by utilizing multiple mechanisms in one formulation. Many times when materials utilizing different protection mechanisms are placed together or combined, they work synergistically to enhance protection.[46, 47] Even combinations of materials using the same mechanism can increase protective capacity, such as combinations of UV absorbers like those commonly found in sunscreens.

Sunscreens present a commercialized example of combining different mechanisms into the same system. Some consumers are sensitive to UV absorbers, causing a need for “sensitive skin” sunscreens. The active ingredients found in conventional sunscreens are usually all UV absorbers. “Sensitive skin” sunscreens are able to use a lower concentration of UV absorbers by adding physical blockers, usually titanium dioxide, zinc oxide, or both. These sunscreen formulations work by both absorbing and scattering UV radiation. Studies have also shown that combining the UV absorber and antioxidant mechanisms may create a superior sunscreen, as the absorber

will absorb radiation and the antioxidant can neutralize radicals created either by the absorbers or the skin.[14, 47]

Using multiple active ingredients with different mechanisms in a sunscreen is merely changing the formulation. Applying sunscreen and wearing protective clothing combines a barrier and UV absorbers (or physical blockers) on a larger scale. Applying UV absorbers to the fabric used for clothing is a way to enhance the barrier mechanism through the addition of materials using the absorbing mechanism.[12, 13]

Encapsulating a protective material, such as a UV absorber, in a particle combines the absorbing mechanism of the absorber and the scattering mechanism of the particle. The particle surface scattering light also reduces the amount of radiation that reaches the absorber, affording it less opportunity to degrade.[48] Further combinations can be created by encapsulating more than one mechanism, such as an absorber and an antioxidant, utilizing three protection mechanisms. In such a system the particle would scatter light, radiation that reaches the inside of the particles can be absorbed by the absorber, and the antioxidant can stabilize the absorber so that the absorber degradation rate decreases.

1.3 Effect of proximity

While the mechanisms for the various forms of UV protection are well known, they have mainly been studied with the goal of protecting a large surface, such as human skin or an automotive coating. With the exception of antioxidants, protection on a molecular level is not generally examined. The question then remains: does the proximity

of a UV protective molecule to a photosensitive molecule affect the level of UV protection attained?

The effect that proximity has on UV protection was investigated by collaborators at Brown University using solutions.[49] Beta-carotene was chosen as a photosensitive molecule and octyl-4-methoxycinnamate (OMC) as a UV absorber. Core/shell, homogeneous, and hybrid particle geometries were simulated using solutions and either a conventional or tandem cuvette, as shown in figure 1.2. The amount of beta-carotene left intact after exposure was measured using a fluorimeter. The beta-carotene in the core/shell particle degraded with the fastest rate, followed by the hybrid particle, and the homogeneous particle had the lowest rate of degradation. A body centered cubic unit cell was used to approximate the distance between beta-carotene and OMC molecules, and a range of distances between 28 nm and 2 nm were examined in the homogeneous configuration by varying the concentration of OMC. The differences in degradation rates suggest that the closer in proximity the protective molecule is to the photosensitive molecule, the more protection is provided. This observation was confirmed by the proximity experiments, which showed an increase in beta-carotene concentration after 60 minutes of exposure as the distance between beta-carotene and OMC molecules was decreased. The proximity requirement would be expected of an antioxidant, as it can only neutralize a radical when it is in proximity of the radical. The fact that different protection rates were measured given the same amount of absorber but different proximity to the photosensitive molecule suggests that proximity plays a large role in the efficacy of photoprotection.

1.4 Dissertation objectives

The importance and vast applicability of UV protection has been summarized in previous sections. Current and upcoming UV protection methods tend to focus on protection on a macro-scale, such as human skin or a pharmaceutical tablet. While this approach has had some success and is suitable for various systems, many materials could benefit from protection focused on the photosensitive molecule itself, for instance the active pharmaceutical ingredient inside the tablet. Morabito *et al.* has shown that the proximity between a protective and photosensitive molecule can affect the level of protection,[49] so a new method to protect a photosensitive material on the molecular level is needed. In addition, an understanding of how the proximity affects the different protection mechanisms both alone and in combination would be beneficial in creating new and more efficient protection systems.

Particles are a logical vehicle in which to further study proximity and build a protective framework for photosensitive molecules. Compared to solutions, molecules in polymer particles are kept stationary, meaning the proximity between protecting and sensitive molecules is fixed rather than constantly changing. An additional advantage to encapsulating photosensitive molecules is that some UV protection is provided by encapsulation itself via scattering by the particle, similar to a physical blocker.[46] Particles can also be used in a wide range of applications, such as encapsulating a sunscreen to increase protection provided and decrease degradation of the sunscreen, or encapsulating a pharmaceutical ingredient to be included in a tablet formulation.

Before creating complex particle geometries, the proximity effect in particles can be estimated using uniform particles. In such a simple particle environment, proximity can be altered by varying the amount of the protective material added to the particle formulation. Chapter 2 is dedicated to protection provided by uniform particles. Protection provided without the use of protectants is evaluated, along with absorbers or an antioxidant, and a combination of protectants. Preliminary conclusions are made on the effect of proximity when the concerned materials are encapsulated in a simple uniform particle system.

Core-shell particle geometries are a good candidate for studying proximity because different additives can be placed in the core and shell. Additionally, the geometry may provide more surfaces for reflection and therefore a higher protective capability. Before the core-shell geometries can be used, they must be synthesized. Chapter 3 focuses on the synthesis of two core-shell geometries that will be used as protective vessels for a photosensitive molecule.

Once the particle geometries are created, they can be tested for their protective capacity and protectants can be added selectively to the compartments. Varying the compartment in which a protectant is contained will aid in determining the proximity necessary for protection within a particle and suggest any mechanistic changes that occur when encapsulating a protectant. Chapter 4 discusses the data, results, and conclusions that can be drawn from varying the protectant and the compartment containing it for core-shell particle geometries. The result of this chapter is a particle geometry and formulation that offers increased protection when compared to encapsulation in a uniform particle.

Some particle characteristics were not explored in previous chapters in regard to their effect on UV protection, and those are discussed in chapter 5. Properties such as particle size and the shell thickness of core-shell particles may have an effect on UV protection. The photosensitive molecule may also react differently to the protective capacity of the particles, so examining another photosensitive species would give insight into the applicability of particles. The dimensionless quantity the Damköhler number may give explanation as to how the particles protect from UV, and may also be able to predict protection. Depending on whether the decay rate is controlled by diffusion or reaction, the shrinking core model can give an estimate of beta-carotene decay in a single particle. While particles are the focus of this work, other work has been done with solutions and films, and comparison can offer insight as to the different protection mechanisms of the systems.

Conclusions regarding the work as a whole are outlined in chapter 6. Applications in which the particles and the ideal formulation would be of use are reviewed. Future work optimizing and utilizing the core-shell particle geometries and protectants is also discussed.

1.5 Figures for Chapter 1

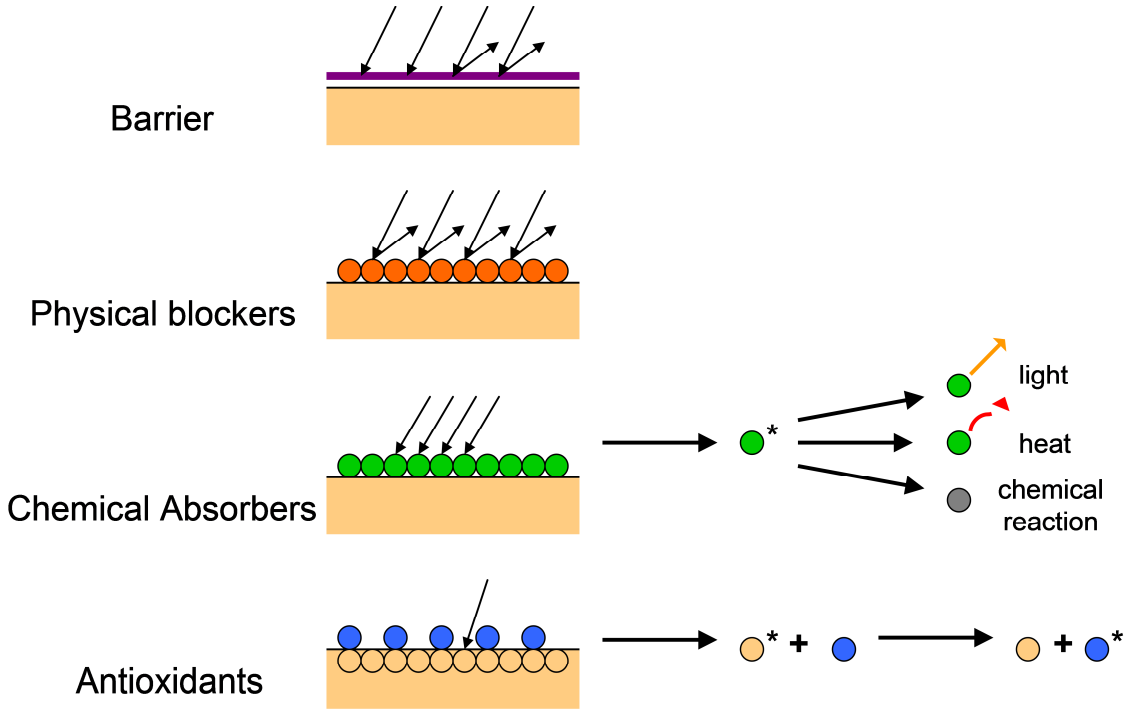

Figure 1.1: Schematic detailing the various protection methods: (a) a barrier, (b) physical blockers (c) chemical absorbers, and (d) antioxidants.

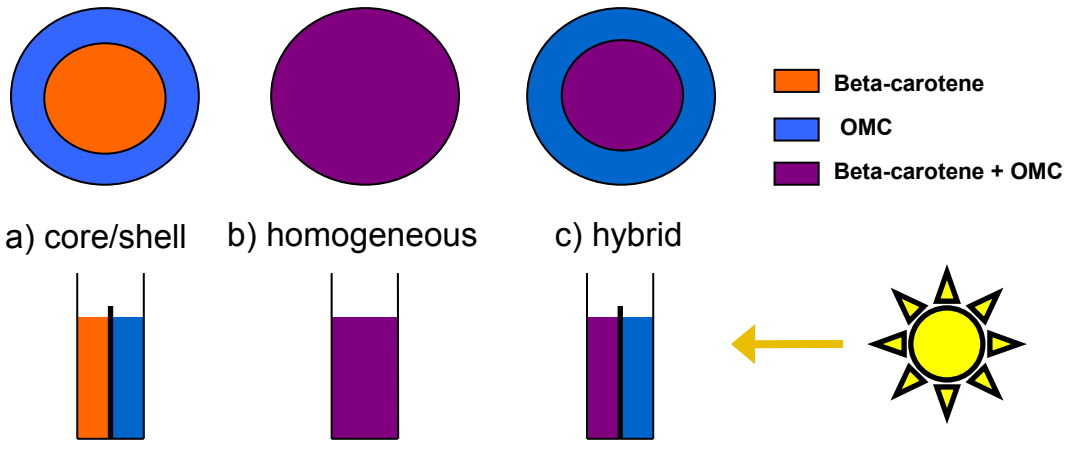

Figure 1.2: Diagrams of the (a) core/shell, (b) homogeneous, and (c) hybrid particle geometries and their respective solutions in cuvettes as studied in Morabito *et al.*[49]

Chapter 2 Protection provided by uniform particles

Particles were created via the single emulsion solvent evaporation method to study the protection of a photosensitive molecule when encapsulated with protective molecules. Particles were exposed to UV radiation and the concentration of photosensitive material left intact was determined using ultraviolet visible spectrophotometry (UV/Vis). The protection provided by various formulations was analyzed using decay curves, a comparison of the protectant amount in a formulation to the normalized absorbance at a specific time, and decay rate constants.

2.1 Single emulsion solvent evaporation method

The solvent evaporation method is a popular and versatile method for creating nano- and microparticles. There is a wealth of literature both on the solvent evaporation process[50-57] and its various applications.[58-61] The method can be modified to create different geometries of particles and include a range of additives. The most elementary form of the process is to use an oil-in-water (O/W) single emulsion method to make uniform particles composed of a hydrophobic polymer and additive.

The process begins by creating an oil phase, which includes a solvent that is mostly immiscible with water as well as everything the particle will be comprised of, such as polymer and sunscreen. In this case the particle contents must be both hydrophobic and soluble in the chosen solvent. The oil phase is blended into an aqueous phase containing water and surfactant. The emulsion is then stirred until the solvent

completely evaporates. The solvent used must be partially miscible in water, as the solvent will migrate to the water before evaporation. As the solvent moves into the aqueous phase, the particle components precipitate and form particles. The entire process can be seen as a diagram in figure 2.1.

There are many parts of the process that can be altered in order to fine-tune particle production. Solvent is an important parameter as it can affect many particle characteristics. The miscibility of the solvent in water affects the amount of time required for the solvent to migrate to the aqueous phase. Over time the aqueous phase becomes saturated with solvent and cannot continue until solvent evaporates. The volatility of the solvent determines how quickly the solvent evaporates to allow more solvent to enter the aqueous phase. These two solvent properties, miscibility and volatility, determine the rate of particle production. For example dichloromethane (DCM) has a very high vapor pressure (and therefore is very volatile) and is slightly miscible in water, and particles are made in approximately four hours. The vapor pressure for toluene is much lower than that of dichloromethane and it is less miscible in water, causing particles to take up to 24 hours to synthesize. The rate of particle production also affects the encapsulation efficiency. A longer rate provides the additive with more time to migrate to the aqueous phase before the particles are solid.[62] The miscibility of the solvent in water contributes to particle porosity as well, since a high miscibility causes the solvent to migrate from the emulsion droplet so quickly as to leave behind pores.[63]

The stability of the emulsion has a large impact on the characteristics of the particles. Emulsion stability can be ensured by the addition of a surfactant. As the surfactant concentration is increased, the solution is able to stabilize smaller emulsion

droplets, leading to smaller particle sizes.[64] Increasing the amount of surfactant can also cause the particle size distribution to narrow, likely due to an increase in emulsion stability.[57] Increasing the stirring speed during evaporation also decreases both the particle size and the particle size distribution.[50] The presence of a surfactant has a positive effect on the encapsulation efficiency, as the encapsulation efficiency decreases as surfactant concentration is decreased.[55] Although increasing the surfactant concentration has advantages, an excess of surfactant can lead to foaming which decreases particle yield.[57]

The polymer used determines characteristics of the resulting particles. Encapsulation efficiency has been found to increase with increased molecular weight of the polymer.[52] Increasing the amount of polymer in the oil phase, while keeping other parameters like volume of the solvent constant, results in an increase of particle size and decrease of particle porosity.[55]

The single emulsion solvent evaporation method is an ideal way to create particles to study the effectiveness of protection of a UV sensitive molecule by encapsulating it with UV protecting materials. The method is well studied and versatile. Particles can be tailored to specific needs by varying parameters such as the solvent, surfactant concentration, and polymer characteristics.

2.2 Synthesis of uniform particles

Uniform particles were formulated to include the UV sensitive molecule beta-carotene and the UV protective materials oxybenzone, avobenzone, octyl-4-

methoxycinnamate, and vitamin E. Poly(methyl methacrylate) was used for the majority of the work, and poly(lactic-*co*-glycolic acid) was studied at some formulations for comparison to a biodegradable polymer. The particles were synthesized using a single emulsion solvent evaporation method.

2.2.1 Materials

UV sensitive additive. Beta-carotene is a pigment found in foods such as carrots, and it acts as an antioxidant[65] and vitamin A precursor in the human body. Beta-carotene gets its color from a chain of conjugated bonds, which also cause beta-carotene to possess some stability when excited.

Beta-carotene was chosen as the UV sensitive additive to assess the amount of UV protection being provided by the particles and their various formulations. Beta-carotene is a good candidate for the study of UV degradation when encapsulated because its photosensitivity and degradation due to UV exposure are well documented.[65-70] Beta-carotene is also highly hydrophobic, so it can be encapsulated using the conventional O/W solvent evaporation method, and should have a high encapsulation efficiency due to it's hydrophobicity.[71]

Attributes of beta-carotene also make it an appealing choice when it comes to data analysis. As beta-carotene degrades due to UV exposure, it transitions from being orange to having no color; therefore degradation is easily confirmed visually by the orange color fading. Beta-carotene also has three distinct absorbance peaks, shown in figure 2.2 that can be observed using an ultraviolet visible spectrophotometer (UV/Vis). Since

absorbance is directly proportional to concentration, the values of the absorbance peaks decline as the beta-carotene concentration is reduced due to degradation. A decay curve of absorbance values will correlate with the concentration decay. Collecting absorbance peaks via UV/Vis is a rapid process that is nondestructive to samples. The maximum beta-carotene absorbance peak can be observed at approximately 465 nm.

Protective additives. As outlined previously, there are three main types of materials used to increase UV protection. Encapsulation offers protection similar to a physical blocker, so addition of compounds such as zinc oxide to particles is not necessary. Most conventional sunscreens are composed of UV absorbers, so three were chosen for study: oxybenzone, avobenzone, and octyl-4-methoxycinnamate (OMC). One antioxidant, alpha-tocopherol (vitamin E) was also included to study the difference in protection when compared to UV absorbers, and to examine the impact of combinations of multiple protection mechanisms.

Oxybenzone is a very common ingredient in sunscreen formulations due its broad spectrum absorbance, which protects in both the UVA and UVB regions, as shown in figure 2.3. After absorbing UV radiation, oxybenzone remains stable by delocalizing the excess energy over two benzene rings separated by a carbonyl group.[72] Frequent use of oxybenzone in sunscreens is despite many cases of photocontact allergy attributed to the UV absorber.[73] It has been proposed that encapsulating oxybenzone allows it to provide UV protection without coming into direct contact with the skin, which should decrease incidences of photocontact allergy.[74] Oxybenzone has also been the center of controversy due to beliefs that it has the potential to disrupt hormones in humans,[75] but

there is considerable information disproving hormonal interference by oxybenzone as well.[76]

Avobenzone, a UVA absorber whose absorbance spectrum is in figure 2.3, is also commonly used in commercial sunscreens. Formulations containing avobenzone usually also contain a stabilizer and a UVB absorber to make the formulation broad spectrum. Avobenzone has a similar structure to oxybenzone, except that the benzene rings have different substituents and there are two carbonyl groups between the rings. As with oxybenzone, the excited molecule is stabilized by delocalization throughout the molecular structure.

OMC is a UVB absorber as shown in figure 2.3, often used since the number of photoallergic cases connected to OMC is very low [77] and it is derived from natural materials. OMC is usually paired with a UVA absorber in formulations in order to offer broad spectrum protection. OMC is stabilized by resonance created by a benzene ring whose substituents are a methoxy group and an electron-accepting group.[78]

Vitamin E is a chain-breaking antioxidant, which means that it hinders the propagation reactions of an excited molecule by reacting with the radical and producing a stable product. Vitamin E also absorbs UV radiation as displayed in figure 2.3, allowing it to use both UV absorber and antioxidant mechanisms in order to protect a photosensitive material. The antioxidant is present in the human body to protect it from harmful reactions such as photooxidation. Vitamin E has even been shown to provide protection when applied as a topical sunscreen.[79]

Polymers. Poly(methyl methacrylate) (PMMA) was chosen as the encapsulating polymer for many reasons. It has been used as an encapsulating material in many solvent evaporation method studies, which confirms its versatility and compatibility with the process.[80-88] PMMA can also be obtained in bulk easily and cheaply, making it ideal for creating large amounts of particles. The biocompatibility of PMMA has been proven in many situations, which increases the scope of possible applications.[89-92]

PMMA is a practically clear polymer, so any UV protection provided to beta-carotene would have to be attributed either to scattering due to encapsulation, or to protection by the UV absorber or antioxidant also encapsulated. Figure 2.2 is an absorbance spectrum for PMMA, showing that it does absorb light, but such a small amount and in such a short range that its effect would be minimal. Studies have also shown that PMMA undergoes negligible decay when exposed to UV radiation.[93]

Poly(lactic-*co*-glycolic acid) (PLGA) is a copolymer composed of lactic acid and glycolic acid. It is approved by the FDA and known for its biocompatibility and biodegradability, which leads to its frequent use in the pharmaceutical industry. PLGA has very similar properties to PMMA, such as being nearly transparent and absorbing very little light.

Solvents. As discussed in the previous section, solvent choice for a single emulsion solvent evaporation method can have a large impact on the characteristics of the synthesized particles. Uniform particles were created using toluene as the solvent. Particles made with toluene have a tendency to be compact and devoid of pores. Toluene is also a good solvent for PMMA and all of the additives.

For studies involving the biocompatible polymer PLGA, chloroform was used as the oil phase solvent. PLGA particles synthesized with chloroform have been shown to have a higher encapsulation efficiency than particles prepared with other solvents. The use of chloroform also produces smaller particles with a more narrow particle size distribution.[94]

Surfactant. The surfactant employed was poly(vinyl alcohol) (PVA), a hydrophilic, nonionic, biodegradable polymer often used as a stabilizer.[95] PVA is a common choice of surfactant when utilizing the solvent evaporation method, especially when the particles are composed of a biodegradable and biocompatible polymer like PLGA.[50, 96, 97] During particle synthesis, the hydrophobic portion of PVA binds to the surface of the particles, which can affect particle properties.[96, 98]

2.2.2 Production of uniform particles

Uniform particles were synthesized using a single emulsion solvent evaporation method, as elaborated upon in section 2.1. Briefly, an oil phase is prepared using a water-immiscible solvent and the particle formulation (polymer and additives). The oil phase is blended into an aqueous phase containing water and a surfactant. The resulting emulsion is agitated until the solvent evaporates, leaving behind solid particles.

Particles were created following the basic solvent evaporation procedure. The oil phase consisted of 3 mg of beta-carotene, 0.2 g of PMMA with a molecular weight of 15000, and a varied amount of protectant dissolved in 3 ml of toluene. The protectants

included oxybenzone, avobenzone, OMC, and vitamin E. The varied amounts of protectant added to the formulation are specified in table 2.1. The aqueous phase was prepared using 175 g of deionized water and 25 g of a stock 4% aqueous solution of poly(vinyl alcohol) (PVA), creating a 0.5% solution of PVA. In a hood vent, the oil phase was poured into the aqueous phase and blended using an UltraTurrax T25 basic disperser by IKA at 15000 rpm for 3 minutes. After blending the emulsion was stirred on a magnetic stir plate for at least 16 hours to allow for evaporation of the toluene. Particles were collected by centrifuging at 10000 rpm for 10 minutes. The supernatant was disposed of and the particles were resuspended in 20 ml of deionized water by sonication. The particles were stored in a jar covered by aluminum foil to prevent accidental UV exposure. The resulting particles were approximately 900 nm in diameter, as determined using a Zetasizer Nano ZS90 (Malvern Instruments). An image of the particles taken with an Amray 1830 I scanning electron microscope is shown in figure 2.4.

Particles were also made with PLGA to compare to a polymer that is both biocompatible and biodegradable. The process used was very similar to that described previously in literature.[94] The formulation was identical to that used for PMMA particles, except that PLGA was used and the particle contents were dissolved in 10 ml of chloroform. The oil phase was blended into 190 g of 5% PVA solution at 15000 rpm for five minutes. The emulsion was added to an additional 100 g of 5% PVA solution and stirred for four hours until the chloroform was completely evaporated. The process of collecting and resuspending the particles was identical to that used for PMMA particles. Two lactic acid to glycolic acid ratios were used, 50:50 and 75:25. Both ratios yield particles using the solvent evaporation method, but the 75:25 ratio shares the more

hydrophobic nature of the other additives. Each copolymer ratio was studied in two formulations, one containing no protectant, and the other containing the 1:10 beta-carotene:oxybenzone ratio.

2.3 Testing and analysis

Beta-carotene decays as it is exposed to ultraviolet radiation and this decay can be tracked by monitoring the concentration of beta-carotene left intact after intervals of UV exposure. The rate of beta-carotene decay in different systems can be compared to assess which system offers the best protection. Four systems were explored: beta-carotene in solution, particles composed of beta-carotene and polymer, single protectants at various concentrations, and combinations of protectants. Each system was exposed to UV radiation for intervals of time, and the beta-carotene absorbance determined to relate to the concentration of beta-carotene left undecayed.

The samples were exposed to UV radiation using a 365 nm Pen Ray Mercury Lamp by UVP. The spectrum of the lamp is given in figure 2.5 with the UVA and UVB sections highlighted in orange and yellow, respectively. The radiation given off by the lamp is predominantly UVA, which is consistent with reality where 95% of the UV radiation that reaches the Earth's surface is UVA.[6] A hole was drilled into an opaque slide box and the lamp fitted inside, ensuring that no light would escape the box. A quartz cuvette with a 10.00 mm path length containing 3.7 ml of sample was placed inside the previously described box with a clear side of the cuvette facing the light source, and the lamp illuminated. A diagram of the experimental setup is in figure 2.6. The exposure

times included five minute intervals from 0-30 minutes, and 10 minute intervals from 30-60 minutes, for a total of 10 exposures. The exposure intervals are shorter for the first 30 minutes because this is when the greatest rate of beta-carotene degradation is observed. The samples were stored in capped centrifuge tubes after exposure.

A solution of beta-carotene in acetone was examined as a baseline to determine the rate of beta-carotene degradation when not encapsulated. The 19 μM solution was exposed as described above, except that the cuvette was capped and sealed with Teflon tape to discourage acetone evaporation. After all 10 exposures were completed, each sample was poured into a graduated cylinder and acetone was added to replace any acetone that may have evaporated. The total sample volume was 3.7 ml. The samples were then analyzed by an ultraviolet visible spectrophotometer (UV/Vis) (Lambda XLS+ by Perkin Elmer) with acetone as a reference sample, and the maximum beta-carotene peak noted.

The procedure for exposing particles was very similar to that for the beta-carotene solution. Samples consisted of 3.7 ml of suspensions containing approximately 19 μM beta-carotene. This means that the suspension of particles contained the same amount of beta-carotene as a 19 μM solution. These suspensions were created by diluting the stock suspensions created in the previous section. The particles in suspension accounted for approximately 1% of the volume fraction, meaning the suspension was dilute enough to discourage particle-particle interactions. The cuvette was not capped since water is not as volatile as acetone. After exposures, samples were centrifuged and the supernatant was disposed of. Particles were resuspended in 3.7 ml of Triton X-100 by sonication. Triton X-100 was used to match the refractive index of PMMA (or PLGA), so the PMMA peak

should be subtracted with the background and not interfere with the beta-carotene peaks. The samples were analyzed via UV/Vis with Triton X-100 as a reference and the maximum beta-carotene peak recorded.

The maximum beta-carotene peaks for each formulation were normalized by dividing by the maximum peak of unexposed particles from the same batch. This normalization is necessary to account for batch to batch variations. For example, the amount of beta-carotene in one batch of particles may be slightly different than that from another batch. Unexposed particles from the two batches would display different absorbance peaks due to differing concentrations. When normalizing using the peak from unexposed particles from the same batch, the decay becomes relative to the amount of beta-carotene in that batch of particles, allowing batch-to-batch comparisons to be made. After normalization, samples without any decay should have a value of one whereas samples with complete decay should have a value of zero.

2.4 Effect of protectants

Three types of formulations were examined: those with no protectant added, one protectant, or a combination of two protectants. The particles devoid of protectant were studied along with a solution of beta-carotene in order to determine whether or not encapsulation possessed a protective effect. The single protectant cases established which protectant offered the best protection, as well as the effect of protectant concentration. Two types of combinations were investigated, two absorber-absorber combinations and three absorber-antioxidant combinations. Each formulation was analyzed using decay

curves and charts comparing the protectant amount to normalized absorbance for specific times.

2.4.1 No protectants

In order to determine whether the addition of protectants to particles improves beta-carotene stability, the effect of encapsulation itself had to be established. It has been found in the literature that encapsulation offers protection to a UV sensitive material due to scattering by the particle surface [46, 99, 100] and by limiting molecular movement as a result of a lack of available free volume.[101] Both of these mechanisms are observed in the particle environment, but not in solutions. Figure 2.7 shows the normalized absorbance of beta-carotene in the acetone solution and encapsulated in PMMA as it is exposed to UV radiation. Each data point is the average of three experiments, and the error bars represent the standard deviation as a result of those three runs. Beta-carotene in solution was completely degraded after 40 minutes of exposure, whereas approximately 25% of the encapsulated beta-carotene was left undegraded after the same amount of exposure. After 60 minutes of UV exposure the encapsulated beta-carotene is still not completely degraded. Figure 2.7 confirms that found by Perugini *et al.*[46] that encapsulation is a UV protective mechanism in itself. Figure 2.7 also shows that the fastest decay takes place in the first 30 minutes of exposure, which is why exposure intervals are shorter during that time. Since PMMA absorbs very little, the protection mechanism employed by encapsulation must be the same as that of physical blockers. Encapsulation in a polymer matrix scatters light, causing less to reach the UV sensitive

molecule embedded in the matrix. Another mechanism of protection is the polymer matrix itself, restricting movement of the beta-carotene molecule which inhibits it from undergoing reaction and degrading.[101]

The solution and suspension in figure 2.7 are not in identical photochemical systems since different solvents were used. Acetone was used for the solution experiments because beta-carotene is insoluble in water, and acetone could not be used to suspend the particles because it would dissolve them, destroying the particle geometry and any benefits attained from that geometry. While the systems are different, the increase in photostability by encapsulation as shown in figure 2.7 is undeniable. Comparing the two systems quantitatively, such as calculating a numerical increase in photostability due to encapsulation, may not yield accurate results due to the use of different solvents. The qualitative observation of increased protection, however, is apparent.

The decay of encapsulated beta-carotene was used to determine the amount of additional protection provided when protectants were added to the particle formulation. Since this decay curve will be often used as a reference in subsequent analysis, a more in depth look at the decay is valuable. Figure 2.8 shows the beta-carotene absorbance spectrum at different times of UV exposure. The unexposed beta-carotene has the three peaks characteristic of the molecule. The middle, maximum peak was recorded to compile decay curves. As the particles were exposed, the absorbance peaks become smaller. After 30 minutes of exposure it is difficult to discern three separate peaks. As mentioned earlier, figure 2.8 shows that the majority of the decay takes place during the first 30 minutes of exposure.

Since beta-carotene is an antioxidant molecule it is necessary to determine if it could provide protection to itself when present in larger quantities. Figure 2.9 shows beta-carotene decay curves for particle formulations synthesized using four different concentrations of beta-carotene. There is a positive effect of higher concentrations of beta-carotene, and this could be a result of the antioxidant mechanism or that the number of photons the particles are being exposed to has remained the same while the number of beta-carotene molecules has increased.

2.4.2 Single protectant

The effectiveness of oxybenzone, avobenzone, OMC, and vitamin E to protect beta-carotene in a particle environment was studied by synthesizing particle formulations containing each protectant individually at four concentrations. Two additional concentrations of oxybenzone were studied to determine protection provided at very low concentrations of protectant. The exposure times 10, 20, 30, 40, and 60 minutes were performed in triplicate for all oxybenzone concentrations, and for each formulation containing the 1:10 ratio of protectant. These particles were chosen for repetitions so that a set of standard deviations could be calculated for each ratio and protectant.

Effect of protectant. Decay curves of the normalized absorbance for each single protectant formulation are shown in figure 2.10. The error bars are the standard deviations as a result of three repetitions. The “beta-carotene” curve represents particles comprised of only beta-carotene and PMMA. Comparing figures 2.10a-d, it is obvious

that the protecting species plays a large role in the amount of protection provided. Oxybenzone and avobenzone formulations display the most similar behavior, offering minimal protection at the 1:1 ratio and protection increasing with concentration until the 1:33 ratio, where it reaches a plateau. Both absorbers also result in approximately 65% beta-carotene left undegraded after 60 minutes for the highest concentration, offering the best protection for a single protectant. Vitamin E still protects very well, but not quite as well as oxybenzone and avobenzone, at approximately 50% beta-carotene left after an hour of exposure for the 1:100 ratio. OMC performed the worst, with the decay curves for all concentrations overlapping with that of beta-carotene encapsulated without a protectant. The ineffectiveness of OMC could be attributed to its sensitivity to both UVA and UVB radiation.[102]

Another way to look at the data is to compare the normalized absorbance over the amount of protectant added for different exposure times, such as in figure 2.11. While this kind of chart speaks more about the effect of concentration, a comparison between the protectants confirms observations made from the decay curves. Figures 2.11a and c show the similar behavior between oxybenzone and avobenzone, including the plateau in effectiveness at the 1:33 ratio (0.1 g) and the high amount of beta-carotene left after 60 minutes of exposure at high concentrations. The ineffectiveness of OMC is also apparent by all points hovering around that for zero protectant, and the practically horizontal line when increasing protectant amount.

Effect of concentration. Figures 2.10a and c show a strong dependence on protectant concentration for oxybenzone and avobenzone. Oxybenzone and avobenzone provide

increased UV protection as concentration is increased until a plateau at the 1:33 ratio, as the 1:33 and 1:100 curves possess significant overlap. This maximum in protection is also present in figure 2.11, where there is a sharp increase in protection from zero to 0.1 g (1:33 ratio), and nearly no increase between 0.1 g (1:33 ratio) and 0.3 g (1:100 ratio). This plateau could arise either because the beta-carotene is already surrounded by protectant molecules at the 1:33 ratio, or because additional protectant cannot be incorporated into the particles since as protectant concentration is increased it reaches a point where there is more protectant than polymer. In a case where the most protection is desired for the least amount of additive material, the plateau suggests that 0.1 g of either oxybenzone or avobenzone would be a good choice.

Vitamin E shows an increase in protection with an increase in vitamin E concentration, as displayed by the decay curves in figure 2.10d. Other than the sharp increase between 0.03 g (1:10 ratio) and 0.1 g (1:33 ratio), vitamin E has a nearly linear increase in protection as the amount of protectant is increased as shown in figure 2.11d. OMC displays the opposite trend, as it's decay curves all cluster around the beta-carotene curve (figure 2.10b) and the protection it provides is nearly horizontal with the zero protectant point when comparing the absorbance at different times with respect to concentration (figure 2.11b).

Effect of polymer matrix. PLGA is a polymer known for its biocompatibility and biodegradability. In order to determine whether findings with PMMA could be extrapolated to PLGA, particle formulations both with and without a protectant were completed to compare the performance. Figure 2.12 shows beta-carotene decay curves

for particles containing just beta-carotene and each polymer, and particles that also contain a 1:10 ratio of oxybenzone. The beta-carotene curves overlap significantly, suggesting that all three polymers offer similar protection by encapsulation alone. There is more variation between the curves of the three polymers when oxybenzone is added to the formulation, but the curves are still in an obvious cluster and display overlap. Although there is some slight variance between the polymers, figure 2.12 shows that similar results should be obtained with different particle formulations regardless of whether PMMA or PLGA is used.

Effect of particle concentration. While every effort was made to ensure that each sample contained a similar amount of particles, it was impossible for each sample to have the exact same concentration. To determine whether this difference in concentration would have an effect on the amount of UV protection provided, the beta-carotene decay of a formulation containing the 1:33 ratio of oxybenzone was studied at the 19 μM concentration discussed previously, as well as a 57 μM concentration. The 57 μM suspension uses the exact same particles as the 19 μM suspension, just three times more of them, resulting in the higher beta-carotene concentration. Figure 2.13 shows decay curves for the 19 μM and 57 μM suspensions of particles containing the 1:33 ratio of oxybenzone. Both decay curves begin almost identically and variation increases as exposure time increases. Even with the variation, there is considerable overlap between the two curves, suggesting that the decay rate is the same. This not only confirms that concentration of the particles is not a factor when the suspensions are dilute, but also proves that at dilute concentrations particle shielding is not a factor. Lack of particle

shielding effects means that the particles are not protecting each other; therefore the scatter by encapsulation and the particle formulation are the main contributors to protecting beta-carotene in the particles.

2.4.3 Combinations of protectants

Using a single protectant proved to significantly extend the life of beta-carotene in a particle environment in most cases. Many commercial UV protective systems, such as sunscreens, utilize a cocktail of protective materials. In order to study the effect of adding multiple protectants to a formulation, combinations with oxybenzone and vitamin E were synthesized. These formulations contained the same amount of each protectant as the previous section, so the overall amount of protectant was doubled, creating an overall beta-carotene:protectant ratio of 1:20. Beta-carotene decay profiles for all of the combinations are shown in figure 2.14.

Absorber-absorber combinations were studied by creating formulations of oxybenzone with another absorber. Oxybenzone was chosen for these combinations because it is broad spectrum, absorbing in both the UVA and UVB regions, so it could offer protection in parts of the UV spectrum not covered by the UVA or UVB absorber in the formulation. Decay curves for particles containing oxybenzone in combination with OMC and avobenzone are shown in figures 2.14a and b, respectively. Contrary to the hypothesis that more protectant would create more protection, the combinations had a negative or neutral effect. The particles containing oxybenzone and OMC (figure 2.14a) offered less protection than either absorber alone, even though the combination particle

contained as much oxybenzone and OMC as the single protectant particles, resulting in double the amount of absorber overall. The decay curve for the avobenzone and oxybenzone particles (figure 2.14b) overlapped with those for the particles containing each absorber singly, resulting in no increase in protection even though the absorber amount had been doubled. From these results it can be concluded that the addition of oxybenzone hindered protection rather than promoting it in the particle environment. An explanation for this behavior could be that oxybenzone has a tendency to become a photosensitizer when in a polar environment.[102] The particles were in an aqueous suspension as they were being exposed, allowing any oxybenzone on the surface of the particles to come into contact with water. The oxybenzone in close proximity to the water could then become a photosensitizer, acting on either the beta-carotene or the other absorber and causing them to degrade, leading to a decrease in protection.

Particles containing both vitamin E and one of the absorbers were created to study the effect of absorber-antioxidant combinations (figures 2.14c-e). Vitamin E combinations with oxybenzone, OMC, and avobenzone all showed significant improvement over their single protectant counterparts. The OMC combination yielded five times the amount of undegraded beta-carotene after 60 minutes of exposure that the particles containing only OMC did, and a slight increase in protection was found over the single protectant vitamin E particles as well (figure 2.14d). The avobenzone and vitamin E particles resulted in double the protection of the single protectant particles after 60 minutes (figure 2.14e). The oxybenzone and vitamin E particles resulted in the best overall protection with 80% of the beta-carotene left undegraded after 60 minutes, double that of the oxybenzone particles and over double the protective capacity of the vitamin E

particles (figure 2.14c). The increased protection as a result of the absorber-antioxidant particle formulations is most likely due to the combination of protective mechanisms, as has been seen in the literature.[47] The absorber-antioxidant particles actually utilize three UV protective mechanisms, since the particles themselves protect by scattering, the same mechanism as physical blockers like zinc oxide and titanium dioxide.

When comparing all combination particles (as in figure 2.14f), all formulations resulted in more beta-carotene left undegraded after 60 minutes than the particles that contained no protectant. The lowest performing combination particles were the absorber-absorber combinations, as the decay curves for those particles show the quickest decay and least amount of beta-carotene left after exposure. The three absorber-antioxidant combinations are the top three curves, meaning that the rate of decay is the smallest. The best performing particles were those containing the combination of oxybenzone and vitamin E, the absorber-antioxidant combination. While oxybenzone was shown to display photosensitizing properties in the absorber-absorber particles, this trend was not noted in the absorber-antioxidant particles, probably because the antioxidant properties of vitamin E neutralized any oxybenzone that may begin to display photosensitizing behavior.

2.5 Rate constants and proximity

An additional tool for analysis of beta-carotene decay in each particle formulation is to calculate the decay rate constant for each set of particles. Rate constants were compared numerically, as well as graphically with respect to the ratio of the amount of

absorber in each formulation to the amount of beta-carotene. The proximity between the beta-carotene and protectant molecules was estimated and paired with the rate constants to determine the effect of proximity on the amount of UV protection provided by a particle formulation.

2.5.1 Rate constants

Decay rate constants allow formulations to be compared quantitatively, as opposed to the qualitative observation of decay curves. Beta-carotene decay was assumed to be a single exponential decay. Rate constants were calculated by first taking the natural log of the normalized absorbance, then plotting it versus the exposure time, as seen in figure 2.15. The points were nearly linear, and the slope of a line fitted to the data yielded the rate constant. The quality of fit was determined by R^2 values, which ranged from 75% to 91% for the lines fitted in figure 2.15, indicating that the lines adequately fit the data. The standard deviations were calculated for each oxybenzone concentration, but the values were so small that they were indistinguishable graphically, and therefore were not included.

Table 2.2 lists the rate constants for each formulation discussed previously. Figure 2.16 shows the rate constants of the single protectant formulations normalized with the rate constant of particles containing no protectant and compares these values by the number of moles of protectant in a formulation per moles of beta-carotene. The rate constants confirm that oxybenzone and avobenzone behave similarly, and that they are the best protectants for formulations containing a single protectant. The vitamin E rate

constants are just slightly higher than those of oxybenzone and avobenzone, verifying that it is also a good protectant in the specific system. The rate constants also show the instability of OMC in the particle environment, as its rate constants fluctuate and show no trend. The formulation with the smallest rate constant and therefore lowest rate of decay is the formulation containing both oxybenzone and vitamin E, as stated in table 2.2. The rate constant behavior in figure 2.16 is comparable to that observed in polymer films, where a large increase in protection was gained with increased concentration of protectant until 100 moles of protectant per mole of beta-carotene.[103]

2.5.2 Proximity

The ratio between beta-carotene and protectant in a formulation has been used to specify the amount of protectant in a formulation, but this information can also be used to approximate the distance between a beta-carotene molecule and the surrounding protectant molecules within a particle. The effectiveness with respect to proximity can provide additional insight into the behavior of each protectant when encapsulated. Proximity can be estimated using a body-centered cubic unit cell, as described in similar work using solutions.[49]

Using a body-centered cubic unit cell, the beta-carotene molecule is located at the center of the unit cell surrounded by eight protectant molecules, as shown in the schematic in figure 2.17. In most cases examined, the concentration of protectant molecules is much greater than that of the beta-carotene molecules, making this model valid. The volume of the particles is required, and can be estimated by the masses used to

create the particles and the density of the individual materials. The number of protectant molecules present in the formulation can be calculated using the mass of the protectant in the formulation and Avogadro's number. Using these two values, the ratio of the particle volume to that of the protectant molecules can be determined and multiplied by eight since each unit cell contains eight absorber molecules. In order to determine the length of one side of the cube, the result of previous calculations must be raised to the one third power. The distance between the beta-carotene molecule and one of the protectant molecules can then be determined by the multiplication of the square root of three divided by two. These calculations are demonstrated in their entirety in equation 2.1.

$$L_{s,a-b} = \left\{ \left[\frac{m_{PMMA}}{\rho_{PMMA}} + \frac{m_{Beta-carotene}}{\rho_{Beta-carotene}} + \frac{m_{\mathrm{Pr}otec\tan t}}{\rho_{\mathrm{Pr}otec\tan t}} \Big/ \frac{m_{\mathrm{Pr}otec\tan t}}{MW_{\mathrm{Pr}otec\tan t}} \times \left(6.02 \times 10^{23}\right) \right] \times 8 \right\}^{1/3} \times \frac{\sqrt{3}}{2} \quad (2.1)$$

There were some formulations where the number of beta-carotene molecules exceeded the number of protectant molecules, and in these cases the unit cell was changed to contain one protectant molecule surrounded by eight beta-carotene molecules. The calculations were the same, except that the number of beta-carotene molecules was used in the denominator instead of the number of protectant molecules.

Spacing is inversely proportional to protectant concentration, therefore a similar trend would be expected. Figure 2.18 shows the absolute value of the rate constants with respect to the proximity between the beta-carotene and protectant molecules. As expected, the absolute value of the decay rate constant increases as the spacing between the molecules is increased. Oxybenzone, avobenzone, and vitamin E show almost linear increase in the rate constant with an increase in spacing, while the rate constants for

OMC are erratic, confirming observations discussed previously. The smallest rate constants are the result of the beta-carotene to protectant spacing of less than 5 nm, while spacing larger than that provides little protection. At spacing smaller than 5 nm the protectant molecules must completely surround the beta-carotene molecule, absorbing most of the UV radiation before it can reach the beta-carotene. At larger than 5 nm the protectant molecules are not close enough to the beta-carotene molecule to protect it, leaving large enough gaps in the sides of the unit cell to allow significant UV radiation to penetrate it and reach the beta-carotene. In the case of vitamin E, 5 nm may be the limit of how far the antioxidant molecule can travel through the polymer in time to quench the beta-carotene molecule before degradation occurs. Proximity requirements are much different in solution, where a distance as far as 15 nm between a beta-carotene and OMC molecule was found to yield approximately 80% beta-carotene undegraded after an exposure time of 60 minutes.[49]

2.6 Uniform particle conclusions

While encapsulation alone has been shown to protect UV sensitive materials[46, 99, 100] and in this work beta-carotene, the addition of UV protecting materials to the particle formulation proves to increase the capacity for UV protection. Beta-carotene is a suitable molecule for studying the protection of photosensitive materials since its UV degradation has been thoroughly studied.[65-70] Three common sunscreens, oxybenzone, avobenzone, and OMC, along with an antioxidant, vitamin E, were used as protective additives in the particles. Particles were exposed to UV radiation and the degradation of

beta-carotene was tracked via UV/Vis. The effectiveness of particle formulations to protect beta-carotene was analyzed by decay curves and rate constants. Oxybenzone and avobenzone provided significant protection, while vitamin E protected sufficiently, and the protection provided by OMC was insignificant. Concentration of the protectant was a factor, with protection increasing as concentration was increased in most cases, and a plateau reached for oxybenzone and avobenzone when they reached a beta-carotene to protectant ratio of 1:33. Absorber-absorber combinations were created by pairing oxybenzone with another absorber, which resulted in no increase or a decrease in protection, attributed to the capability of oxybenzone to act as a photosensitizer in polar environments.[102] Absorber-antioxidant combinations, created by a formulation containing vitamin E and an absorber, greatly increased protection, probably because of the combination of protective mechanisms. The formulation that offered the best protection overall included both oxybenzone and vitamin E. The effect of the spacing between protectant and beta-carotene molecules was also investigated, and it was found that the maximum distance still providing protection was 5 nm.

2.7 Figures for Chapter 2

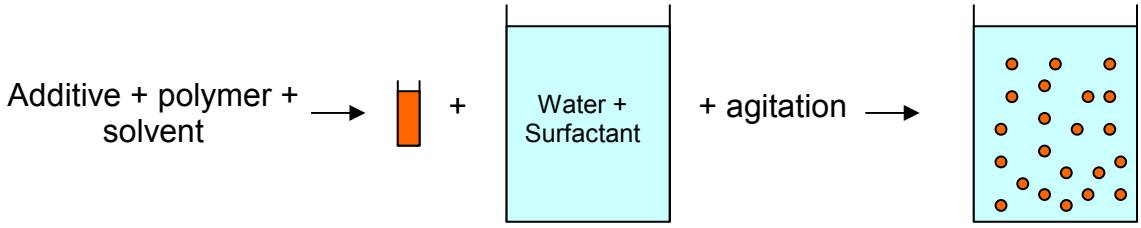

Figure 2.1: A schematic of the single oil-in-water solvent evaporation method for synthesizing particles.

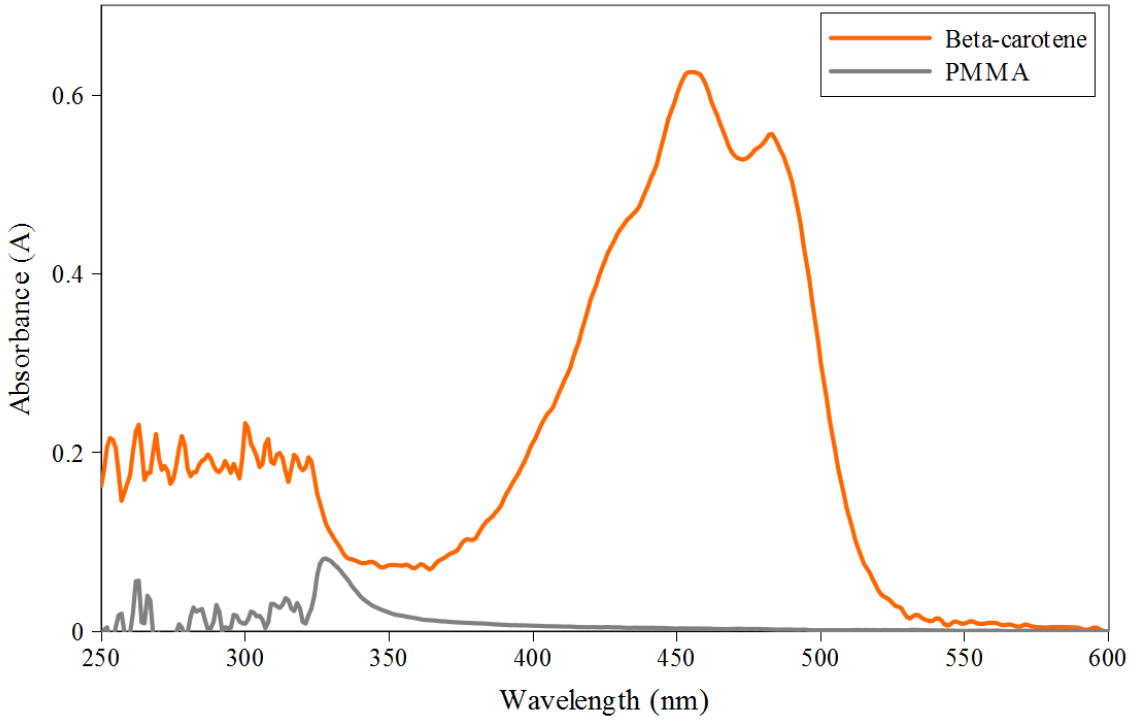

Figure 2.2: Absorbance spectra for beta-carotene, the UV sensitive material, and PMMA, the polymer.

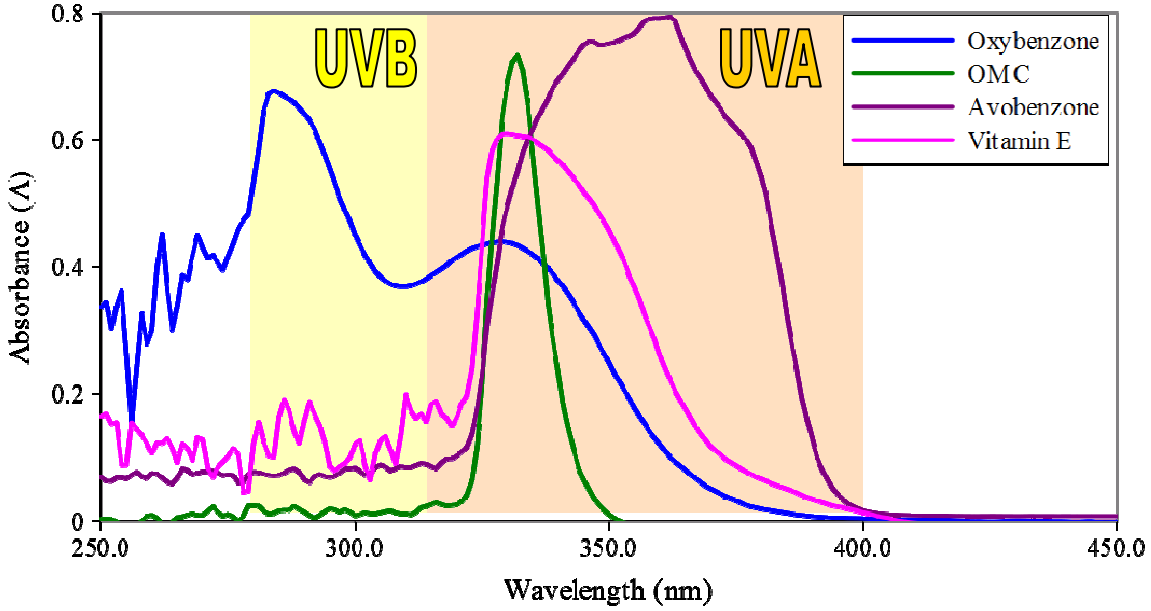

Figure 2.3: Absorbance spectra of the UV absorbers oxybenzone, avobenzone, and OMC, and the antioxidant vitamin E. The UVA region is highlighted in orange, and the UVB region in yellow.

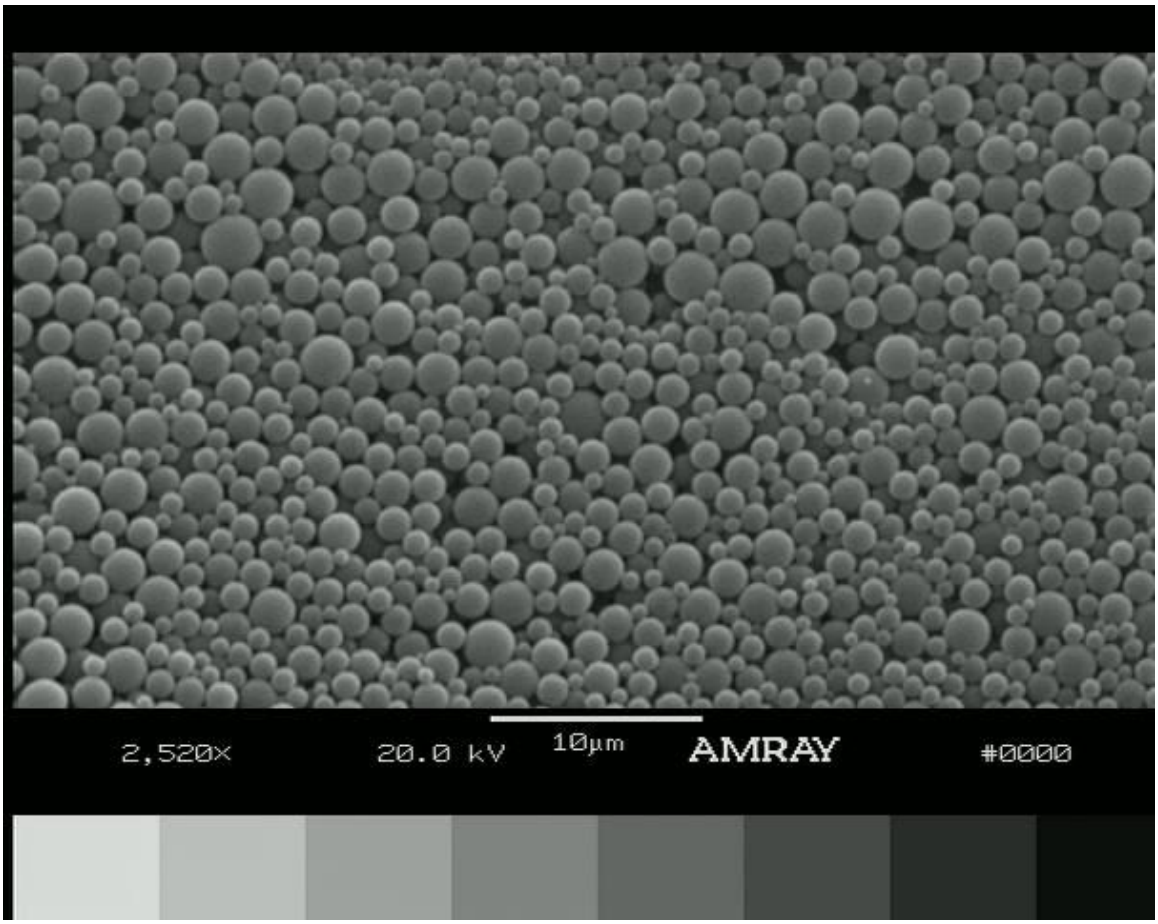

Figure 2.4: Scanning electron microscope image of the uniform particles.

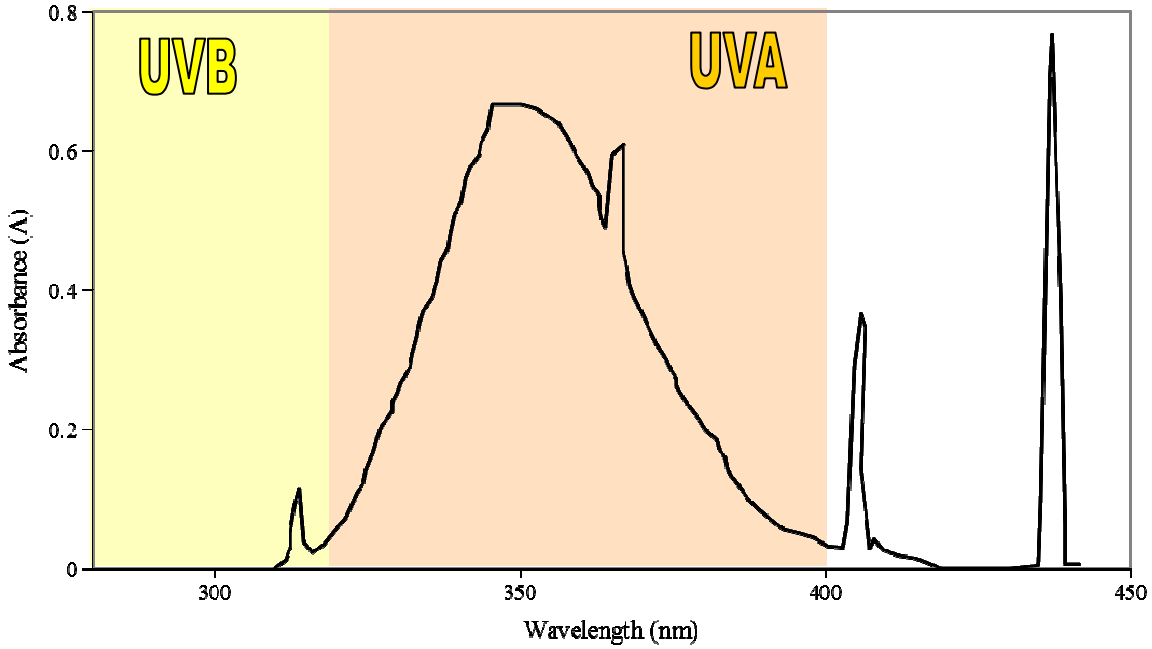

Figure 2.5: Absorbance spectrum of the UV lamp used to expose the particles. The UVA and UVB regions are highlighted in orange and yellow, respectively.

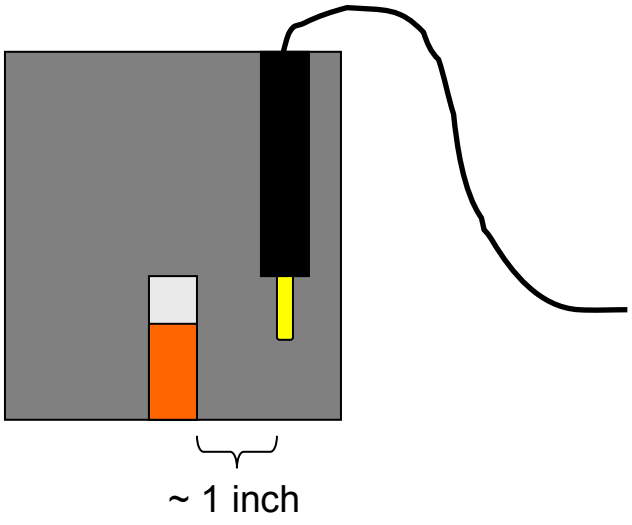

Figure 2.6: Schematic of the system for exposing samples to UV radiation. The cuvette is approximately 1 inch from the light source.

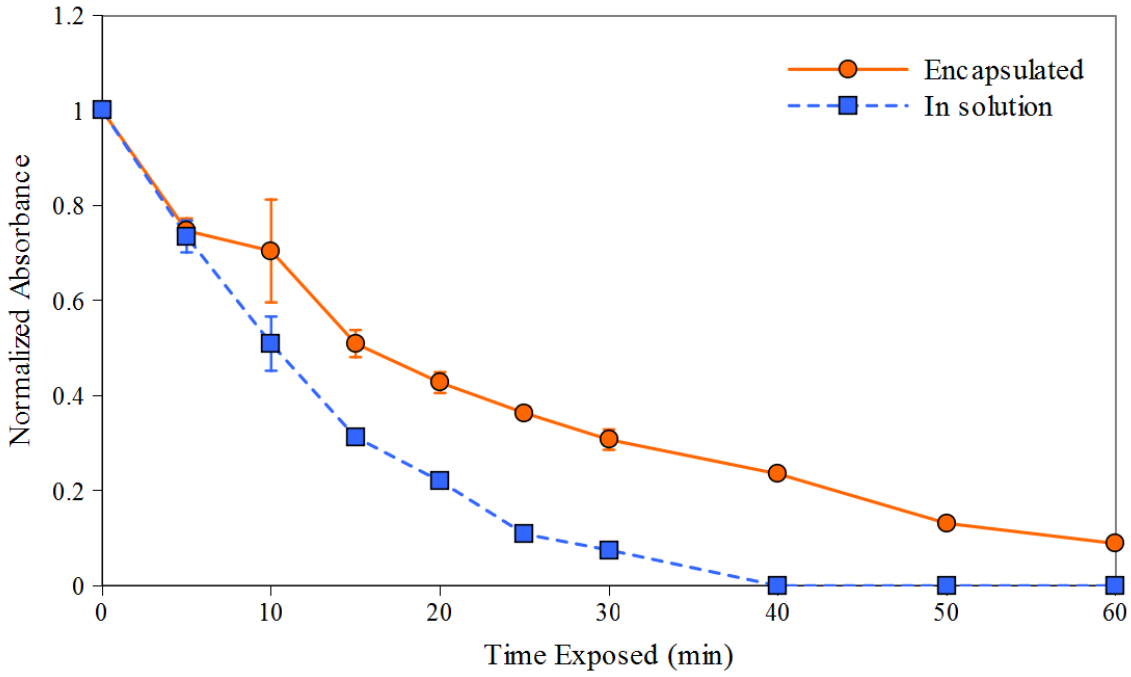

Figure 2.7: The decay of beta-carotene as shown by its decreased absorbance as it is exposed to UV radiation both in solution and encapsulated.

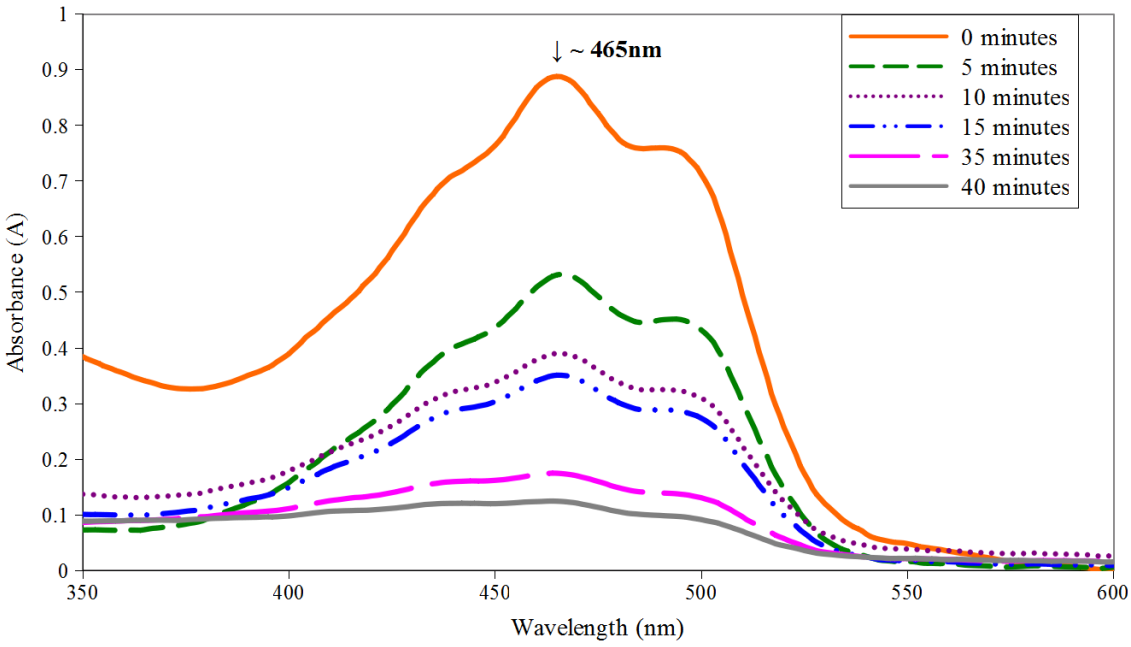

Figure 2.8: The beta-carotene absorbance spectrum at various exposure times.

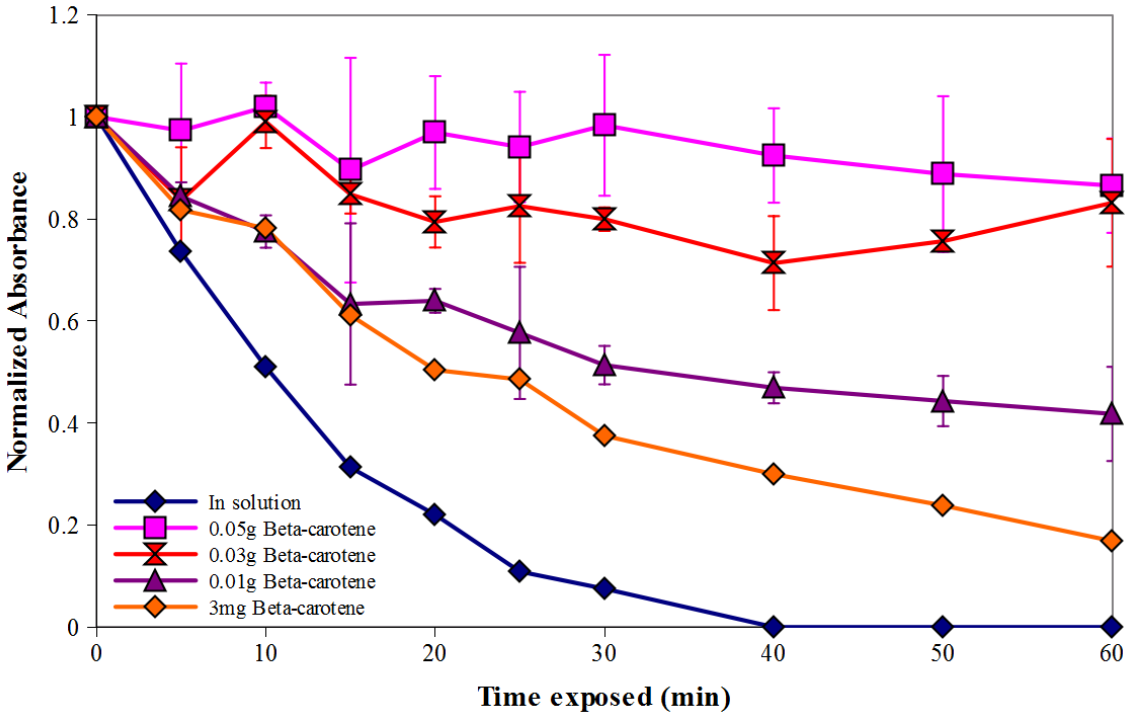

Figure 2.9: Beta-carotene decay curves for particles containing different concentrations of beta-carotene.

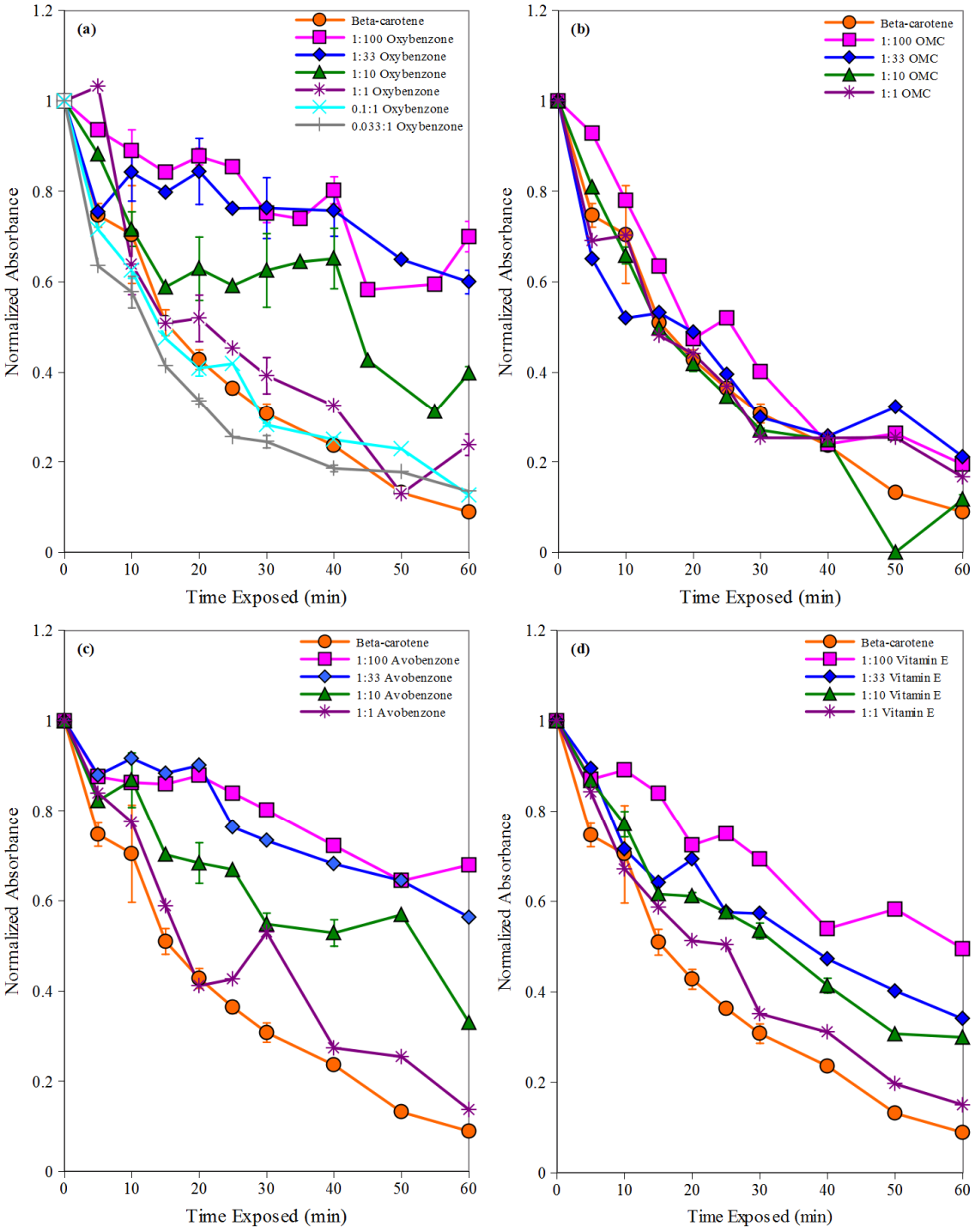

Figure 2.10: Decay curves of normalized absorbance over time exposed for (a) oxybenzone, (b) OMC, (c) avobenzone, and (d) vitamin E individually.

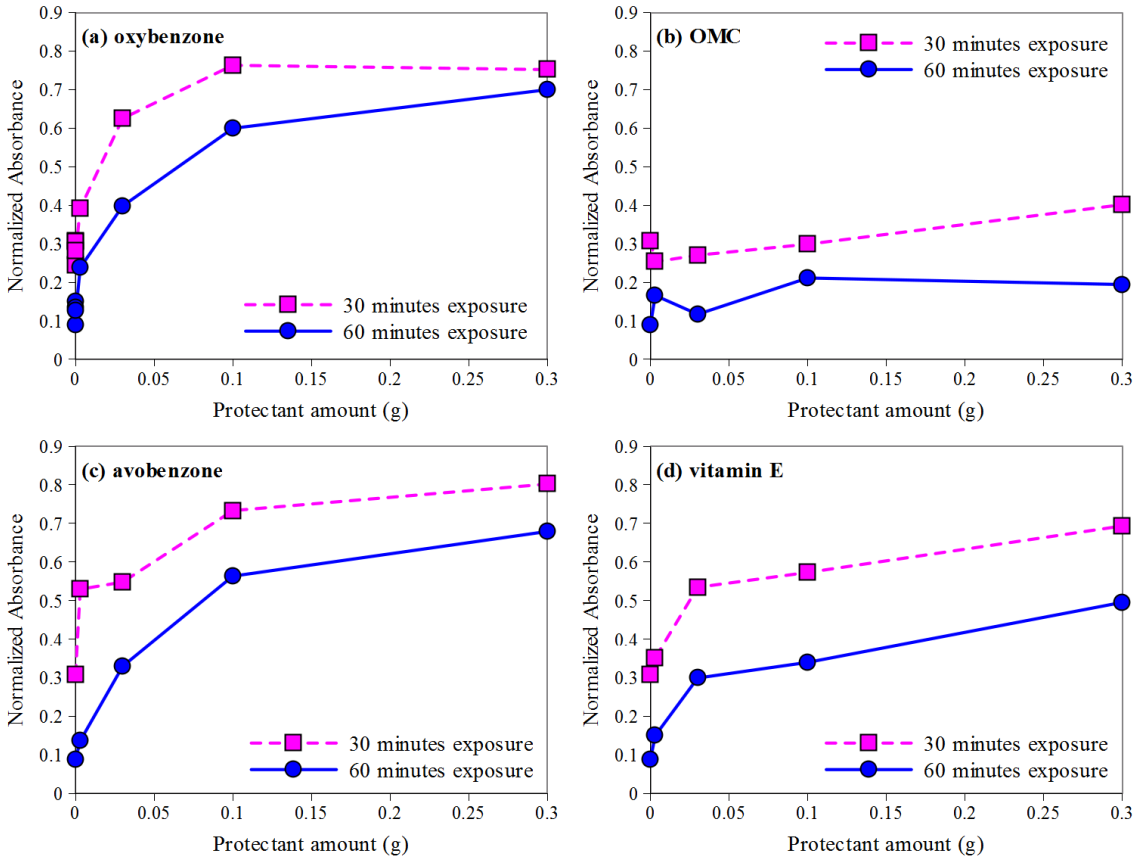

Figure 2.11: The effect of the amount of protectant used in the particle formulations by comparing absorbance at 30 and 60 minutes for particles containing (a) oxybenzone, (b) OMC, (c) avobenzone, and (d) vitamin E.

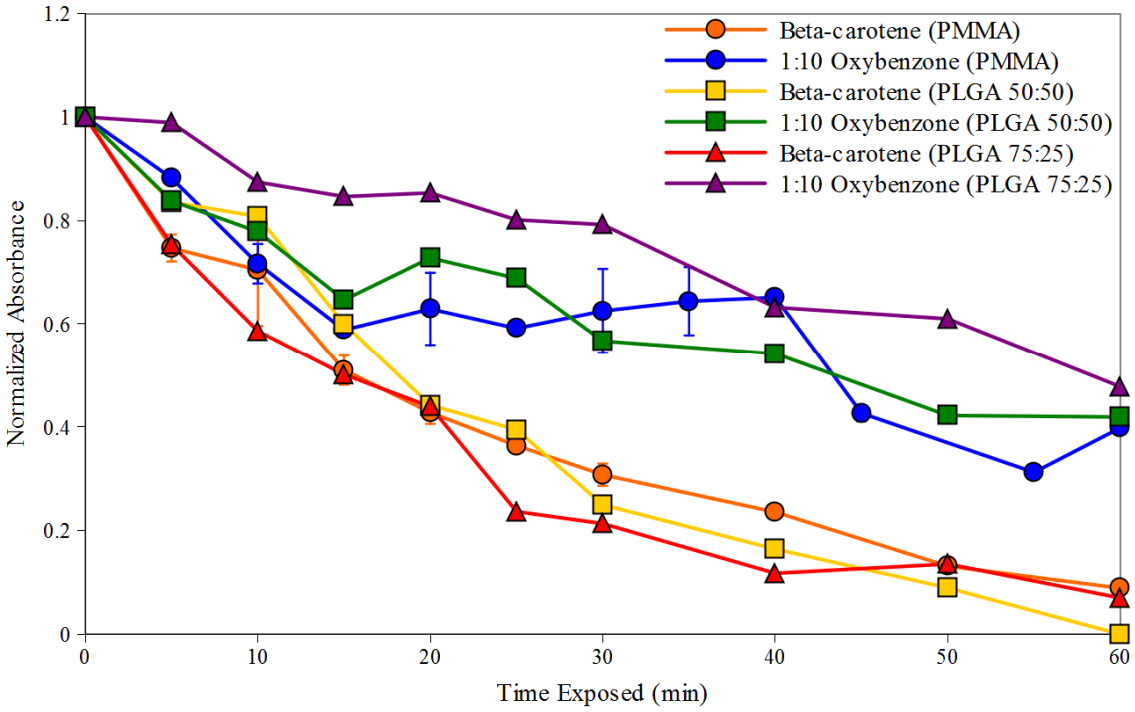

Figure 2.12: Beta-carotene decay for particles containing beta-carotene or beta-carotene and oxybenzone in a 1:10 ratio for PMMA, PLGA (50:50), and PLGA (75:25) polymer matrices.

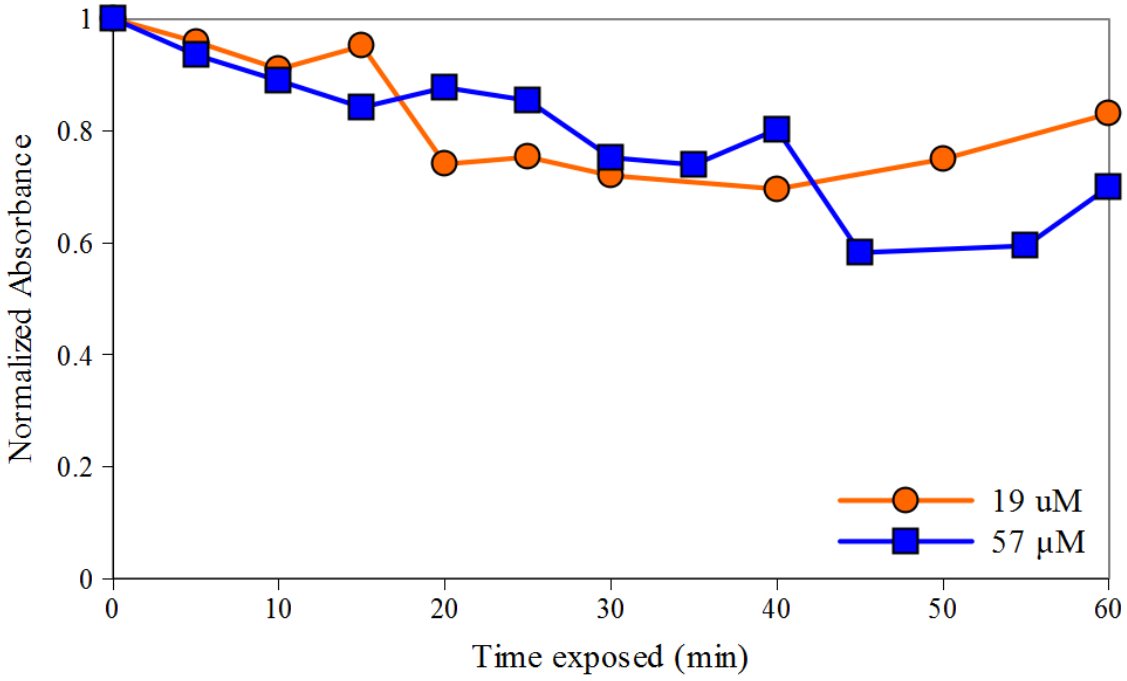

Figure 2.13: Beta-carotene decay curves for two concentrations of the formulation containing 1:33 oxybenzone.

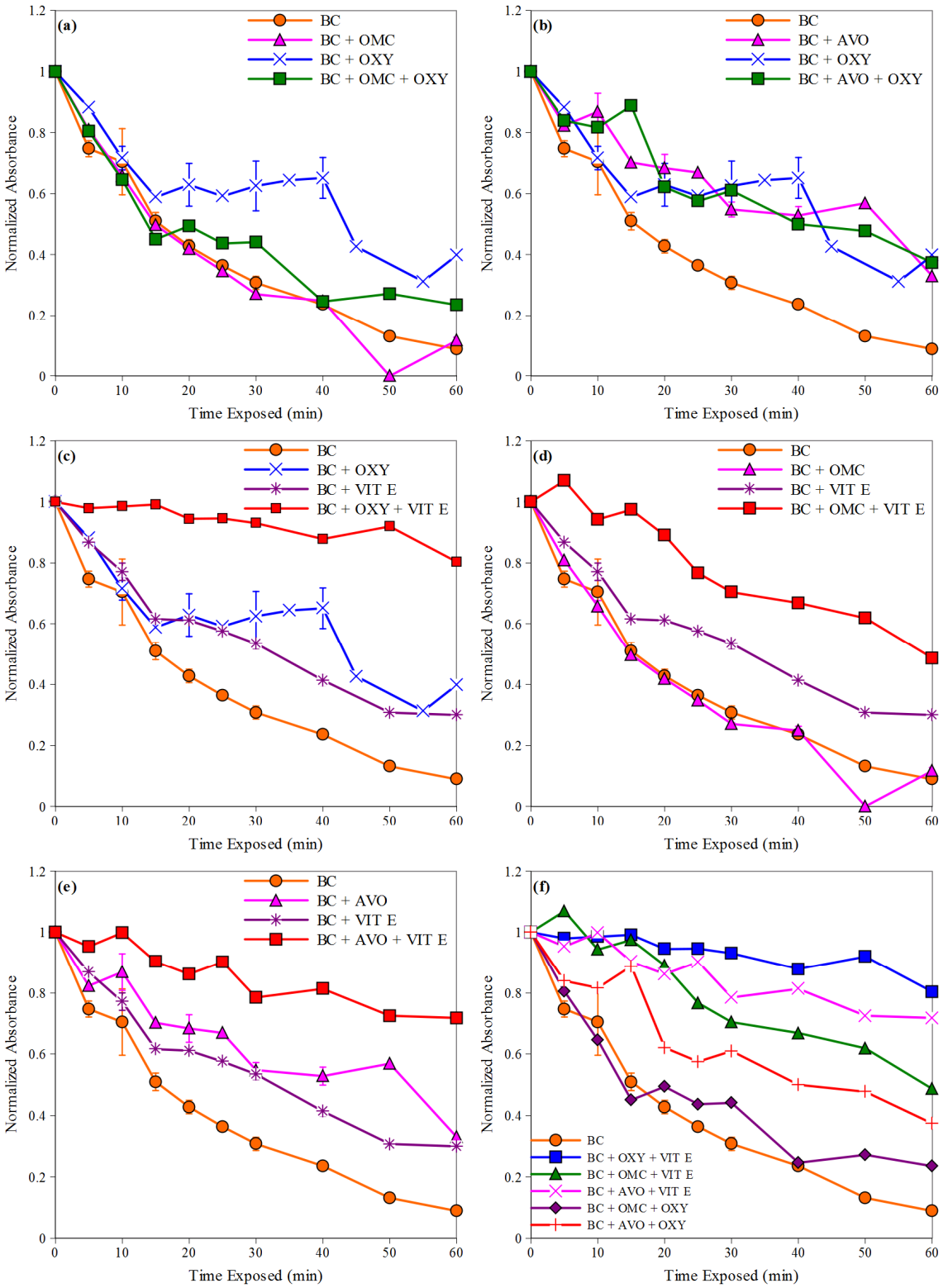

Figure 2.14: Beta-carotene (BC) decay profiles where two protectants are used, such as (a) OMC and oxybenzone (OXY), (b) avobenzone (AVO) and oxybenzone, (c) oxybenzone and vitamin E (VIT E), (d) OMC and vitamin E, (e) avobenzone and vitamin E, and (f) all concentrations.

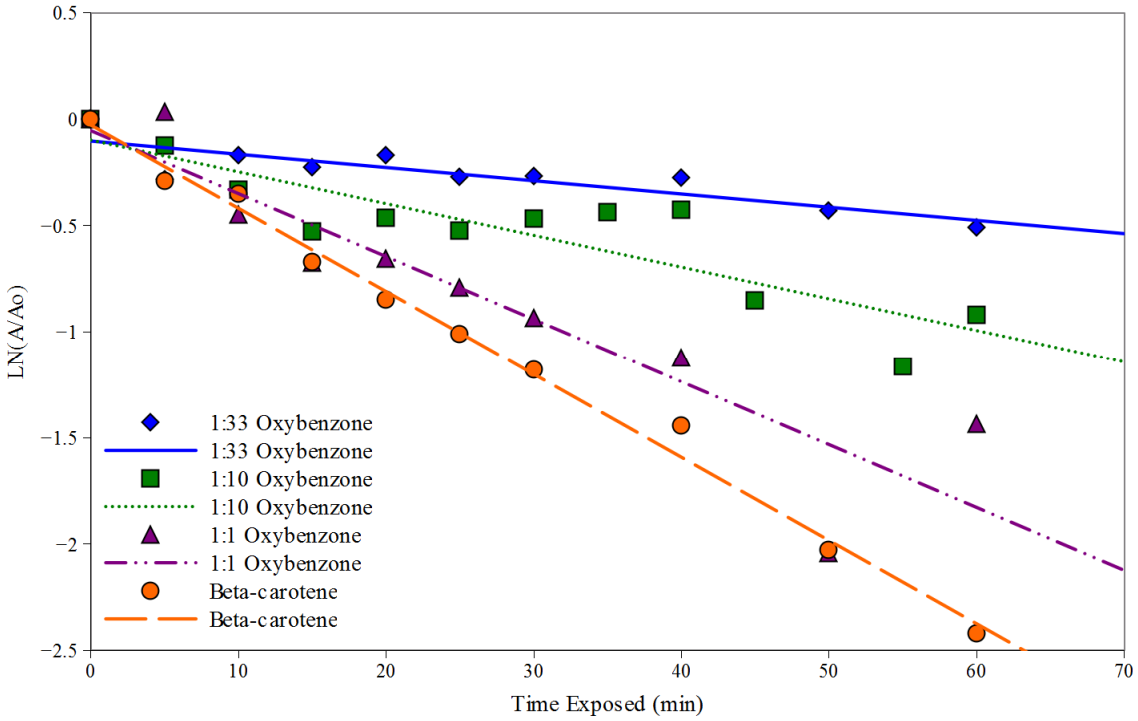

Figure 2.15: The natural log of the normalized absorbance plotted over time. The slopes of the fitted lines are equal to the rate constants of beta-carotene degradation.

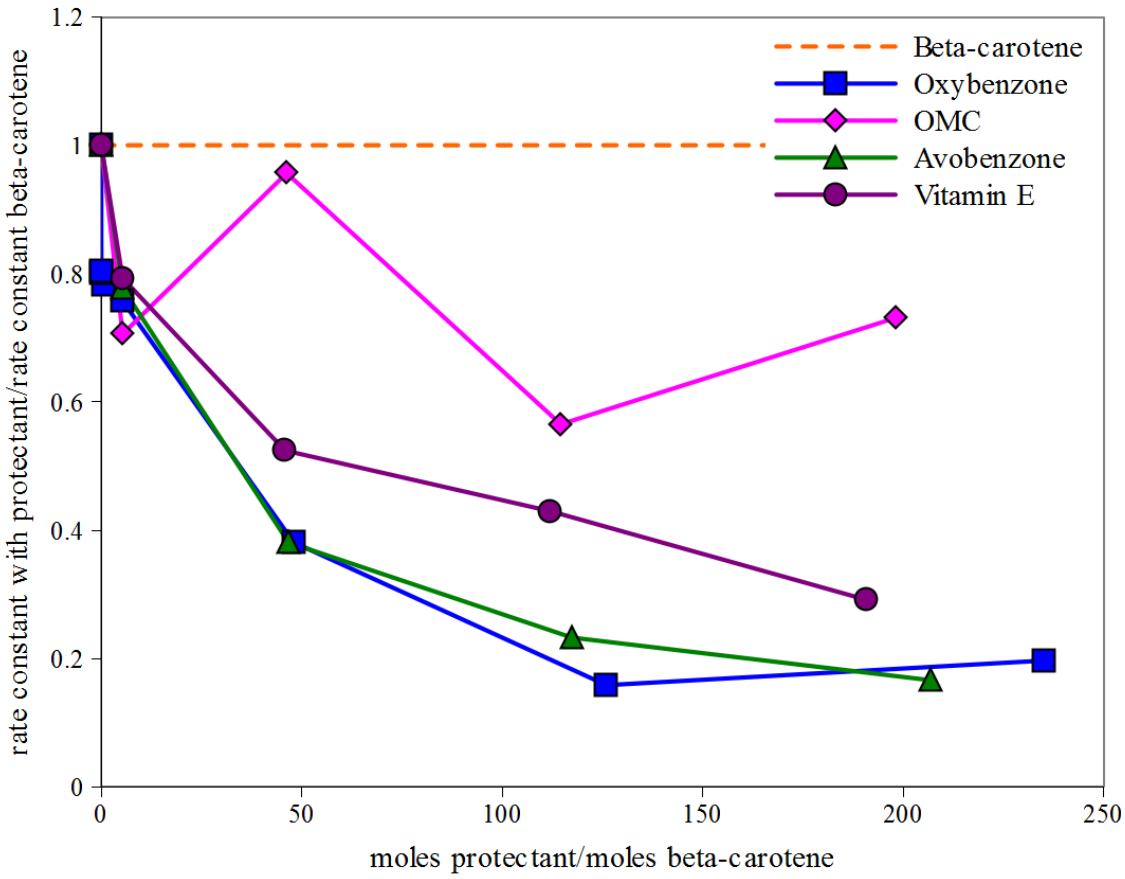

Figure 2.16: The ratio of the amount of protectant to the amount of beta-carotene in the particle formulation versus the ratio of rate constants when protectant is present to particles containing just beta-carotene.

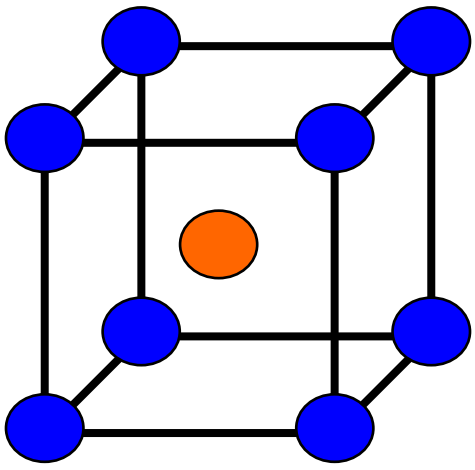

Figure 2.17: Schematic of the body-centered cubic unit cell used to approximate the proximity between a beta-carotene molecule (orange) and protectant molecules (blue).

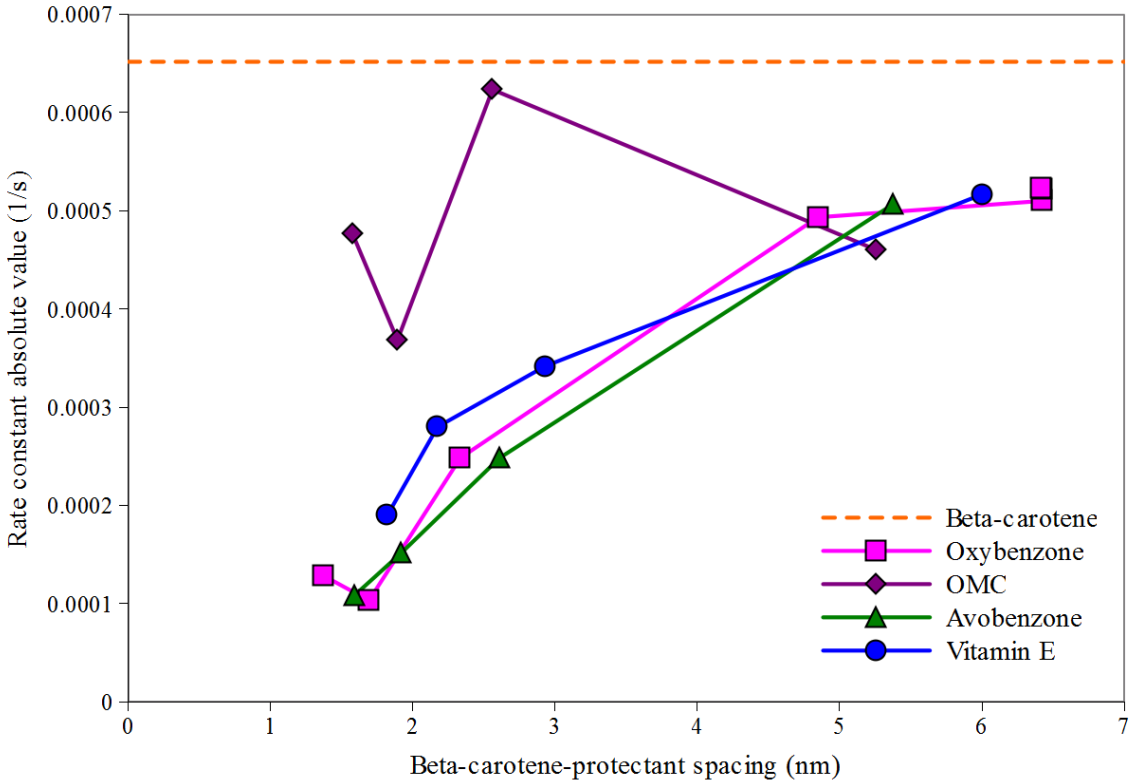

Figure 2.18: The relationship between the absolute value of the rate constant and the estimated spacing between a beta-carotene molecule and a protectant molecule.

2.8 Tables for Chapter 2

<table>
<tr><th colspan="3">Table 2.1: Protectant in uniform particle formulations</th></tr>
<tr><td colspan="3">Beta-carotene + PMMA particles (no absorber)</td></tr>
<tr><th colspan="3">Single protectants</th></tr>
<tr><th>Beta-carotene: protectant weight ratio</th><th colspan="2">Amount of protectant (grams)</th></tr>
<tr><td>1:1</td><td colspan="2">0.003</td></tr>
<tr><td>1:10</td><td colspan="2">0.03</td></tr>
<tr><td>1:33</td><td colspan="2">0.1</td></tr>
<tr><td>1:100</td><td colspan="2">0.3</td></tr>
<tr><th colspan="3">Combinations</th></tr>
<tr><th>Protectants</th><th>Beta-carotene : protectant weight ratio (total)</th><th>Amount of each protectant (grams)</th></tr>
<tr><td>Oxybenzone + OMC</td><td rowspan="5">1:20</td><td rowspan="5">0.03g</td></tr>
<tr><td>Oxybenzone + Avobenzone</td></tr>
<tr><td>Oxybenzone + Vitamin E</td></tr>
<tr><td>Vitamin E + OMC</td></tr>
<tr><td>Vitamin E + Avobenzone</td></tr>
</table>

Table 2.2 Uniform particle decay rate constants		
Material	**Beta-carotene : protectant weight ratio**	**Rate constant (s^{-1})**
Beta-carotene (solution)	1 : 0	-1.5E-03
Beta-carotene (encapsulated)	1 : 0	-6.5E-04
Oxybenzone	1 : 100	-1.0E-04
	1 : 33	-1.1E-04
	1 : 10	-2.3E-04
	1 : 1	-4.3E-04
	1 : 0.1	-5.5E-04
	1 : 0.033	-5.5E-04
OMC	1 : 100	-4.8E-04
	1 : 33	-3.7E-04
	1 : 10	-6.2E-04
	1 : 1	-4.6E-04
Avobenzone	1 : 100	-1.1E-04
	1 : 33	-1.5E-04
	1 : 10	-2.5E-04
	1 : 1	-5.1E-04
Vitamin E	1 : 100	-1.9E-04
	1 : 33	-2.8E-04
	1 : 10	-3.4E-04
	1 : 1	-5.2E-04
Combinations		
Oxybenzone + OMC	1 : 20	-3.9E-04
Oxybenzone + Avobenzone		-2.6E-04
Oxybenzone + Vitamin E		-5.2E-05
OMC + Vitamin E		-2.1E-04
Avobenzone + Vitamin E		-9.8E-05

Chapter 3 Synthesizing microparticle geometries

Proximity was studied in the previous chapter by changing the concentration of protectant in the particle and calculating an average distance between beta-carotene and protectant molecules. Core-shell particles allow separation of beta-carotene and protectant molecules by the core-shell interface, minimizing contact between the molecules. The process for creating the core-shell geometries was determined by multiple experimental designs varying parameters that could potentially affect the particle geometry. The products of the experimental designs were two core-shell particles, one with a solid core of polymer and beta-carotene, and the other encapsulating a suspension of uniform particles consisting of polymer and beta-carotene.

3.1 Double emulsion solvent evaporation method

The solvent evaporation method is a versatile technique to synthesize particles. The single emulsion method, commonly used to make uniform particles, was discussed in chapter 2. The most basic single emulsion technique can efficiently encapsulate hydrophobic materials, but hydrophilic materials have a tendency to migrate to the aqueous phase, resulting in poor encapsulation efficiency. A double emulsion method is used to make core-shell particles, commonly by using a water-in-oil-in-water (W/O/W) emulsion, resulting in microcapsules with an aqueous core. The double emulsion technique has versatility of its own, and has been used in a wide variety of studies.[50-52, 54, 56, 63]

The double emulsion solvent evaporation method is similar to its single emulsion counterpart except that it begins by the creation of a water-in-oil (W/O) emulsion, known as the primary emulsion. The water phase of the primary emulsion is known as the inner aqueous phase and will become the core of the particle. The oil phase must contain solvent as well as any materials that will make up the shell of the particle. The oil phase and inner aqueous phase are emulsified by a technique such as sonication to create the primary emulsion. The primary emulsion is then transferred to an outer aqueous phase. Similar to the aqueous phase in the single emulsion method, the outer aqueous phase is an aqueous solution containing a surfactant. The double emulsion is created by a lower shear mixing technique than the primary emulsion, using a method such as stirring on a magnetic stir plate. As with the single emulsion, the solvent in the oil phase migrates into the outer aqueous phase before evaporating, leaving behind particles with a solid shell and an aqueous core. A schematic of the process can be found in figure 3.1.

The addition of a second emulsion to the process creates more opportunities with which to fine-tune particles. The stability of the primary emulsion determines the geometry of the particles. Primary emulsion stability can be altered by the addition of surfactant to the inner aqueous phase, oil phase, or both. Three types of geometries are generally created: a core-shell structure, a multi-core structure, or a matrix structure. The core-shell structure is a microcapsule with a single core. The multi-core structure contains multiple cores. The matrix structure is made up of numerous small cores, causing the internal morphology of the particle to be porous. The geometry is dependent on which surfactant is used, the concentration of the surfactant, and which phase the surfactant is added to (inner aqueous phase, oil phase, or both).[104]

Encapsulation efficiency is an important characteristic of particles since the goal of synthesizing the particles is to encapsulate a material. As there are more variables in the double emulsion method, there are more factors that can affect encapsulation efficiency. As with the single emulsion method, increasing the molecular weight of the polymer used for encapsulation increases the encapsulation efficiency.[52, 105] Decreasing the volume of the inner aqueous phase while holding the oil phase volume constant also increases the encapsulation efficiency.[50, 105]

There are many physical characteristics of the particles that can also be controlled. As with the single emulsion method, increasing the stir speed during evaporation decreases the particle size.[54] Utilizing a solvent that is more miscible in water will increase the porosity of the particles since the solvent migrates to the outer aqueous phase so quickly as to leave behind pores.[63] The thickness of the shell can also be altered, either by changing the amount of polymer in the oil phase,[106, 107] or by changing the osmotic gradient through addition of sodium chloride to either the inner aqueous phase, outer aqueous phase, or both.[108]

There are many ways to alter the double emulsion solvent evaporation method in order to create core-shell particles with desired characteristics. This flexibility allows for different particle geometries to be made with few changes to the particle synthesis process. The similarity of the process to that of making uniform particles also means that the additional equipment required is minimal and the procedure only involves moderate changes, making the transition from a single emulsion to double emulsion process simple and economical.

3.2 Identifying key parameters

Two types of particle geometries were desired to study the proximity effect between beta-carotene and protectant molecules. The first geometry is a simple core-shell particle, except that both the core and shell will be comprised of polymer and the process must have selectivity of which compartment in which to place a hydrophobic material. The second geometry is a core-shell particle that contains uniform particles in the core. The problem with either geometry is that any solvent used to make the shell could potentially dissolve the contents of the core, causing a lack of selectivity between compartments, or a lack of geometry altogether. The particles were made with the double emulsion solvent evaporation method, but a design of experiments was necessary to determine which parameter values produce each type of geometry.

3.2.1 Particle synthesis

Particle geometries were synthesized using a W/O/W double emulsion solvent evaporation method, as discussed in the previous section. The inner aqueous phase consisted of a concentrated suspension of uniform particles, such as those studied in chapter 2. The only change to the procedure was to use dichloromethane (DCM) as the solvent instead of toluene. Dichloromethane decreases the time needed to synthesize a batch of particles, as well as creates larger particles that can be more easily distinguished with an optical microscope. The concentration of the suspension was approximately 2.2

mM beta-carotene. The particles contained only polymer and beta-carotene, no UV absorbers or antioxidants. The volume of the inner aqueous phase was varied.

The oil phase consisted of 0.2 g of polymer, 10 ml of solvent, and a varied amount of the surfactant Span 80. The oil phase was devoid of any other additive to make the shell of the particles as transparent as possible in order to best distinguish the particle geometry. A volume of the inner aqueous phase was added to a vial of the oil phase and the opening of the vial was covered with Parafilm. The Parafilm was pierced with the sonicator tip and the mixture sonicated until the primary emulsion was formed. The primary emulsion was poured into the outer aqueous phase, consisting of a 0.5% aqueous solution of poly(vinyl alcohol). The secondary emulsion was created by stirring the mixture with a magnetic stir rod at approximately 225 rpm until the solvent had completely evaporated. The evaporation step required four hours for dichloromethane and 24 hours for toluene. Particles were collected by centrifuging at 2000 rpm for 10 minutes. The supernatant was disposed of and the particles resuspended in deionized water.

Particles were analyzed using an optical microscope (Celestron 44350 LCD Digital LDM Biological Microscope). The images were compared to determine visually which produced the desired geometries. One formulation was chosen to create the core-shell particles with a solid core, and another formulation to create particles whose core consisted of a suspension of uniform polymer particles.

3.2.2 Particle characterization design of experiments

In order to find an optimum formulation for creating the particle geometries, a design of experiments was created varying any parameters that could affect the particle geometry. Five parameters were chosen to study at two levels, as shown in table 3.1. A full factorial design was implemented, resulting in 32 particle formulations, as displayed in table 3.2. The experiments were completed in a random order, as shown by the run number in table 3.2. Images of the particles were taken using an optical microscope and the geometry analyzed visually.

The first parameter chosen was solvent, and the two levels were toluene and dichloromethane. Solvent miscibility determines how much of the solvent will enter the inner aqueous phase in the time it takes to synthesize the particles. The solubility of both molecular weights of PMMA in the solvent influence whether or not the particles in the inner aqueous phase will be dissolved by solvent that migrates first to the core rather than to the outer aqueous phase. The combination of these two properties will determine whether the uniform particles present in the inner aqueous phase will remain particles or fuse together as a solid mass.

The molecular weight of the polymer used to create the shell can also impact particle geometry. As mentioned in the previous section, it has been shown in the literature that a higher molecular weight of polymer used for the shell results in higher encapsulation efficiency.[52, 105] This change in encapsulation efficiency will determine whether the particles present in the inner aqueous phase suspension will stay

encapsulated. The inner aqueous phase volume was another parameter that has been shown to influence encapsulation efficiency.[105]

The molecular weight of polymer used to create the particles in the inner aqueous phase combined with the solvent determined the nature of the core of the particles. The lower molecular weight of PMMA was dissolved easier in both solvents than the higher molecular weight, therefore if the solvent migrated to the core of the particles it may dissolve the particles leaving behind a solid mass. Particles made of the higher molecular weight polymer may be more resistant to dissolution from the small amount of solvent that would enter the core.

The concentration of surfactant in the oil phase can determine the particle geometry.[104] Altering the amount of surfactant in the oil phase can change the stability of the primary emulsion. An increased stability by the addition of surfactant may limit the amount of solvent entering the inner aqueous phase, determining whether the core of the final particle contains uniform particles or a solid mass. The concentration of surfactant can also influence whether the particle will contain multiple cores, or one large core.

The experimental design implemented was a full factorial. Using the design of experiments not only can the effect of each parameter be determined, but the effect of interactions between the parameters. For example, both the solvent used and the molecular weight of the polymer particles in the inner aqueous phase will determine whether or not the particles become dissolved during the particle synthesis process. The result of this study will be two formulations, one for a core-shell particle with a solid core, and another for a core-shell particle whose core is a suspension of uniform particles.

Further experimental designs were created around the resulting formulations to determine the best process for making each type of particle.

3.2.3 Particle geometry results

Optical microscope images were taken and compared to determine which formulation offered the most promise for each particle geometry. The solid core formulation was chosen as the particles best displaying a solid core with no discernible individual uniform particles and a clear boundary between the orange core and clear polymer shell. The formulation with uniform particles in the core was chosen as a particle with discernible particles in the core and a clear shell, so that no beta-carotene leached from the core particles to the shell. While the goal of the design of experiments was to find a beginning formulation for each particle geometry, it also gave insight as to the effect of changing each parameter, reaffirming some of the points made in the previous section. Figures 3.2-3.7 are comparisons of formulations where only one parameter is changed, and the formulation details for each figure can be found in table 3.3.

Varying the solvent altered the particle geometry drastically, as seen in figure 3.2. Figure 3.2a shows particles made with toluene, and the large particle in focus has many obvious uniform particles encapsulated inside. Even the smaller particles in figure 3.2b look to have uniform particles inside of them, although they seem to display more of a multi-core geometry than the single-core particle. Figure 3.2b is an image of particles made with dichloromethane, but otherwise the same formulation as the particles in figure 3.2a. The dichloromethane particles appear to have a dense solid core, and no individual

uniform particles can be discerned. Dichloromethane is more miscible in water than toluene, so it is more likely that some solvent entered the core. Also, it was noted during synthesis that dichloromethane dissolves PMMA much faster than toluene, so even limited time in the core could dissolve the uniform particles.

The molecular weight of PMMA used to make particles comprising the inner aqueous phase suspension determines the ease with which the particles are dissolved if solvent enters the core. Figure 3.3a shows particles made with a low molecular weight PMMA for the core, and 3.3b uses a higher molecular weight of polymer for the core particles. The high molecular weight case shows obvious particles present in the core, while the low molecular weight case shows a distribution of beta-carotene throughout the particle. The particles in 3.3a have a grainy appearance, so it is possible that some particles are intact in the core, but the distribution of orange throughout the particle suggests that at least some particles were dissolved during particle synthesis. Figure 3.3 shows the significance that the molecular weight of PMMA comprising the uniform particles used in the core plays in the resulting particle geometry.

The molecular weight of polymer used to create the shell of particles using W/O/W emulsion solvent evaporation method has been shown to affect the encapsulation efficiency.[52, 105] Figure 3.4a shows particles whose shell was made of low molecular weight PMMA, while figure 3.4b is particles with a high molecular weight PMMA shell. The particles with the high molecular weight shell are intact while particles with the low molecular weight shell did not form completely, as uniform particles and pieces of polymer are scattered throughout the image. Figure 3.4 confirms what was found in previous studies.

The internal aqueous phase volume has been shown to affect encapsulation efficiency.[50, 105] Figure 3.5a shows particles synthesized using 200 µl of suspension for the inner aqueous phase, while figure 3.5b displays particles made using 600 µl. Figure 3.5a shows particles that are very obviously encapsulated. Some particles look encapsulated in figure 3.5b, as there are individual orange spheres present in some of the particles, but there are also clear spheres that are most likely large pores or cores that are devoid of particles. Figure 3.5 shows that the smaller inner aqueous phase volume, 200 µl, did in fact encapsulate better than the larger volume, 600 µl.

The amount of surfactant and compartment in which it is added can determine particle geometry.[104] Figure 3.6a shows particles made without any surfactant, and figure 3.6b displays particles made with 3% Span 80 in the oil phase. The amount of Span 80 used was with respect to the mass of the shell components, not including the solvent. The particles created without surfactant appear to be uniform, with the entire particle being an orange color and few, if any, uniform particles present. This is in contrast to the particles in figure 3.6b, which have a clear core and shell. Figure 3.6 displays the importance of adding a surfactant to the oil phase of the formulation.

Since the data is analyzed visually it is difficult to note any interactions between the parameters. One interaction that is apparent is that between solvent and the molecular weight of polymer used for the uniform particles in the core. A grid of images to examine this interaction is shown in figure 3.7. The lower molecular weight PMMA (15000) is generally easier to dissolve and DCM dissolves the polymer faster than toluene. To make the particles containing uniform particles, a solvent must minimally migrate to the core and not be able to dissolve the polymer, while the polymer must have a high enough

molecular weight to be difficult to dissolve. When toluene is paired with the uniform particles of low molecular weight (figure 3.7a) it is obvious that some dissolution has taken place since some particles are completely orange, but there is still some trace of the uniform particles. When toluene is paired with the high molecular weight PMMA (figure 3.7b), the polymer that is more difficult to dissolve is paired with a solvent that takes a long time to dissolve the polymer and is mostly immiscible with water, resulting in encapsulated uniform particles that are intact. Opposite conditions are needed to create the particles with solid cores, the polymer needs to be easily dissolved and solvent needs to be more miscible with water in order to enter the core in a higher quantity. Figure 3.7c displays both of these qualities, using DCM and the lower molecular weight PMMA. Figure 3.7d uses the higher molecular weight PMMA with DCM, and it's apparent that the high molecular weight particles don't dissolve as well since the cores look less uniform and more like an agglomeration of particles. From these observations, figure 3.7 shows the importance of the interaction between the solvent and the molecular weight of polymer in the core.

The formulations chosen for both particle geometries can be found in figure 3.8, with the specifics in table 3.3. Both geometries had the best results when using surfactant in the oil phase, a smaller inner aqueous phase volume (200 μl), and the higher molecular weight PMMA for the shell. These values are not surprising since the addition of surfactant increases the stability of the primary emulsion, and the lower inner aqueous phase volume and higher molecular weight polymer for the shell both should yield higher encapsulation efficiency. Based on the above analysis of the solvent and polymer molecular weight in the core, it isn't surprising that DCM and PMMA with a molecular

weight of 15000 yielded the particles with a solid core while the toluene and PMMA with a molecular weight of 120000 resulted in particles that encapsulated uniform particles. These two formulations were used to create further experimental designs to optimize the parameter values for each geometry.

3.3 Particle optimization experimental designs

The results of the previous section succeeded in identifying a formulation for each particle geometry as well as determining which parameters must adhere to the values found and which can be altered in order to optimize the particle synthesis. The solvent and the molecular weight of the polymer in both the core and shell must stay consistent with the formulations found from the previous studies as it was apparent from figures 3.2-3.4 that these parameters determined the particle geometry.

Figure 3.5 showed that particles were encapsulated with an inner aqueous phase of either 200 μl or 600 μl, but encapsulation was much better with 200 μl. The drastic difference found in the particles when changing the inner aqueous phase volume by 400 μl made it a prime candidate for optimization. The inner aqueous phase volume was studied at three levels: 100 μl, 200 μl, and 300 μl. It can be determined from figure 3.6 that the addition of surfactant is necessary in creating the particle geometries, but the amount can be optimized. Two surfactant amounts were chosen for study, the 3% used in the previous study and 5%. The amount of surfactant used is in relation to the mass of the particle shell without taking into account the solvent mass. One additional parameter, amount of polymer, was added to the optimization studies in order to find whether it

could add to the core-shell contrast of the particle geometries. Polymer amount was studied at three levels: 0.2 g (as in the previous studies), 0.25 g, and 0.3 g.

A factorial design was created around the formulations in figure 3.8. As discussed, three parameters were chosen for study: polymer amount at three levels, inner aqueous phase volume at three levels, and surfactant amount at two levels. The experimental designs can be found in tables 3.4 for particles with solid cores and 3.5 for particles encapsulating uniform particles. Particle synthesis is the same W/O/W double emulsion solvent evaporation method procedure as that used for the previous section. The experiments were completed in a random order and the particles analyzed by optical microscope images.

3.3.1 Particles with a solid core

The aim of the experimental design in table 3.4 was to optimize the formulation found in section 3.2 for particles with a solid core. As in section 3.2, the data must be analyzed visually by comparing optical microscope images. Since the design of experiments is based on a formulation that attained the particle geometry, the aim of this design is to choose the formulation with the best contrast between the core and shell that has a core where no individual uniform particles are discernible. Table 3.6 contains the formulation details for figures 3.9-3.12, which will be used to compare the impact of the polymer amount, inner aqueous phase volume, and surfactant amount on the structure of the particles, respectively.

A visual analysis of the effect of the amount of polymer used to create the shell can be found in figure 3.9. The particles in figure 3.9a were made using 0.2 g of PMMA for the shell, and no clear core-shell boundary is present. The uniform particles used to create the core seemed to diffuse into the shell slightly before solidifying. Figure 3.9b displays particles made with 0.25 g of PMMA for the shell, and the particles have a clear boundary and the cores appear dense with no distinct individual particles. Figure 3.9c shows particles made with 0.3 g of polymer. While the core-shell boundaries in figure 3.9c are obvious, the boundaries are not smooth, as though uniform particles in the core were not completely dissolved before the solvent exited the particle. The differences between the three formulations could be a result of the increased viscosity of the oil phase when the polymer amount is increased. From the observations made from figure 3.9, the ideal amount of polymer to make the shell of the particles with solid cores would be 0.25 g of PMMA with a molecular weight of 120000.

It was determined in the previous section that the inner aqueous phase volume would have an impact on the particle structure. Figures 3.10a, b, and c compare three particle formulations made using 100, 200, and 300 µl for the inner aqueous phase, respectively. The smallest inner aqueous phase volume, 100 µl shown in figure 3.10a, creates particles with the sharpest core-shell contrast and a core devoid of individual particles. As the inner aqueous phase volume is increased in figures 3.10b and c, the core-shell contrast becomes increasingly less distinct and the shell takes on more of an orange color, suggesting that more beta-carotene is leaching into the shell. Figure 3.10c even shows some particles that are misshapen or split open, most likely due to an inner aqueous phase volume that was too large.

Results from the previous section demonstrated the dependence of particle structure on whether or surfactant was present in the oil phase. It had been established that the particle geometries required the surfactant, so an aim of this design of experiments was to determine how much surfactant would be ideal. Figures 3.11a and b used 3% and 5% surfactant, respectively. Both formulations displayed a clear core-shell boundary with no individual particles in the core. Since a similar outcome was observed in both cases, 3% was chosen as the ideal case in order to minimize additives.

After visual analysis of all images produced by the design of experiments in table 3.4, the formulation chosen for core-shell particles with a solid core used 0.25 g of PMMA, an inner aqueous phase volume of 100 μl, and a surfactant concentration of 3%. Particles have an average diameter of 100 micrometers as determined by an analysis of 25 particles using ImageJ. Figure 3.12 shows the particles at two different magnifications. Figure 3.12a displays the overall structure of the particles, while figure 3.12b is a higher magnification image to confirm that the core is solid and contains no individual uniform particles. While the cores of the particles were created using an aqueous suspension of uniform particles, it appears in the images that the water from the inner aqueous phase was expelled from the particles during synthesis. A proposed schematic of the particle synthesis process occurring during the final evaporation step is outlined in figure 3.13. Dichloromethane is slightly soluble in water, so some of the solvent from the oil phase must migrate to the inner aqueous phase. Once in contact with the uniform particles, the DCM dissolves the particles before exiting the core, leaving behind a solid core of uniform particles that are fused together. The water from the inner aqueous phase most likely exits the particle either with the DCM, or through pores in the

shell. Solvents miscible with water have a tendency to create porous particles,[63] so it would be possible for water to exit the particle through the shell even after the shell has formed.

3.3.2 Particles with uniform particles in the core

The optimization experimental design for the particles with uniform particles in the core can be found in table 3.5. The method of analysis was again visual examination of optical microscope images. As for the core-shell particles with solid cores, the effect of polymer amount, inner aqueous phase volume, and surfactant amount was studied and the result was a formulation to be used in studies discussed in subsequent chapters. The three parameters were analyzed by visual comparison of microscope images, and the formulations for the images in figures 3.14-3.16 can be found in table 3.7. The characteristics required of the particles were a clear shell and identifiable particles in the core.

The effect of polymer amount is illustrated in figure 3.14. The polymer amounts used were 0.2 g, 0.25 g, and 0.3 g which correspond to figures 3.14a, b, and c, respectively. In figure 3.14a, it appears that some particles were encapsulated, but the amount of particles contained in the core is small, and most of the particles don't show the core clearly. As the amount of polymer is increased, in figure 3.14b there are more particles with obvious particles in the core. Most of the particles probably have multiple cores, assumed due to the grainy nature in the image, but they do appear to have encapsulated uniform particles. As polymer amount is further increased to 0.3 g in figure

3.14c, there are more particles that show individual uniform particles encapsulated inside. Two particles in the center of the image show a cluster of orange uniform particles in the center of a clear polymer particle. Other particles have the grainy nature similar to the particles in figure 3.14b, seeming to have encapsulated uniform particles, but in multiple cores. An explanation for this behavior could be that since there is more material available to form the shell, more particles are able to be encapsulated.

The inner aqueous phase volume has been shown to affect encapsulation efficiency,[50, 105] but since the inner aqueous phase consists of a suspension of particles, the volume also dictates the amount of particles present to be incorporated into the particle core. Figures 3.15a, b, and c show the effect of the inner aqueous phase volume on particles encapsulating uniform particles as the inner aqueous phase is increased from 100 µl to 300 µl. In figure 3.15a, where the inner aqueous phase volume is 100 µl, there are some orange uniform particles encapsulated within the particles, but only a few particles are noticeable in each core. As the inner aqueous phase volume is increased to 200 µl in figure 3.15b, the increase in particles is shown by the amount present in the core. The inner aqueous phase volume was further increased to 300 µl in figure 3.15c, but this increase proved to be too large of a volume. Particles in figure 3.15c have an orange color, as though beta-carotene has leached from the core, and many uniform particles that aren't encapsulated are scattered about. Figure 3.15 shows that the idea inner aqueous phase volume for the current formulation of particles with a particle core is 200 µl.

Since the design of experiments in section 3.2 determined that the addition of a surfactant is a necessity, the amount of surfactant was increased to find an optimal

amount. Figure 3.16a uses 3% surfactant while figure 3.16b uses 5%. The increase in surfactant seemed to change the particle morphology from one of a single core, to that of a particle with multiple cores. Since a single core is preferable, 3% was chosen as the ideal amount of surfactant.

The formulation chosen to create particles containing uniform particles in the core can be seen in figure 3.16a. In the center of the image are particles with a transparent shell and a core containing orange uniform particles. The formulation resulting in these particles uses 0.3 g PMMA, 200 μl for the inner aqueous phase, and 3% surfactant in the oil phase. While it isn't clear from the image, it is likely that water is present in the core of the particles since toluene is not miscible with water and creates particles without pores. The average diameter for the particles is 50 micrometers as determined by an image analysis using ImageJ. These particles are further used in the next chapter to study the effect of proximity and particle geometry on UV protection.

3.4 Controlling shell thickness

One of the particle attributes that can be easily manipulated in the W/O/W solvent evaporation method is the particle shell thickness. Methods of controlling shell thickness have been reported in the literature. Altering the osmotic gradient of the system by the addition of sodium chloride to the inner aqueous phase, outer aqueous phase, or both, can affect shell thickness by causing swelling of the particles.[108] The amount of polymer used to create the shell also affects the thickness of the particle shell,[106, 107] which is the method that has been used in this study.

To confirm that what has been found in previous studies holds true in the current system, the polymer amount was varied for the particles with a solid core. These were chosen over the particles with uniform particles in the core because DCM can dissolve much more PMMA than toluene can. The polymer amount was varied from 0.15 g to 0.50 g. The shell thickness was determined by analyzing ten particles from each formulation. The diameter of the entire particle was measured, as was the diameter of the particle core, allowing the shell thickness to be calculated. The ratio of the shell thickness to the size of the particle was found for comparison in order to account for the particle size in relation to the shell size.

A visual comparison of particles synthesized using 0.175 g and 0.500 g of PMMA is shown in figure 3.17. The change in shell thickness is obvious; although it also appears that the core-shell boundary is affected. The smaller polymer amount, 0.175 g in figure 3.17a, produces a dense core with a crisp core-shell boundary. The larger polymer amount, 0.500 g in figure 3.17b, produced a particle with a definite core, but there appears to be some migration of beta-carotene between the shell and core at the boundary. This migration may be a result of the larger distance the solvent must travel in order to exit the particle, or the increased viscosity of the oil phase from the addition of more polymer.

A comparison of the average shell thickness:particle radius ratio for all of formulations examined is displayed in figure 3.18. There is a clear increase in the shell thickness:particle radius ratio as the amount of polymer in the formulation is increased. This supports what has been found in literature,[106, 107] and proves that the shell thickness can be controlled in the current system.

3.5 Synthesizing microparticle geometries conclusions

The aim of this chapter was to discover formulations to create two geometries of particles. The first geometry was a core-shell particle with a solid core, where both the core and shell are comprised mostly of polymer and selectivity between the compartments is possible when including an additive. The second geometry was a particle with a solid shell of polymer encapsulating an aqueous suspension of polymer particles, with the same selectivity requirements as the previous particles. An initial design of experiments was created to determine the parameters that affect particle geometry, as well as to gain primary formulations for the particle geometries. Additional designs of experiments were created around each particle geometry to fine-tune the desired attributes.

It was established that the solvent and the molecular weight of the polymer used in both the core and shell impacted the resulting particle geometry. The molecular weight of PMMA used to create the shell of the particles determined the encapsulation efficiency, the higher molecular weight (120000) creating particles with more substance in the core. The interaction between the solvent and the molecular weight of polymer used to create the uniform particles in the inner aqueous phase determined the geometry. Toluene used with uniform particles with PMMA of a molecular weight of 120000 produced particles with uniform particles in the core, while dichloromethane using uniform particles of PMMA with a molecular weight of 15000 created particles with a solid core. The combination of the ease with which DCM can dissolve the low molecular

weight particles and the slight miscibility with water resulted in the solid core, while the immiscibility of toluene and its difficulty in dissolving high molecular weight polymer particles allowed particles to remain intact in the core.

Two additional designs of experiments were created to fine-tune the formulations resulting from the previous design of experiments. The inner aqueous phase volume was varied at three levels, the surfactant concentration at two levels, and an additional parameter of polymer amount was added and varied at three levels. Each design resulted in a formulation for a particle geometry. The particles with a solid core were created using dichloromethane, 0.25 g of PMMA with a molecular weight of 120000 for the shell, 3% surfactant, and 100 µl of inner aqueous phase consisting of uniform particles of PMMA with a molecular weight of 15000. The particles encapsulating a suspension of uniform particles were created using toluene, 0.3 g of PMMA with a molecular weight of 120000 for the shell, 3% surfactant, and 200 µl of inner aqueous phase consisting of uniform particles of PMMA with a molecular weight of 120000.

In addition to forming the geometries, it was desired to have the capability of controlling the thickness of the shell of the particles. The particles with a solid core were chosen to study since DCM more easily dissolves PMMA. The shell thickness was varied by changing the amount of polymer in the oil phase using amounts between 0.15 g to 0.5 g. A near linear increase was observed when increasing the polymer amount.

The initial design of experiments resulted in an understanding of which parameters influence the particle geometry, as well as gaining formulations for each particle geometry desired. The fine-tuning designs resulted in final formulations for each geometry that will be used in studies in the subsequent chapters. The method of varying

the shell thickness of the particles by altering the polymer amount in the oil phase was also verified. The resulting particles were used in the studies in chapter 4 to examine the effect of particle geometry on UV protection, as well as the proximity between beta-carotene and protectants.

3.6 Figures for Chapter 3

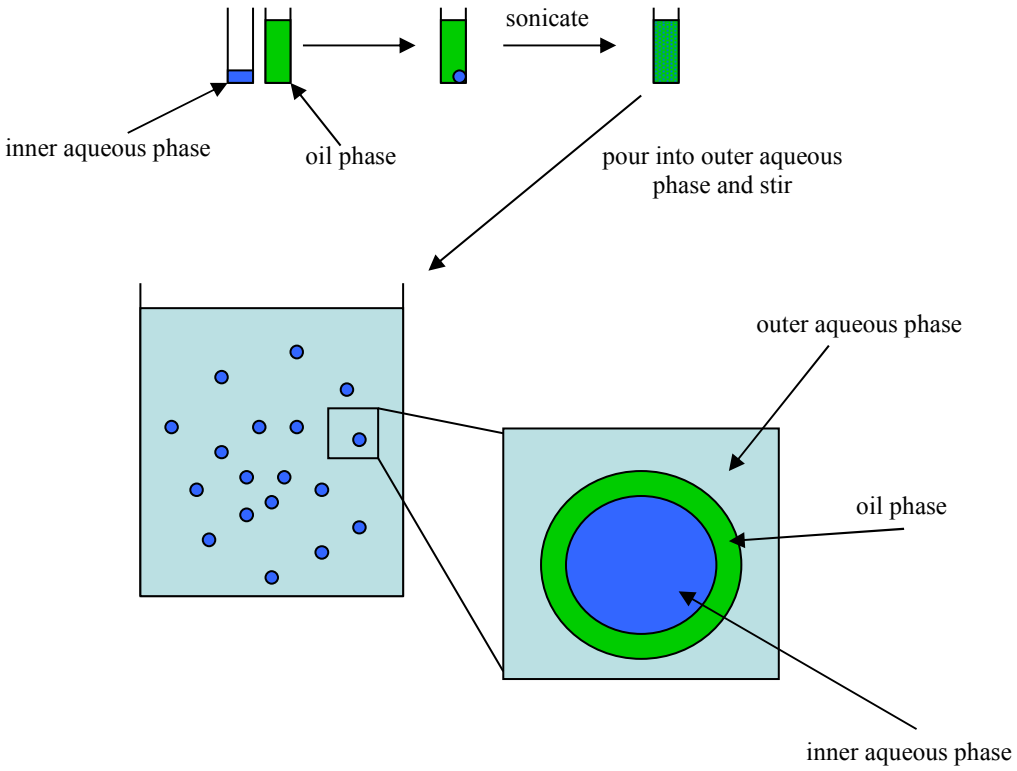

Figure 3.1: Schematic of the W/O/W double emulsion solvent evaporation method.

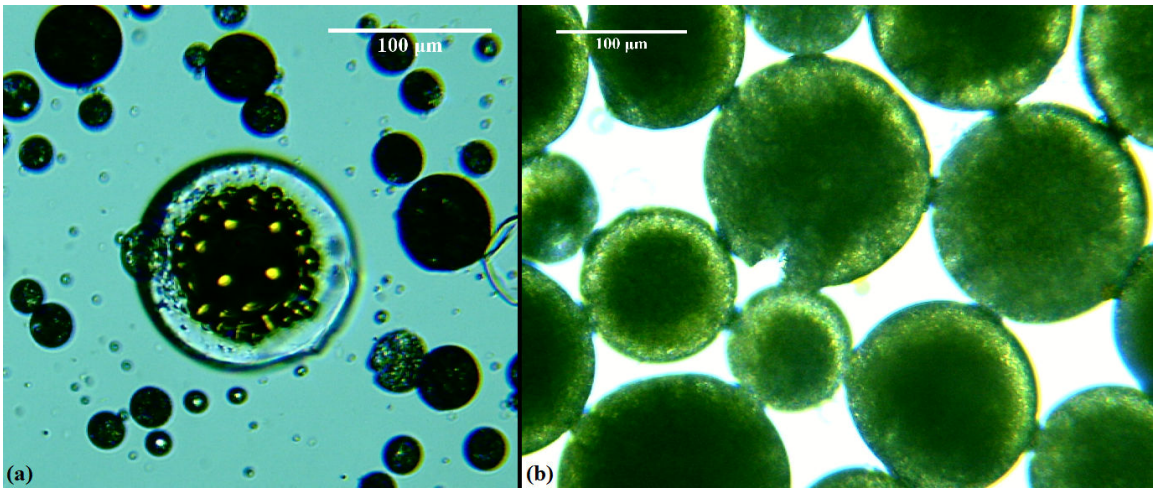

Figure 3.2: Particles made with (a) toluene and (b) dichloromethane to distinguish the effect of the solvent. Formulation details can be found in table 3.3.

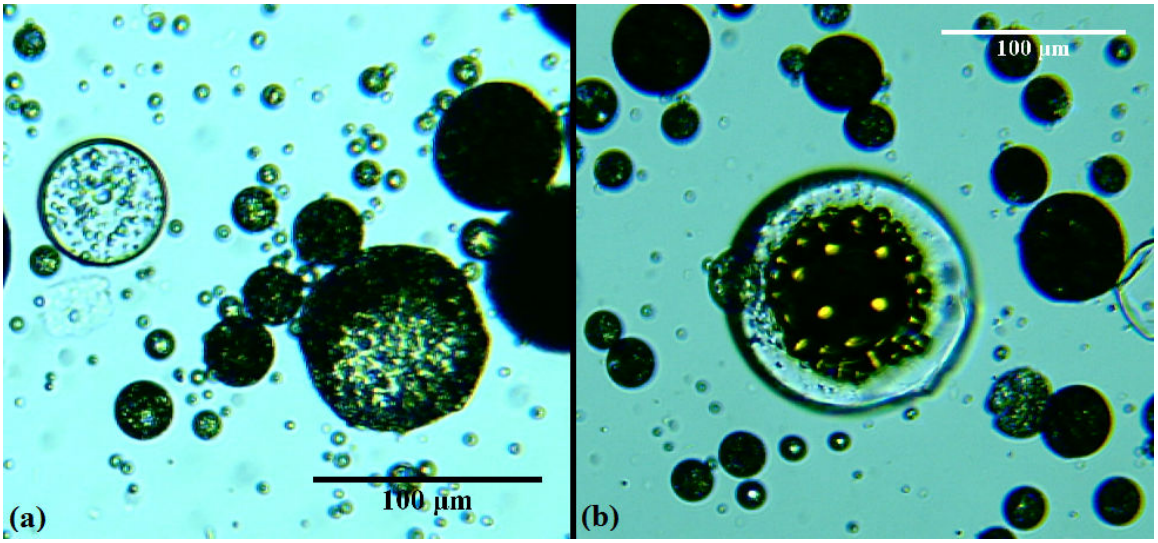

Figure 3.3: Particles made with an inner aqueous phase made up of a suspension of uniform particles comprised of PMMA with a molecular weight of (a) 15000 and (b) 120000 to determine the effect of polymer molecular weight in the core. Remaining formulation details are in table 3.3.

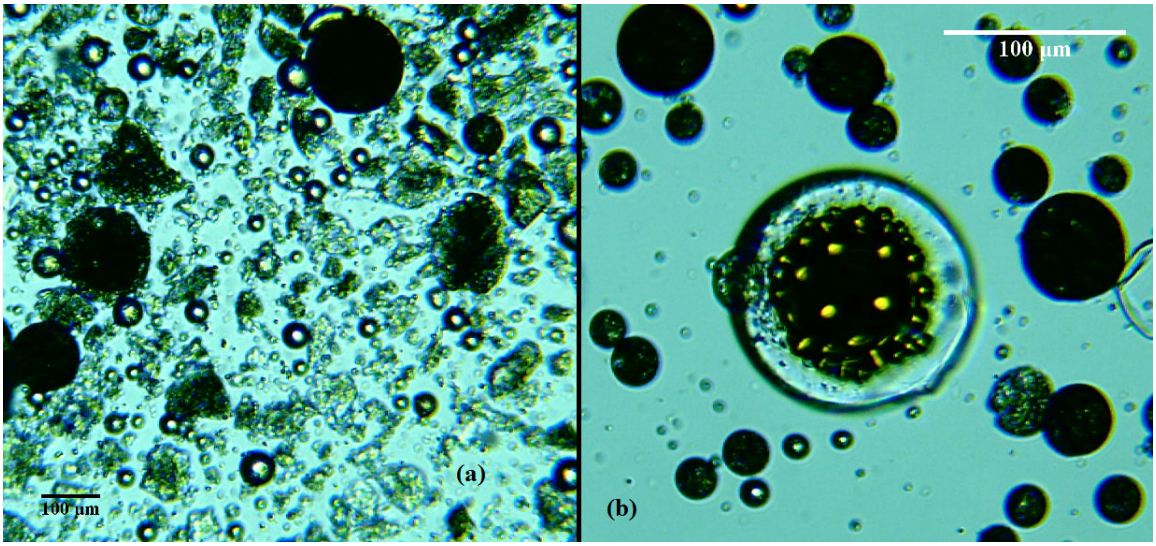

Figure 3.4: Particles made with PMMA with a molecular weight of (a) 15000 and (b) 120000 for the shell in order to observe the effect of polymer molecular weight in the shell. Additional formulation details can be found in table 3.3.

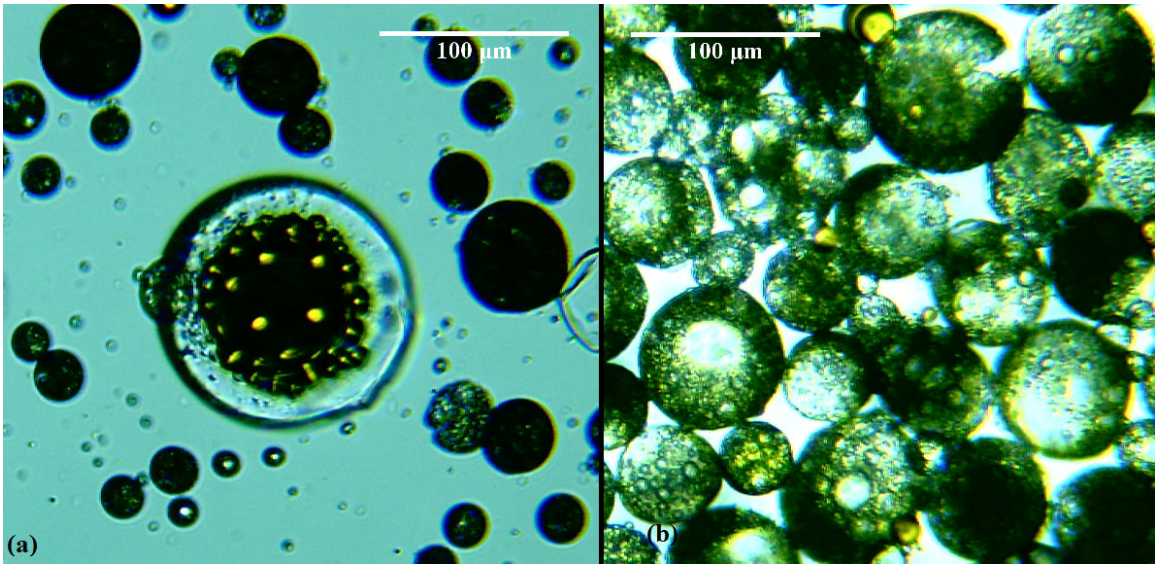

Figure 3.5: Particles made with an inner aqueous phase volume of (a) 200 µl and (b) 600 µl to determine the effect of inner aqueous phase volume on the particle geometry. More details on the formulations can be found in table 3.3.

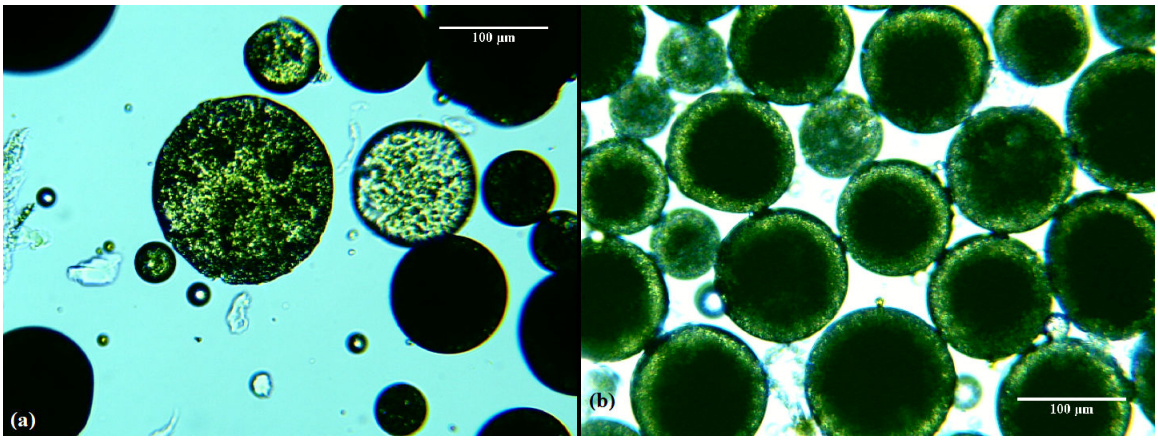

Figure 3.6: Particles made with (a) 0% and (b) 3% surfactant in the oil phase to observe whether the addition of a surfactant aided in creation of the particle geometry. Remaining formulation details are in table 3.3.

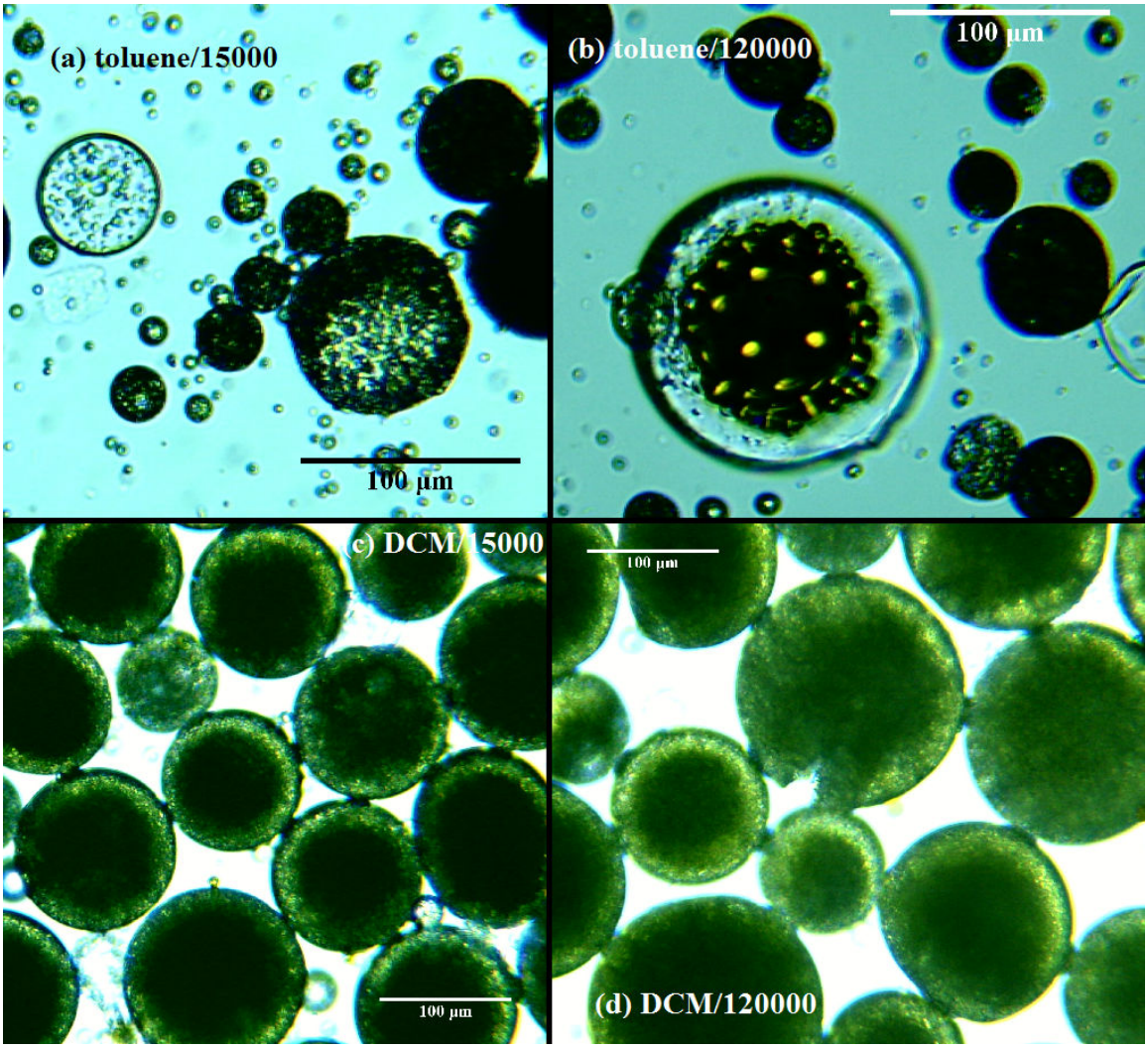

Figure 3.7: A graphical comparison of four formulations (detailed in table 3.3) to demonstrate the interaction effect between solvent and the molecular weight of PMMA of the uniform particles used in the core.

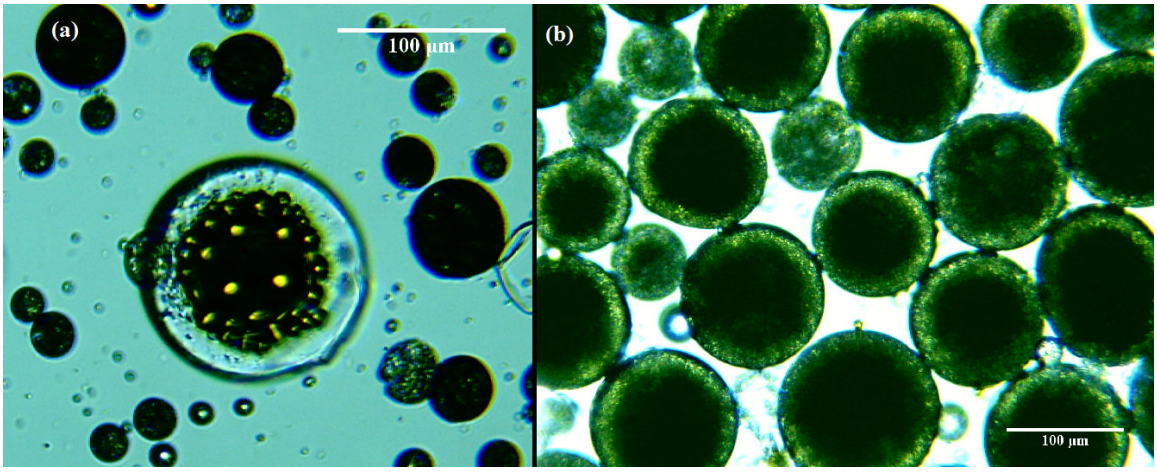

Figure 3.8: Particles displaying the formulations chosen for further study for the particles with (a) particles in the core and (b) a solid core. Formulation details can be found in table 3.3.

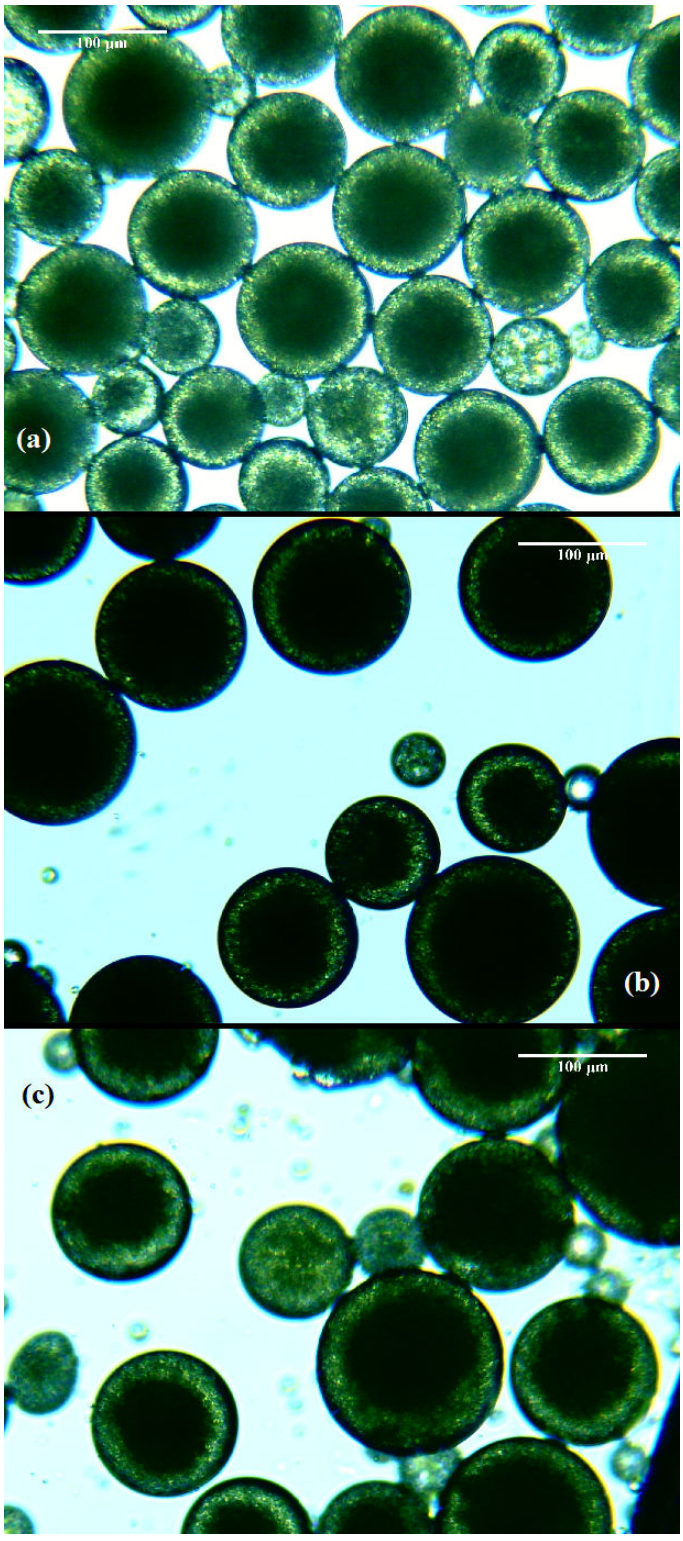

Figure 3.9: Particles with a solid core made with (a) 0.2 g, (b) 0.25 g, and (c) 0.3 g of PMMA to determine the effect of polymer amount. Formulations detailed in table 3.6.

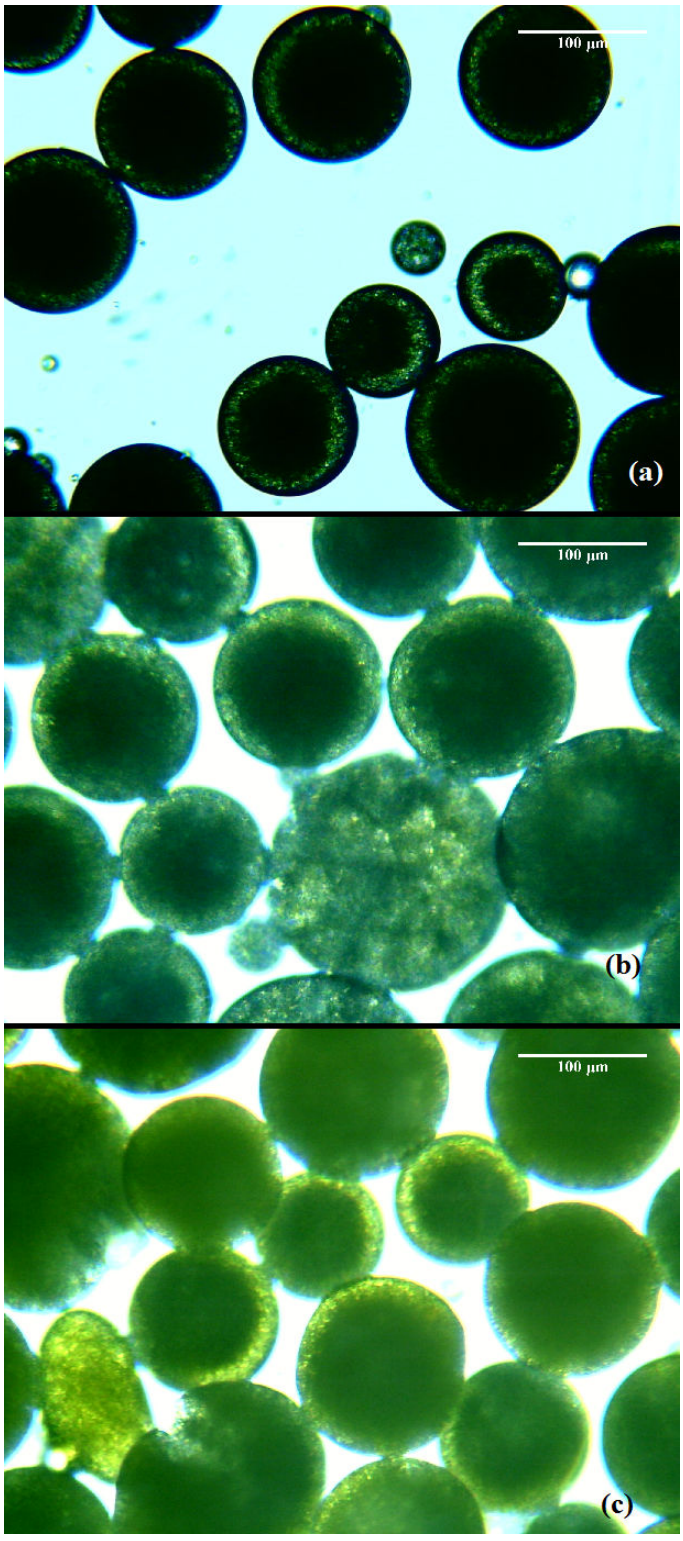

Figure 3.10: Particles with a solid core made with an inner aqueous phase volume of (a) 100 µl, (b) 200 µl, and (c) 300 µl. Formulations detailed in table 3.6.

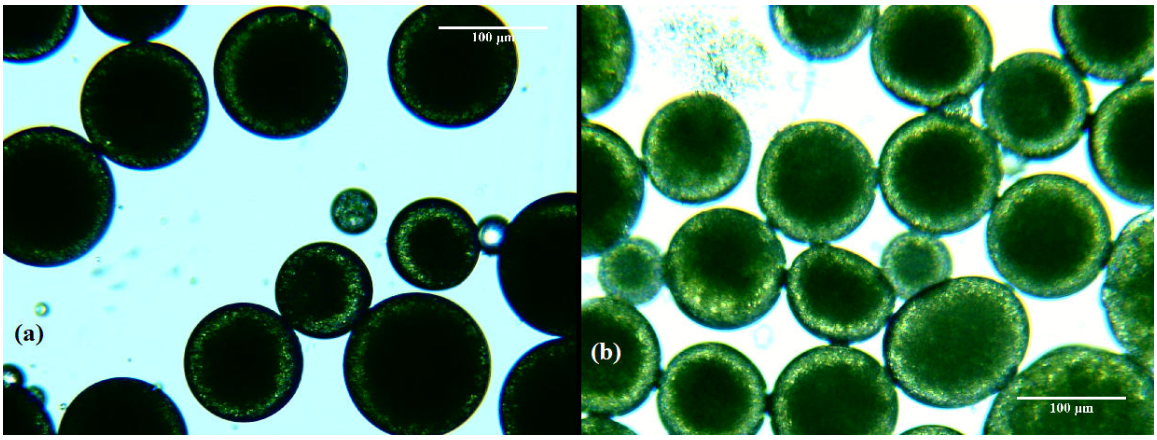

Figure 3.11: Particles with a solid core made with (a) 3% and (b) 5% of surfactant in the shell to determine the optimum surfactant amount. Formulations detailed in table 3.6.

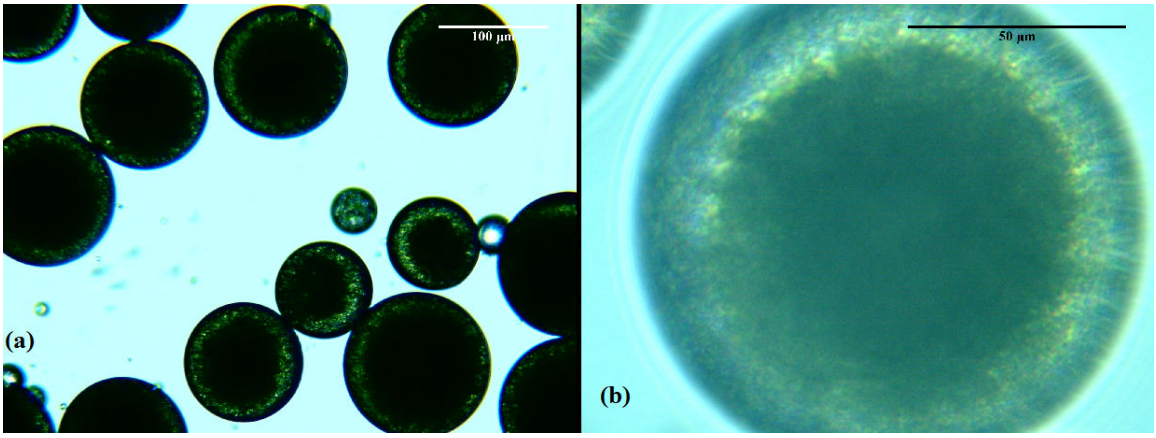

Figure 3.12: Particles chosen as the formulation to be used for further studies at (a) 10x and (b) 40x (formulation in table 3.6).

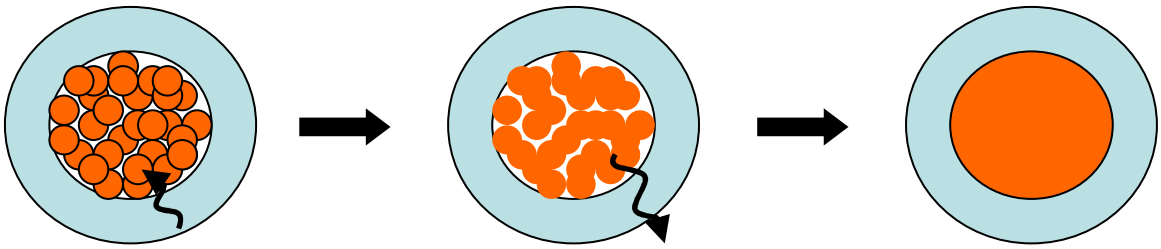

Figure 3.13: A schematic of the proposed mechanism for creating the core-shell particles with a solid core. The solvent first migrates into the inner aqueous phase, dissolving the uniform particles before exiting the particle entirely, leaving behind a solid core.

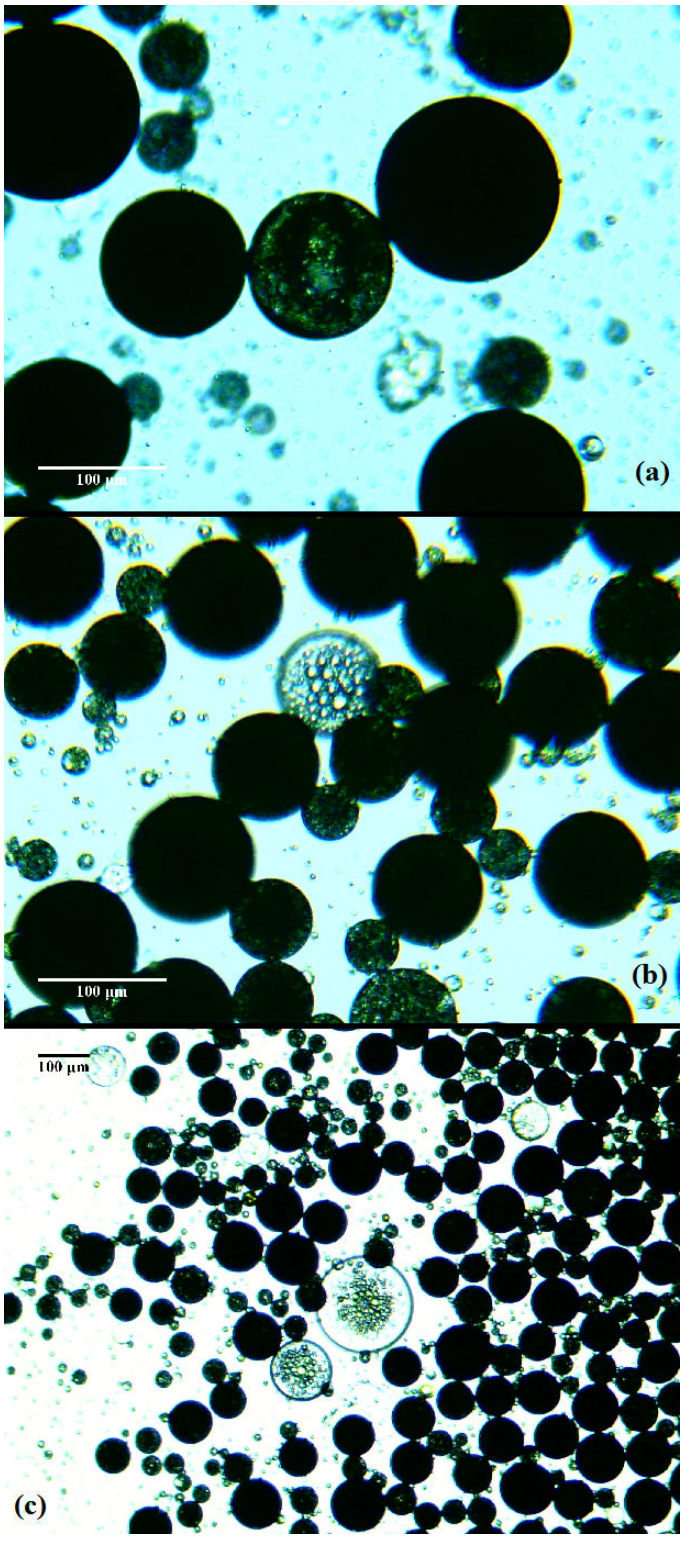

Figure 3.14: Particles with a core of particles made using (a) 0.2 g, (b) 0.25 g, and (c) 0.3 g of PMMA. Formulations detailed in table 3.7.

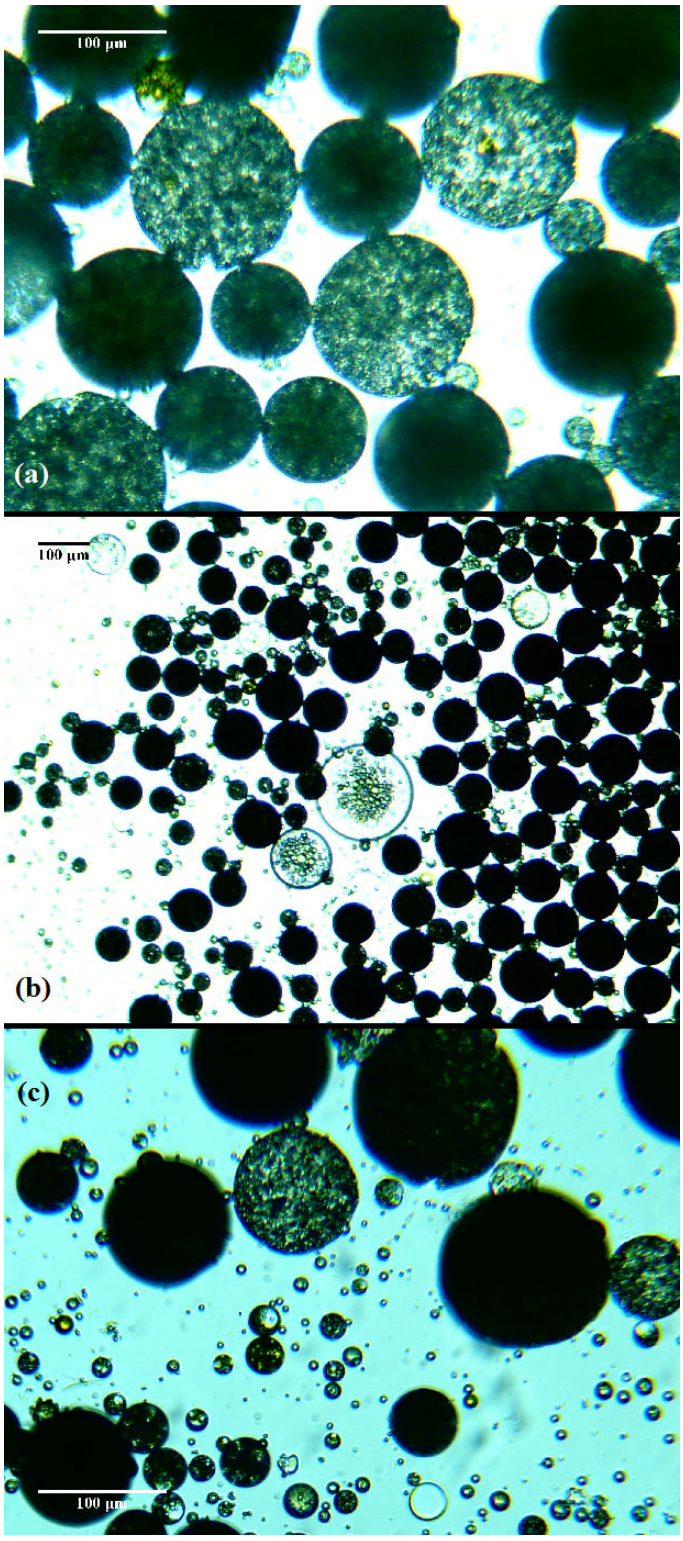

Figure 3.15: Particles with a core of uniform particles made with an inner aqueous phase volume of (a) 100 µl, (b) 200 µl, and (c) 300 µl. Formulations detailed in table 3.7.

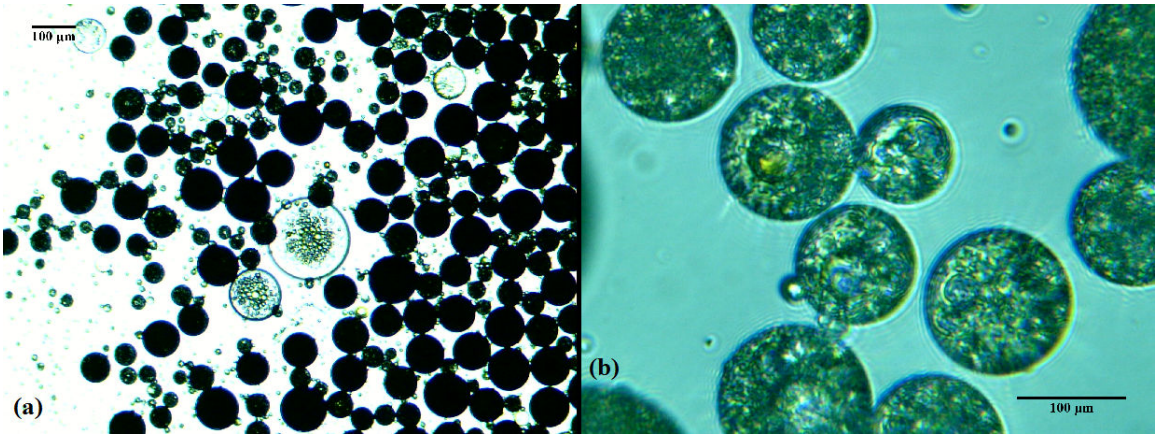

Figure 3.16: Particles with a core of uniform particles made with (a) 3% and (b) 5% of surfactant in the shell to determine the optimum surfactant amount. Formulations detailed in table 3.7.

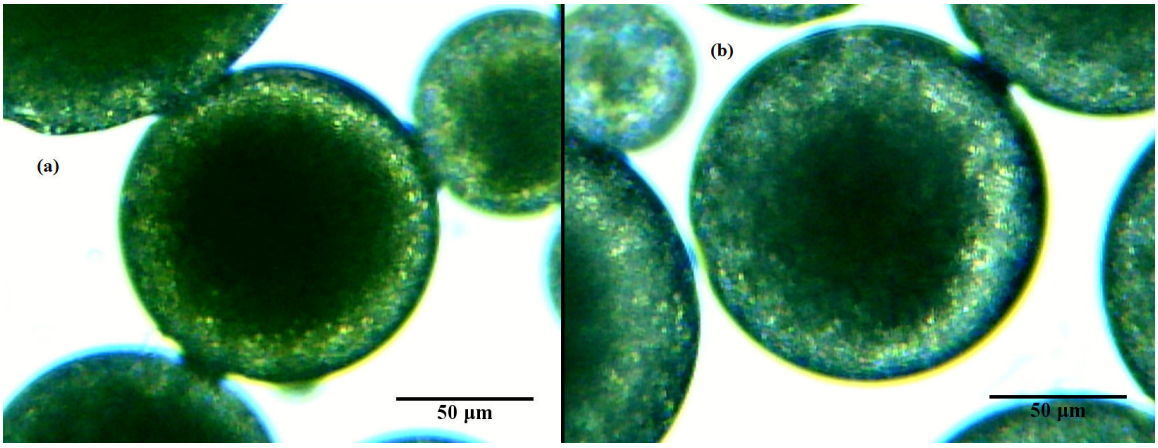

Figure 3.17: A visual comparison of the shell thickness of particles with a solid core prepared using (a) 0.175 g and (b) 0.500 g of PMMA.

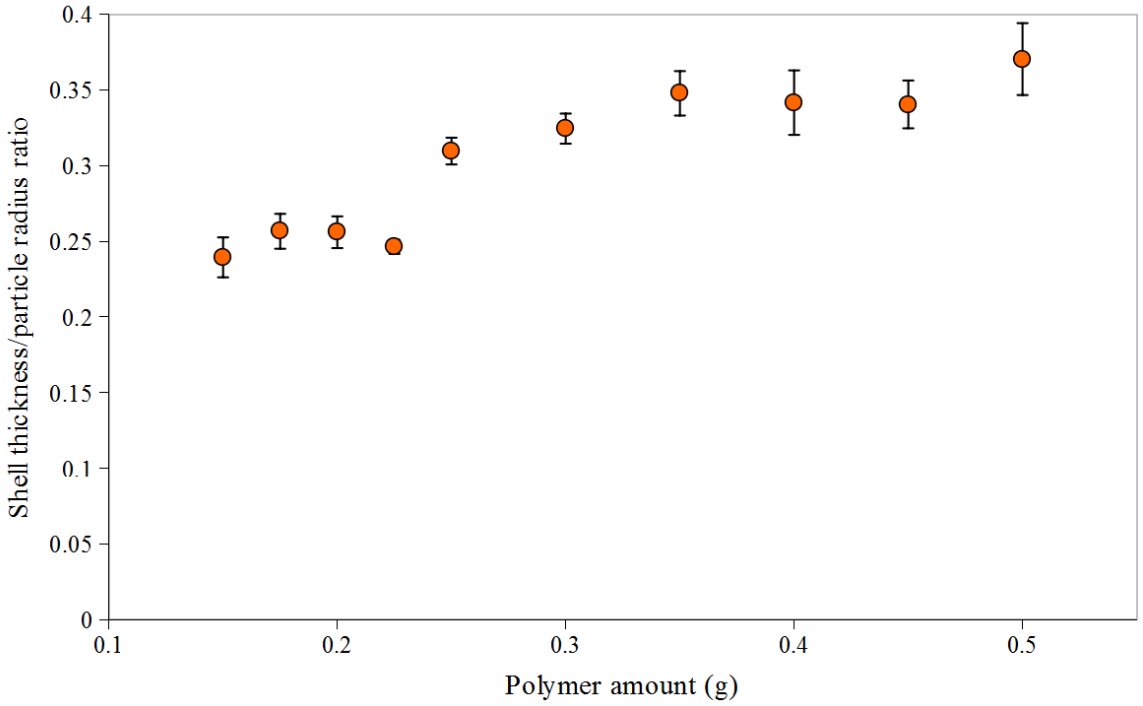

Figure 3.18: A comparison of the shell thickness to particle radius ratio averaged over 10 particles for polymer amounts ranging from 0.15 g to 0.5 g.

3.7 Tables for Chapter 3

Table 3.1: Parameters for design of experiments	
Parameter	**Values**
Solvent	Toluene
	Dichloromethane
Molecular weight of PMMA (core)	15000
	120000
Molecular weight of PMMA (shell)	15000
	120000
Inner aqueous phase volume (µl)	200
	600
Oil phase surfactant concentration	0%
	3%

Table 3.2: Design of experiments for creating particle geometries					
Randomized run number	**Solvent**	**MW PMMA core**	**MW PMMA shell**	**Inner aqueous phase (µL)**	**Oil phase surfactant concentration**
29	Toluene	15000	15000	200	0%
17	DCM	15000	15000	200	0%
26	Toluene	120000	15000	200	0%
2	DCM	120000	15000	200	0%
1	Toluene	15000	120000	200	0%
31	DCM	15000	120000	200	0%
19	Toluene	120000	120000	200	0%
15	DCM	120000	120000	200	0%
18	Toluene	15000	15000	600	0%
14	DCM	15000	15000	600	0%
7	Toluene	120000	15000	600	0%
24	DCM	120000	15000	600	0%
8	Toluene	15000	120000	600	0%
28	DCM	15000	120000	600	0%
12	Toluene	120000	120000	600	0%
21	DCM	120000	120000	600	0%
6	Toluene	15000	15000	200	3%
30	DCM	15000	15000	200	3%
27	Toluene	120000	15000	200	3%
22	DCM	120000	15000	200	3%
13	Toluene	15000	120000	200	3%
4	DCM	15000	120000	200	3%
32	Toluene	120000	120000	200	3%
10	DCM	120000	120000	200	3%
16	Toluene	15000	15000	600	3%
3	DCM	15000	15000	600	3%
25	Toluene	120000	15000	600	3%
20	DCM	120000	15000	600	3%
9	Toluene	15000	120000	600	3%
23	DCM	15000	120000	600	3%
5	Toluene	120000	120000	600	3%
11	DCM	120000	120000	600	3%

Table 3.3 Formulations for particles in figures 3.2-3.6					
Figure	**Solvent**	**Molecular weight of PMMA (core)**	**Molecular weight of PMMA (shell)**	**Inner aqueous phase volume (µL)**	**Oil phase surfactant concentration**
3.2a	toluene	120000	120000	200	3%
3.2b	DCM	120000	120000	200	3%
3.3a	toluene	15000	120000	200	3%
3.3b	toluene	120000	120000	200	3%
3.4a	toluene	120000	15000	200	3%
3.4b	toluene	120000	120000	200	3%
3.5a	toluene	120000	120000	200	3%
3.5b	toluene	120000	120000	600	3%
3.6a	DCM	15000	120000	200	0%
3.6b	DCM	15000	120000	200	3%
3.7a	toluene	15000	120000	200	3%
3.7b	toluene	120000	120000	200	3%
3.7c	DCM	15000	120000	200	3%
3.7d	DCM	120000	120000	200	3%
3.8a	toluene	120000	120000	200	3%
3.8b	DCM	15000	120000	200	3%

Table 3.4: Factorial around figure 3.8b (particles with a solid core)			
Randomized run number	**Polymer amount (g)**	**Inner aqueous phase (µL)**	**Surfactant amount**
1	0.2	200	3%
3	0.2	200	5%
8	0.2	300	3%
10	0.2	300	5%
14	0.2	100	3%
13	0.2	100	5%
17	0.25	200	3%
11	0.25	200	5%
7	0.25	300	3%
6	0.25	300	5%
18	0.25	100	3%
5	0.25	100	5%
9	0.3	200	3%
15	0.3	200	5%
12	0.3	300	3%
16	0.3	300	5%
2	0.3	100	3%
4	0.3	100	5%

Table 3.5: Factorial around figure 3.8a (particles in the core)			
Randomized run number	**Polymer amount (g)**	**Inner aqueous phase (µL)**	**Surfactant amount**
12	0.2	200	3%
2	0.2	200	5%
4	0.2	300	3%
8	0.2	300	5%
13	0.2	100	3%
14	0.2	100	5%
17	0.25	200	3%
9	0.25	200	5%
3	0.25	300	3%
10	0.25	300	5%
11	0.25	100	3%
7	0.25	100	5%
15	0.3	200	3%
6	0.3	200	5%
18	0.3	300	3%
5	0.3	300	5%
16	0.3	100	3%
1	0.3	100	5%

Table 3.6 Formulations for particles in figures 3.9-3.12			
Figure	**Polymer amount (g)**	**Inner aqueous phase (µL)**	**Surfactant amount**
3.9a	0.2	100	3%
3.9b	0.25	100	3%
3.9c	0.3	100	3%
3.10a	0.25	100	3%
3.10b	0.25	200	3%
3.10c	0.25	300	3%
3.11a	0.25	100	3%
3.11b	0.25	100	5%
3.12	0.25	100	3%
All particles made with: dichloromethane, PMMA with a molecular weight of 120000 in the shell, and PMMA with a molecular weight of 15000 in the core.			

Table 3.7 Formulations for particles in figures 3.14-3.16			
Figure	**Polymer amount (g)**	**Inner aqueous phase (µL)**	**Surfactant amount**
3.14a	0.2	200	3%
3.14b	0.25	200	3%
3.14c	0.3	200	3%
3.15a	0.3	100	3%
3.15b	0.3	200	3%
3.15c	0.3	300	3%
3.16a	0.3	200	3%
3.16b	0.3	200	5%
All particles made with: toluene and PMMA with a molecular weight of 120000 in both the core and shell.			

Chapter 4 Geometric effect of particles on UV protection

4.1 Geometric and proximity effects on UV protection

Materials in a wide variety of fields are photosensitive and require some form of UV protection. As discussed in chapter 1, other than preventing exposure to UV radiation altogether via a barrier, there are three types of materials with which to formulate a protection method: physical blockers, UV absorbers, and antioxidants. Physical blockers offer protection by scattering UV radiation, a mechanism which can be attributed to the material's physical characteristics. UV absorbers protect by absorbing UV radiation before it reaches the sensitive material, and the protection is dependent upon the proximity of the absorber to the photosensitive molecule. Antioxidants are also dependent on proximity since they must be in contact with an excited molecule in order to quench it. These two characteristics, geometry and proximity, can be manipulated using the particles formulated in chapters 2 and 3.

Structured particle geometries devoid of protectants can be used to assess the effect of geometry on UV protection. Since no protectant is present, all protection provided must be due to scatter as a result of the geometry of the particle. The particles formulated in the previous two chapters can be used as tools to assess the geometric effect on protection. Figure 4.1 is a schematic view of the three types of geometries examined in this study, showing how a cross-section would appear when they are made without protectant.

When protectant is added to structured particle geometries, the effect of proximity can be analyzed. Proximity changes can be approximated in uniform particles by changing the concentration of the protectant in the particle formulation, therefore changing the average distance between a beta-carotene molecule and a protectant molecule. The core-shell particles formulated in the previous chapter provide a discrete method of separation between the core and shell of the particle. Protectant and beta-carotene can be selectively added to the core or shell, creating a more distinct partition than is possible with uniform particles. Using these particle formulations, protectant can be added to the core, the shell, or both to study the effect. A schematic view of particles where protectant is added to one compartment is shown in figure 4.2 with the introduction of pomegranate, raspberry, and orange particles.

Understanding the role of proximity and geometry in protecting photosensitive molecules will aid in creating and modifying UV protective systems. The particle environment has the added advantage of being a physical blocker by nature of geometry. Encapsulation also has some unique properties when compared to other systems. Unlike a solution of photosensitive and protective materials, the particle environment holds the proximity between the photosensitive and protective molecules practically constant. The particle geometry itself is also different from other polymer systems, such as films, which scatter light differently. Typically, small particles with sharply curved interfaces scatter a much larger fraction of the incident light than flat films. There are many applications, such as sunscreens and pharmaceuticals, in which particles such as those that will be discussed in the coming sections would be a logical choice of UV protection.

4.2 Geometric effect

As discussed in the previous section, the effect of utilizing various particle geometries for the purpose of UV protection can be determined by comparing the particles when their formulations do not contain protectants, as in figure 4.1. When protectants are not used it can be assumed that all the protection provided is due to the particle geometry since no other method of protection has been identified. A solution of beta-carotene and uniform particles whose only additive was beta-carotene were exposed for 60 minutes with three repetitions. The orange (solid core) and pomegranate/raspberry (particle core) geometries containing no protectant were exposed for 120 minutes, with three repetitions of the 0-60 minute exposure times. The core-shell geometries were exposed for longer times because they provided so much protection that they were difficult to compare over just 60 minutes. The core-shell particles were stirred during exposure to discourage settling, while only 2.5 ml were exposed at a time to ensure the suspension was well mixed. After exposure, the particles were centrifuged and resuspended in 2.5 ml of acetone. In order to remove interfaces for scatter, the suspensions were then capped and stirred until the particles were completely dissolved. This allows the UV/Vis to measure the beta-carotene absorbance unimpeded. Figure 4.3 displays the beta-carotene decay curves for each particle geometry.

All particle geometries offered better protection than beta-carotene in solution, as the beta-carotene in solution was completely degraded after 40 minutes of exposure and all of the particles still contained beta-carotene at that time. As discussed in chapter 2, the increase in protection when encapsulated is due to scatter by the particle[46] as well as a

lack of available free volume for the molecule's conformation to change during chemical reaction.[101] Both of the core-shell geometries retained approximately 50% beta-carotene by 120 minutes of exposure, while the uniform particles only retained approximately 25% undegraded beta-carotene at the same exposure time. The drastic increase in protective capacity of the core-shell particles when compared with the uniform particles proves the importance of the shell for UV protection. Beta-carotene is distributed uniformly throughout the uniform particles, meaning that a substantial amount of beta-carotene is present on the surface of the particles, easily accessible to rays of UV radiation. Both of the core-shell geometries possess a layer of polymer over the core that contains beta-carotene. Since beta-carotene is not present in the shell of the core-shell particles, the fraction of UV radiation that is scattered by polymer instead of absorbed by beta-carotene must increase, increasing the efficiency of the particles to protect from UV radiation. The beta-carotene in the core of core-shell particles is also protected from any free radicals that may form in the water of the aqueous suspension.

The pomegranate/raspberry particle conformation seems to perform better than the orange particle geometry for the first 75 minutes of exposure. Over the next 45 minutes of exposure both decay curves level out and the orange and pomegranate/raspberry particles perform similarly with approximately 50% of the beta-carotene left intact after 120 minutes of exposure. While the two particle geometries appear to behave similarly, the error bars representing the standard deviations over three repetitions show that there is much more variation in the protection provided by the orange particles. This larger variation suggests that the orange particles do not provide as much stability as the pomegranate/raspberry particles. This superior stability found in the

pomegranate/raspberry particles is most likely a result of increased scatter due to the core-shell boundary and the particles in the core. The pomegranate/raspberry particles contain water in the core, which increases scatter at the core-shell boundary, whereas the orange particles do not have as specific a boundary since both the core and the shell are primarily composed of polymer. The particles in the core of the pomegranate/raspberry particles also offer additional highly curved interfaces with which to scatter light, further protecting the beta-carotene. So while the orange and pomegranate/raspberry particles seem to offer similar protection, the pomegranate/raspberry particles offer the largest increase in stability due to the particle geometry.

4.3 Proximity effect – one protectant

A significant increase in UV protection was achieved by creating a more complicated particle geometry than that studied in chapter 2. The core-shell geometries synthesized in chapter 3 provided more protection than uniform particles without the addition of a UV protective molecule, suggesting that particle geometry affects UV protection. This section examines the effect of adding a protectant to the particle geometries to study the effect of proximity. As in chapter 2, oxybenzone, OMC, avobenzone, and vitamin E were used as protectants. Oxybenzone was studied at three beta-carotene:oxybenzone ratios, while the other protectants were studied solely at the 1:33 ratio. Since the effect of geometry has already been established, proximity is discussed in this section by the comparison of particles with similar geometries, such as

the uniform particle with the orange particle or the pomegranate particle with the raspberry particle.

4.3.1 Solid particles

The uniform and orange particle geometries can be compared to assess effect of proximity since both particles are solid throughout, ruling out the effects of geometry. The uniform particles contain protectant and beta-carotene throughout the particle, so there is always potential for a protectant molecule to come into contact with a beta-carotene molecule. The orange molecules have a core-shell structure with beta-carotene in the core and protectant in the shell. Protectant and beta-carotene molecules are mostly separate in the orange particles, except at the interface between the core and shell. The differing frequency of beta-carotene and protectant molecule interactions in the two geometries allows the effect of proximity to be examined.

The amount of protectant in the particle formulations determines the number of molecules available to absorb UV or quench radicals to increase protection, as well as the number of molecules available to interact with beta-carotene. During comparison of the various particle geometries, the mass ratio of beta-carotene to protectant was held constant while the location of the protectant varied. The amount of oxybenzone added to the particle geometries was varied, and a comparison of decay curves is shown in figures 4.4a-c. Decay curves for the smallest amount of oxybenzone, a 1:10 beta-carotene to oxybenzone ratio, are shown in figure 4.4a. The curves overlap for the majority of the exposure time and after 60 minutes of UV exposure there is approximately 40% of the

beta-carotene left undegraded in both cases. The 1:33 ratio in figure 4.4b behaves similarly with significant overlap, except that approximately 60% of the beta-carotene is left undegraded at the end of 60 minutes. The largest oxybenzone concentration, the 1:100 ratio, also displays significant overlap, although by the end of 60 minutes of UV exposure the orange particles showed slightly less degradation with 90% of the beta-carotene remaining as opposed to 70% for the uniform particles.

The data in figures 4.4a-c show increasing UV protection as the oxybenzone concentration is increased for both orange and uniform particles. This result is intuitive as the increase in oxybenzone concentration results in an increase in the amount of protective molecules present in the particles. The figures also suggest that uniform particles and orange particles offer similar protection over a range of oxybenzone concentrations when exposed to UV radiation for 60 minutes. The similarity in decay curves for the smaller concentrations of oxybenzone suggest that the proximity between beta-carotene and oxybenzone molecules does not affect UV protection. The larger concentration of oxybenzone, however, does exhibit a higher protective capacity when beta-carotene and oxybenzone are separated into the core and shell, respectively. The orange and uniform particle curves in figure 4.4c behave similarly for the first 40 minutes of exposure, but at exposure times greater than 40 minutes the decay curves split and the orange particles offer more protection. The oxybenzone concentrations in figures 4.4a and b may not be large enough to ensure beta-carotene and oxybenzone molecule interaction in the uniform particles, whereas the 1:100 ratio surrounds beta-carotene with enough oxybenzone molecules to differentiate the uniform and orange particle structures. Oxybenzone also decays over time due to UV exposure, but the separation provided by

the orange particles reduces the amount of excited oxybenzone molecules that can react with beta-carotene.

As discussed in chapter 2, each protectant affects beta-carotene decay differently when the two are encapsulated together. The UV protection provided by each protectant when encapsulated in uniform particles was reviewed in chapter 2. Oxybenzone and avobenzone provided the best protection in uniform particles, followed by vitamin E and finally OMC. Figure 4.5 shows the decay of beta-carotene when encapsulated with each protectant in orange particles at a 1:33 beta-carotene to protectant ratio. The decay curves for all particle formulations overlap significantly for the early exposure times, with the avobenzone and vitamin E curves separating at 30 minutes. Oxybenzone and OMC showed similar protective capacity to orange particles that contain no protectant, with approximately 60% of beta-carotene left undegraded after 60 minutes of UV exposure. Avobenzone and vitamin E provided more protection, with only 10-20% of beta-carotene degraded at the end of 60 minutes. OMC offered no additional protection when added to the uniform particle formulation, so the absence of additional protection in the orange particles is not unexpected. The lack of improvement when oxybenzone was added to the formulation could be a result of absorber available to react with beta-carotene as a photosensitizer at the core-shell interface, as was observed in uniform particles containing a combination of oxybenzone and another absorber.

The orange and uniform particle geometries are compared with respect to each protectant in figure 4.6. Each protectant is present in the 1:33 ratio. Orange and uniform particles containing oxybenzone are compared in figure 4.6a, and the comparison was previously discussed during analysis of figure 4.4b. Oxybenzone provides similar

protection in the orange and uniform geometries at the 1:33 ratio, making the separation provided by the orange particle unnecessary. OMC, avobenzone, and vitamin E all showed a decrease in beta-carotene degradation when the protectant was added as seen in figures 4.6b-d, respectively. The increase in protection exhibited by OMC and avobenzone was expected as separating the absorber from the beta-carotene decreases the chance that an absorber radical can interact with beta-carotene. The orange particle geometry was not expected to increase the protection provided by vitamin E since it is an antioxidant and must be in contact with beta-carotene to quench beta-carotene radicals. Figure 2.3, however, shows that vitamin E also acts as a UV absorber, so the orange configuration may provide a better location for vitamin E to protect from UV since it can intercept the radiation before it reaches the beta-carotene. Note that any increases of intensity with exposure time present in the decay curves are due to concentration fluctuations in the measured samples and are typically smoothed with additional repetitions of the experiment.

Orange and uniform particles were compared to assess the role of protectant proximity in solid particles. Both particles show increased protection when the concentration of oxybenzone is increased, as shown in figure 4.4. The uniform and orange particles also show similar protection for the 1:10 and 1:33 beta-carotene:protectant ratios, while the orange particle performs better for the 1:100 ratio probably because the oxybenzone more completely surrounds the beta-carotene. For the uniform particles in figure 2.14, oxybenzone and avobenzone provide the best protection, followed by vitamin E, and OMC protects very little. For the orange particles all of the formulations overlap for the first 30 minutes, then avobenzone and vitamin E emerge as

the best protectants while oxybenzone and OMC provide similar protection to particles containing no protectant in figure 4.5. The orange particles resulted in less beta-carotene degradation than the uniform particles for formulations containing OMC, avobenzone, and vitamin E, while protection was the same for particles containing oxybenzone in figure 4.6. Overall the orange particles offer the same if not better protection than the uniform particles, proving that the greater separation distance between the protectants and beta-carotene promotes UV protection due to separation between protectant radicals and beta-carotene.

4.3.2 Encapsulated particles

The pomegranate and raspberry particles are identical except for the location of the protectant. In pomegranate particles, the protectant is present in the shell, whereas for the raspberry particles, the protectant is in the core particles along with beta-carotene. Comparing the pomegranate and raspberry particles allows the effect of proximity to be analyzed without needing to account for additional scatter due to the particles and any water present in the core.

The amount of oxybenzone present in particle formulations was varied to determine the impact that protectant concentration has on UV protection. The amount of oxybenzone present can affect UV protection in two ways: it can influence protection by changing the number of molecules available to absorb UV radiation before it can reach a beta-carotene molecule, or it can vary the amount of molecules present around beta-carotene that can absorb UV and become a radical. The effect of oxybenzone

concentration was studied in 1:10, 1:33, and 1:100 beta-carotene:oxybenzone mass ratios. A comparison between pomegranate and raspberry particles with respect to oxybenzone concentration is shown in figures 4.4d-f. Increasing the amount of oxybenzone from the 1:10 ratio to the 1:33 ratio enhanced protection for raspberry particles, with the amount of beta-carotene left after an hour of exposure increasing from approximately 60% to 80%. The further increase in oxybenzone from 1:33 to 1:100 did not yield an increase in protection. The plateau of protection reached when increasing oxybenzone was also observed with the uniform particles as seen in figure 2.8a. While the behavior when increasing oxybenzone concentration is the same, the overall protection was better, suggesting that the two particle geometries utilize the same protection mechanism with the raspberry particles having additional scatter due to the shell. The pomegranate particles show little to no benefit from the addition of oxybenzone to the particle formulation, as the amount of beta-carotene left after an hour of exposure remains at approximately 80% for all three ratios. The absence of additional protection suggests that the pomegranate particles have already reached their largest potential without the addition of more oxybenzone.

The raspberry particle geometry initially offers less protection than the pomegranate configuration at the 1:10 ratio, but the performance of the raspberry particle increases to match that of the pomegranate particle as the amount of oxybenzone is increased, shown in figures 4.4d-f. The raspberry particle requires more oxybenzone than the pomegranate particle to provide the same protection, suggesting that the ideal placement for oxybenzone is in the shell of the particles. This inference implies that the

best protection is provided when oxybenzone molecules surround beta-carotene molecules without being in close proximity to them.

Each particle geometry reacts differently in terms of protection provided when various protectants are present in the formulation. A comparison between each of the protectants in the pomegranate particles at a 1:33 ratio is examined in figure 4.7. All of the decay curves overlap except for that of OMC, which has values larger than one. Normalized absorbance cannot exceed a value of one since beta-carotene is not created during exposure, so the OMC curve can be approximated by having a value of one throughout the exposures. Assuming a value of one for OMC, all curves exhibit significant overlap through 40 minutes of exposure, where OMC and avobenzone separate and show superior protective properties than oxybenzone, vitamin E, and a particle devoid of protectant. Therefore avobenzone and OMC offer the best protection for pomegranate particles.

The effect of varying the protectant in raspberry particles was also investigated at the 1:33 ratio, with the results in figure 4.8. Vitamin E and OMC provided the least protection, less even than the particle not containing protectant. Oxybenzone and avobenzone provide the most protection; approximately 80% of the beta-carotene is left after 60 minutes of exposure in both cases. The poor performance of OMC mirrors that of the uniform particles containing OMC from chapter 2, which is expected since uniform particles of the same formulation comprise the core of the particle. The vitamin E results are surprising because vitamin E is primarily an antioxidant, a protection mechanism that requires molecules to be in close proximity, such as within the same uniform particle. It is possible that the polymer matrix hinders movement of the antioxidant to the point

where the molecule is acting solely as a UV absorber and no benefit is retained from the molecule's ability to quench beta-carotene radicals.

Each protectant studied behaves differently, even the three UV absorbers discussed do not protect in identical fashions though they are all effective by absorbing UV radiation. A comparison of the raspberry and pomegranate particle geometries with respect to each protectant at a 1:33 ratio is visualized in figure 4.9. The pomegranate and raspberry particles offer almost identical protection at the 1:33 ratio of oxybenzone, as was concluded in the discussion of figure 4.4e and as seen again in figure 4.9a. OMC offers significantly different protection in the two geometries, shown in figure 4.9b. Pomegranate particles containing OMC offer nearly complete protection over an hour of UV exposure, whereas only 40% of the beta-carotene is remaining in the OMC formulation of the raspberry particles. The pomegranate particle configuration offers nearly complete protection when avobenzone is included in the formulation while the raspberry configuration leaves approximately 80% beta-carotene undegraded after an hour of exposure, as depicted in figure 4.9c. The pomegranate particle geometry also shows greater performance when vitamin E is used as the protectant, with approximately 35% more beta-carotene left at the end of 60 minutes of exposure than the raspberry particle geometry, as illustrated in figure 4.9d. With the exception of oxybenzone, for which both particle geometries yielded nearly identical results, the pomegranate particle configuration outperforms the raspberry particle. The superior results obtained using the pomegranate particle supports the conclusions from figure 4.4, that the best protection occurs when beta-carotene is surrounded by protectant molecules, but not in close proximity to them.

Core-shell particle geometries with a suspension of uniform particles in the core were analyzed. The raspberry particles contain both beta-carotene and a protectant in the core, while pomegranate particles are configured with beta-carotene in the core particles and a protectant in the shell. Concentration of protectant had no effect for pomegranate particles and only increased protection for raspberry particles for the initial increase in concentration. The raspberry and pomegranate offered similar UV protection after the first protectant increase for the raspberry, suggesting that the pomegranate configuration is superior. Avobenzone performed well in both particle geometries, while vitamin E performed poorly. Oxybenzone increased protection for raspberry particles but not for pomegranate particles, while OMC increased protection for pomegranate particles but not raspberry particles. When comparing the geometries with each protectant, the pomegranate particles outperform the raspberry with every protectant except for oxybenzone, with which both particles perform similarly. Avobenzone was the most ideal protectant overall since it performed very well for both geometries, while the pomegranate particle often showed better protective properties than the raspberry.

4.3.3 Conclusions

Two types of core-shell particles were studied, those with a solid core and those whose core contained a suspension of uniform particles. The particles with a solid core (orange particles) were compared to uniform particles, and two configurations of the particles containing particles in the core (pomegranate and raspberry particles) were created to compare. The two types of core-shell particles were compared in section 4.2 to

determine the effect of geometry, where the pomegranate/raspberry particle configuration yielded the most beta-carotene undegraded after two hours of exposure. Since the geometric effect of the particles has already been determined, this section compared particles with similar geometries with the aim of determining the effect of protectant proximity.

Orange particles and uniform particles were examined to establish whether there is an advantage to having the protectant in the shell instead of throughout the particle. Both geometries exhibited an increase in protective capacity when the concentration of oxybenzone in the particle formulations was increased. Avobenzone proved to be a UV absorber that performed well in both particle geometries. In most cases the orange configuration produced better results than the uniform particle, proving that the ideal UV protective particle surrounds beta-carotene molecules without being in close proximity to them.

Pomegranate and raspberry particles were compared to study the effect of proximity when the geometry contains a suspension of submicron particles in the core of a microparticle. When varying the oxybenzone concentration in the particle formulations, no effect was observed for pomegranate particles and a small increase was noted for the initial concentration increase for the raspberry particles. As with the orange and uniform particles, avobenzone proved to be a UV absorber that provided a substantial increase in protection for both the pomegranate and raspberry geometries. In many of the formulations studied, the pomegranate particles performed significantly better than the raspberry particles, strengthening the conclusion drawn from the orange and uniform

particles that the ideal placement for a protectant is not in close proximity to beta-carotene.

Although the purpose of these comparisons was to segregate the extreme differences in particle geometry, some general conclusions can be made. Avobenzone was the one protectant that performed well for every particle geometry examined, so it has proven to be a good choice of protectant when using polymer particles. Also, the pomegranate and orange particles outperformed the particles that contained both beta-carotene and protectant in the core, so conclusions can be made about proximity. The best protection from UV radiation was achieved when beta-carotene was surrounded by the protectant, but not near enough to interact. Separating the photosensitive and protecting molecules by placing beta-carotene in the core and the protectant in the shell allowed the protectant to absorb UV before it reached beta-carotene without being in close enough proximity for protectant radicals to damage beta-carotene. When creating particles to protect molecules from UV radiation, the protectant should be close enough to surround the photosensitive molecules without being close enough to interact with them.

4.4 Proximity effect – multiple compartments

An advantage of the core-shell particles that has not been discussed is the ability to place protectants in multiple compartments. The particles in the previous section either segregated the protectant away from beta-carotene, or placed the two molecules together in the same compartment. By utilizing both compartments and multiple protectants, a wide range of different particle formulations can be synthesized and studied. Initially the

1:33 protectant to beta-carotene ratio was preserved, but the protectant was spread equally between the core and the shell, creating a "split" configuration. Vitamin E is known for protection via the antioxidant mechanism, so another particle design contains a UV absorber in the shell to absorb UV radiation before it reaches beta-carotene, and vitamin E in the core to quench beta-carotene that may become radicals due to exposure to UV radiation. Additional absorber-antioxidant configurations were explored using oxybenzone and vitamin E, since oxybenzone has been used most extensively in previous sections and chapters. These additional configurations include oxybenzone and vitamin E in the shell, oxybenzone and vitamin E in the core, and oxybenzone and vitamin E in the shell with vitamin E also in the core. These particles further explore the proximity effect specific to each protectant.

4.4.1 Core-shell particle splits

When the protectant amount is split between the core and shell of the particles, the positive and negative aspects of core and shell placement compound. The effects resulting from the close proximity of the protectant to beta-carotene in the uniform and raspberry particles combine with those characteristic of the larger distance created in the orange and pomegranate particles. The split particles can highlight which effect is stronger, providing further evidence toward the effect of proximity.

Oxybenzone has been shown to provide adequate UV protection in previous particle geometries. Results of the oxybenzone split particles are presented in figure 4.10. The solid particles are compared to their split in figure 4.10a, where the uniform particle

offers the best protection, followed closely by the orange, and the split particle provides the least protection. These results suggest that the split configuration does not contain enough oxybenzone in the shell to effectively screen UV, and enough is present in the core to photosensitize beta-carotene. All configurations in figure 4.10b overlap significantly, suggesting that the placement of oxybenzone is not important when a suspension of particles is encapsulated. Comparing the charts side by side, it is apparent that oxybenzone behaves very differently in the two types of core-shell particles, as the geometry has no effect on the pomegranate/raspberry split, but a large negative impact for the orange split.

OMC performed very poorly for uniform, orange, and raspberry particles, but well for pomegranate particles in the previous section. Splitting the OMC concentration between the core and shell has a significantly positive effect for the solid particles, as seen in figure 4.11a, where the split particles greatly outperform the orange and uniform particles with nearly complete protection. Spreading the concentration of OMC over both compartments must take advantage of positive aspects of OMC, allowing the absorber in the shell to screen UV radiation while the OMC in the uniform particles of the core are stabilized by the core-shell environment. For the encapsulated particles, however, figure 4.11b shows that the split provides more protection than the raspberry particles, but less than the pomegranate particles. This sort of a response is intuitive, as the split particles are only partly as effective as the pomegranate particles since only some of the concentration is in the shell, yet performance is better than the raspberry particles for the same reason.

In the previous section, avobenzone was found to be the best protectant overall when used as the only protectant in the particles. For solid particles, figure 4.12a displays that the orange maintained the geometry with the best protection, while the uniform and split geometries retained approximately the same amount of undegraded beta-carotene at the end of 60 minutes of UV exposure. The proximity conclusions from section 4.3.1 hold true in this case, as the best geometry is that where no avobenzone is present in core in close proximity to beta-carotene molecules. The pomegranate/raspberry split is examined in figure 4.12b, where it overlaps significantly with the pomegranate particle for the first 25 minutes of exposure before degrading and ultimately performing worse than the pomegranate and slightly worse the raspberry particles. This solidifies that avobenzone performs the best when present in the shell, such as in the pomegranate particle. The difference in protection between the raspberry and split particles is minimal, inferring that any avobenzone present in the core impedes protection.

A UV absorber was used as the protectant in the previous three particle configurations, and as such the addition of the protectant to the core either aided in surrounding the beta-carotene to prevent UV radiation from reaching it, or hindered protection by becoming radicals acting as photosensitizers. Vitamin E, on the other hand, exhibits UV absorber properties while primarily acting as an antioxidant. Figure 4.13a compares the solid particles, where all geometries overlap for the first 25 minutes of exposure, then degradation continues for the uniform particle while the orange and split geometries continue to offer substantial protection. The encapsulated particles behave similarly, as shown in figure 4.13b. All encapsulated particle geometries possess overlapping decay curves through 20 minutes of exposure, at which time the beta-

carotene in the raspberry particle continues to degrade and the pomegranate and split geometries degradation plateaus with approximately 80% beta-carotene remaining. These results imply two characteristics of the behavior of vitamin E as a protectant in the particle environment: vitamin E requires a UV absorber in the shell of the particle, and as long as an absorber is present in the shell, vitamin E may act as an absorber, antioxidant, or both in the core.

The addition of the same protectant to both compartments adds a new dynamic to the particle geometries. While the OMC split performed well for the orange particles and the oxybenzone split offered sufficient protection for the pomegranate/raspberry particles, vitamin E was the only protectant to achieve good protection for both split geometries. The fact that the antioxidant performed well for the splits, but not the absorbers, explains a lot about protectant mechanism and effective proximity. UV absorbers protect by absorbing UV radiation before it reaches the photosensitive molecule, but if the protectant is in close proximity then the protectant radical can react with the photosensitive one, encouraging decay. Antioxidants, on the other hand, quench radicals, so close proximity is favored. The interesting aspect of antioxidant protection in the core-shell particle mechanism is the necessity of an absorber in the particle shell. This requirement suggests that the antioxidant mechanism cannot provide adequate protection on its own in the core-shell particle geometry, but can greatly improve protection when used in conjunction with a UV absorber.

4.4.2 UV absorber-antioxidant hybrid particles

A significant increase in protection from UV radiation has been observed in most cases when a protectant molecule has been added to a particle formulation. Previously only one protectant has been used per core-shell particle configuration. It was noted in section 4.3 that vitamin E did not offer as much protection as the UV absorbers when it was the only protectant present in a formulation. Section 4.4.1 suggested that vitamin E could offer significant protection when placed in the core of the particle geometries, but this increased protection only occurred when another protectant was present in the shell. To further explore the protective capacities of vitamin E in the core-shell particle environment, particle configurations featuring vitamin E in the core and a UV absorber in the shell, known as hybrid particles, have been created and analyzed. These particles contain the same 1:33 ratio of total protectant to beta-carotene, except that half of the protectant is the vitamin E in the core and the other half is the UV absorber in the shell. The hybrid particles are compared to particles containing the 1:33 ratio of vitamin E in the core and particles containing the 1:33 ratio of UV absorber in the shell.

Uniform particles containing both oxybenzone and vitamin E were synthesized in chapter 2 and found to perform very well. A chart of the decay curves for the core-shell version of such particles is presented in figure 4.14. The solid hybrid particles offered significantly more protection than their orange and uniform counterparts, as demonstrated in figure 4.14a. The pomegranate/raspberry hybrid particles offered much more protection than the raspberry particles, although they overlap with the pomegranate particles through 30 minutes of exposure and have slightly less beta-carotene degraded at

the end of 60 minutes. Overall, the oxybenzone and vitamin E hybrid particles offer better protection from UV radiation than oxybenzone or vitamin E alone.

The OMC and vitamin E combination for the uniform particles provided much greater protection than OMC alone, as OMC was very unstable in the uniform particles and vitamin E acted as a stabilizer. Figure 4.15 shows the OMC and vitamin E hybrid particles, whose performance as a combination does not mimic their uniform particle counterparts. In figure 4.15a all of the particle configurations cluster together, and the hybrid particle ultimately does slightly worse than the orange and uniform particles. Initially figure 4.15b appears as though the pomegranate particle greatly outperforms the hybrid particle. Normalized absorbance, however, has a maximum value of one. The green dashed line in figure 4.15b represents this assumption, under which the pomegranate and hybrid particles offer similar protection. The lack of increased protection could be attributed to the separation between OMC and vitamin E. While vitamin E in the core can stabilize beta-carotene, it cannot stabilize OMC except at the interface.

As with oxybenzone, the vitamin E and avobenzone combination provided a substantial amount of protection in uniform particles in chapter 2. The hybrid core-shell particles behaved similarly to their uniform particle combination formulations. The orange hybrid offered near perfect protection, as shown in figure 4.16a. The decay curve for the orange hybrid particle was comprised of values above one for the majority of the exposure, but beta-carotene cannot be created in this process so the normalized absorbance cannot have a value larger than one, so a dashed line was added to provide a more accurate estimate of protection offered by the orange hybrid particle. Even with the

aforementioned assumption, the orange hybrid particle outperforms both the orange particle with avobenzone and the uniform particle with vitamin E. The pomegranate/raspberry hybrid particle also had a decay curve whose values were greater than one, so a gray dashed line has been added to figure 4.16b to account for the inability of the particles to create beta-carotene. The hybrid performs significantly better than the raspberry particle, and the decay curve (not the dashed line) makes it appear that it also provides more protection than the pomegranate particle. When assuming a value of one for the hybrid particle, though, it is clear that the protection provided is similar to that of the pomegranate particle.

Particle configurations containing the antioxidant vitamin E in the core and a UV absorber in the shell were analyzed. The protectants were present in a 1:33 ratio, where half of the protectant was vitamin E and the other half was an absorber. A decrease in protection was observed with OMC for both orange and pomegranate/raspberry hybrid particles, whereas an increase in protection was seen when avobenzone and oxybenzone were used. The lack of response of the OMC particles could be due to an insufficient amount of absorber in the shell to protect effectively, or to the instability of the OMC molecule, as was discussed in chapter 2. OMC reacts differently from oxybenzone and avobenzone when absorbing UV radiation, as it contains only one aromatic ring while oxybenzone and avobenzone molecules have two. Since section 4.3 found OMC to be very effective in the core-shell geometries when OMC comprised the whole of the 1:33 ratio and sections 4.3 and 4.4.1 discovered the requirement that vitamin E be used with an effective protectant in the shell, it is likely that the problem with OMC is one of concentration. Oxybenzone and avobenzone, however, are relatively stable and provide

adequate UV protection, so decreasing the concentration of the absorber to add vitamin E to the core proved to enhance UV protection. The hybrid particles have determined that as long as there is a sufficient amount of a stable absorber in the particle shell, adding vitamin E to the core will have positive effects.

4.4.3 Additional oxybenzone and vitamin E configurations

Vitamin E behaves differently in the core-shell particle configurations from how it did in the uniform particles, as evidenced in previous sections. Chapter 2 saw vitamin E performing well as a protectant by itself, and offering superior protection when coupled with a UV absorber. It was expected that vitamin E would be most effective in the core of a core-shell particle, where its antioxidant mechanism could work best by being in direct contact with beta-carotene. The opposite effect was observed; in section 4.3 it was found that vitamin E offered adequate protection when present in the shell of the particle, but only moderate protection when located in the core. Sections 4.4.1 and 4.4.2 showed that vitamin E could be a very effective protectant when present in the core of a particle, as long as a protectant was also present in the shell.

Formulations containing both oxybenzone and vitamin E have been shown to provide ample UV protection. Additional particle configurations containing the two protectants were studied to observe the effect of UV absorber and antioxidant placement. The first configuration was a shell hybrid particle, where the shell contained 0.05g of each oxybenzone and vitamin E, resulting in a total of 0.1g of protectant (or a 1:33 beta-carotene to protectant ratio). Comparing the shell hybrid to the oxybenzone and vitamin E

hybrid in section 4.4.2 will shed light on the importance of the compartment that vitamin E is located in. The second hybrid is a combination of the shell hybrid and that examined in section 4.4.2. This core/shell hybrid will be identical to the shell hybrid, except it will be made with the same seeds as that in section 4.4.2. The aim of this hybrid is to determine if it would be beneficial to have vitamin E in both the core and shell of the particle.

The shell hybrid particles call on vitamin E to act as both a UV absorber and an antioxidant. The tendency of vitamin E to absorb UV radiation aids oxybenzone in shielding the core of the particle from exposure to UV. The antioxidant properties of the molecule can quench oxybenzone radicals before the absorber degrades, slowing the loss of protection. An analysis of the shell hybrid particles is shown in figure 4.17, with orange-type particles in figure 4.17a and pomegranate-type particles in figure 4.17b. The beta-carotene in the shell hybrid particles degrades slower than in the orange particles with oxybenzone, but at the end of 60 minutes 45% of the beta-carotene is degraded in both particles. The orange particle with vitamin E performs the best, with the hybrid containing oxybenzone in the shell and vitamin E in the core close behind. The pomegranate-type particles behave very differently, with both hybrid particles outperforming their single protectant counterparts, the shell hybrid offering the most protection.

The core/shell hybrid particle containing oxybenzone and vitamin E in the shell along with vitamin E in the core of the particles was only explored with the pomegranate particle configuration since it has continually offered the best UV protection. The decay curve for this particle along with particles representing each absorber individually

(pomegranate with oxybenzone, pomegranate with vitamin E, raspberry with vitamin E) are shown in figure 4.18. Only slight beta-carotene decay was observed after 60 minutes, so exposures were completed through 120 minutes to better evaluate the particles' performances. The decay curve for the core/shell hybrid particle fluctuates during the first 60 minutes of exposure, although the protection remains similar to that provided by the other particles. During the second half of the exposures the core/shell hybrid particle curve stabilizes and approximately 90% of the beta-carotene was retained after 120 minutes of UV exposure. The pomegranate particle with vitamin E performs similarly, and both outperform the other particles only slightly. This suggests that the protective capacity of the particle with a single protectant is so high, that using a combination of protectants may not be necessary to achieve optimum UV protection.

The goal of this section was to determine the best performing hybrid particle containing both oxybenzone and vitamin E. Figure 4.19 contains a comparison of the hybrid from section 4.4.2 (oxybenzone in the shell, vitamin E in the core), the shell hybrid, and the core/shell hybrid (oxybenzone and vitamin E in the shell, vitamin E in the core). A dotted line was used to approximate a 100% retention of beta-carotene for the latter half of shell hybrid exposures since a normalized absorbance value of greater than 1 is not possible. The decay curves for the hybrids fluctuate dramatically for the first 40 minutes of exposure, but at exposures greater than 40 minutes they all show only 0-10% decay of beta-carotene. The nearly perfect protection observed for all of the hybrids implies that the vitamin E and oxybenzone combination is so effective that the placement of the protectants has no significant effect. The level of protection and similarity of the decay curves for all of the hybrid particles are due to both the ability of oxybenzone and

vitamin E to work well together as well as the tendency of the vitamin E particle to act as both a UV absorber and an antioxidant. When vitamin E is present in the core of the particles, it acts as a last line of defense for beta-carotene by both absorbing UV radiation before it can reach the beta-carotene molecule, and by quenching beta-carotene radicals that form. In the shell of the particles vitamin E is again able to call upon its tendency to absorb UV radiation to protect the beta-carotene in the core of the particle, but it also quenches oxybenzone radicals, slowing the decay of the protectant.

Various combinations of oxybenzone and vitamin E were examined to determine the particle configuration that provides superior UV protection. The shell hybrid was not effective for orange particles, but did slightly increase protection in pomegranate particles. When compared to its constituent particles, the core-shell particle slightly outperformed pomegranate with oxybenzone particles and raspberry with vitamin E particles, but provided similar protection to pomegranate with vitamin E particles. When the hybrids were compared, all retained 90-100% beta-carotene after 120 minutes of exposure. Overall, combination particles marginally increased UV protection over particles containing one effective protectant. The placement of the vitamin E and oxybenzone did not affect protection for exposure times through 120 minutes, suggesting that a formulation containing oxybenzone and vitamin E is so effective that placement is not a factor.

4.4.4 Conclusions

Uniform particles were examined in chapter 2 to determine the UV protection that encapsulation within a polymer particle can provide to a photosensitive molecule, both with and without the addition of UV protectants. This chapter studied the effects that change in the particle geometry can have on UV protection of an encapsulated molecule. Core-shell particles were tested with no protectant present, with one protectant in the core or shell, with one protectant in the core and shell, and with multiple protectants in various compartments. The single protectant core-shell particle schematics are in figure 4.2.

The effect of the particle geometry itself was studied by not adding protectant to the particle formulations. Figure 4.3 shows the decay of beta-carotene in solution as a reference. Beta-carotene encapsulated in uniform particles was better protected than the beta-carotene in solution, and protection increased further when beta-carotene was placed in the core of the core-shell particles. While the orange and pomegranate/raspberry particles offered similar UV protection over time, there was far less variation for the pomegranate/raspberry particles, suggesting that they offer the best protection.

The core-shell particles were examined with each formulation consisting of a single protectant, and the effectiveness was gauged by comparison to like particles (uniform vs. orange and pomegranate vs. raspberry). The effect of concentration was studied by varying the amount of oxybenzone in each formulation. Orange and uniform particles saw an increase in protection with the increase in oxybenzone concentration. The protection provided was similar until the 1:100 ratio, where the orange particles were superior. Oxybenzone and avobenzone provided the best protection in uniform particles,

while avobenzone and vitamin E protected best in the orange configuration. The orange particles generally protected better than the uniform particles, most likely because of the addition of the particle shell. Raspberry particles also saw an increase in protection when oxybenzone was increased from the 1:10 to 1:33 ratio, but a plateau was reached and no further protection was observed when increasing to the 1:100 ratio. The pomegranate particle was unaffected by the change in oxybenzone concentration, but pomegranate particles offered better protection than raspberry particles until the 1:100 ratio. The ideal formulation for pomegranate particles contained either OMC or avobenzone, while raspberry particles benefitted from the use of vitamin E or OMC. Pomegranate particles generally offered more protection than raspberry particles, suggesting that the shell is the ideal location for protectant placement.

Additional particle configurations were examined where protectant was present in multiple compartments within the particle. Split particles contained the same amount of protectant as the single protectant formulations, except the amount of protectant was split equally between the core and shell. The orange particle performed well when OMC was split, while oxybenzone worked best for the pomegranate/raspberry split. Vitamin E had a positive impact on the split particles for both geometries. Hybrid particles with a UV absorber in the shell and vitamin E in the core were also examined. Formulations including avobenzone and oxybenzone saw improvements in the hybrid configuration, while OMC received no benefit. A shell hybrid was also studied with oxybenzone and vitamin E in the shell. The shell hybrid saw no increase in protection for the orange particle, but the pomegranate particle did see an increase in protection. An additional hybrid was the core/shell hybrid, where oxybenzone and vitamin E were placed in the

shell of the particle, and vitamin E was also present in the core. All of the oxybenzone and vitamin E hybrid particles performed similarly, suggesting that the specific combination of UV absorber and antioxidant protects well enough that the location of the protectants has no significant effect.

The differences in UV protection when the location of the protectants was varied allowed analysis of the effect of proximity. In solid particles, the orange particles provided similar if not better protection than the uniform particles. This suggests that the larger distance between the beta-carotene and protectant molecules is desired for the best UV protection. The same was observed for the encapsulated suspensions, as the pomegranate particles provided the same or better protection than the raspberry particles. The only case where it was beneficial to have protectant in the core was when the protectant was vitamin E, but even then optimal protection was achieved with a UV absorber in the shell. Overall, UV absorbers provide the most protection when the distance between beta-carotene and UV absorber molecules is maximized.

The core-shell particles offer more UV protection than the uniform particles since they are aided by the addition of a protective shell that completely surrounds all of the beta-carotene. The addition of a single protectant to the formulations had a positive effect in most cases, as did an increase in protectant concentration. The best protection was observed when protectant was present in both the core and shell, most notably with hybrid particles containing both oxybenzone and vitamin E.

4.5 Figures for Chapter 4

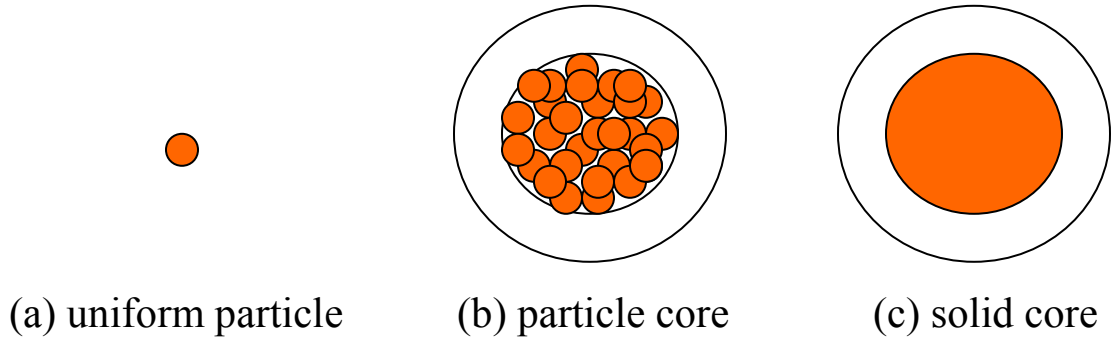

Figure 4.1: Schematic view of the geometries obtained when no protectant is used for (a) uniform particles, (b) particles with particles in the core, and (c) particles with a solid core. The white areas represent polymer with no protectant or beta-carotene, and the orange areas represent a composite of polymer and beta-carotene.

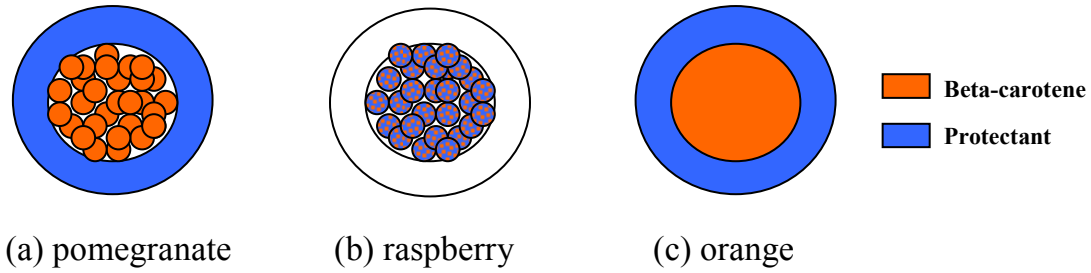

Figure 4.2: A schematic view of the particle geometries when protectant is added to one compartment. The (a) pomegranate particle is a core-shell particle with protectant in the shell and a core of particles containing beta-carotene. The (b) raspberry particle is a particle with particles in the core where the shell contains no additive and the particles in the core contain both protectant and beta-carotene. And the (c) orange is a solid core particle with protectant in the shell and beta-carotene in the core.

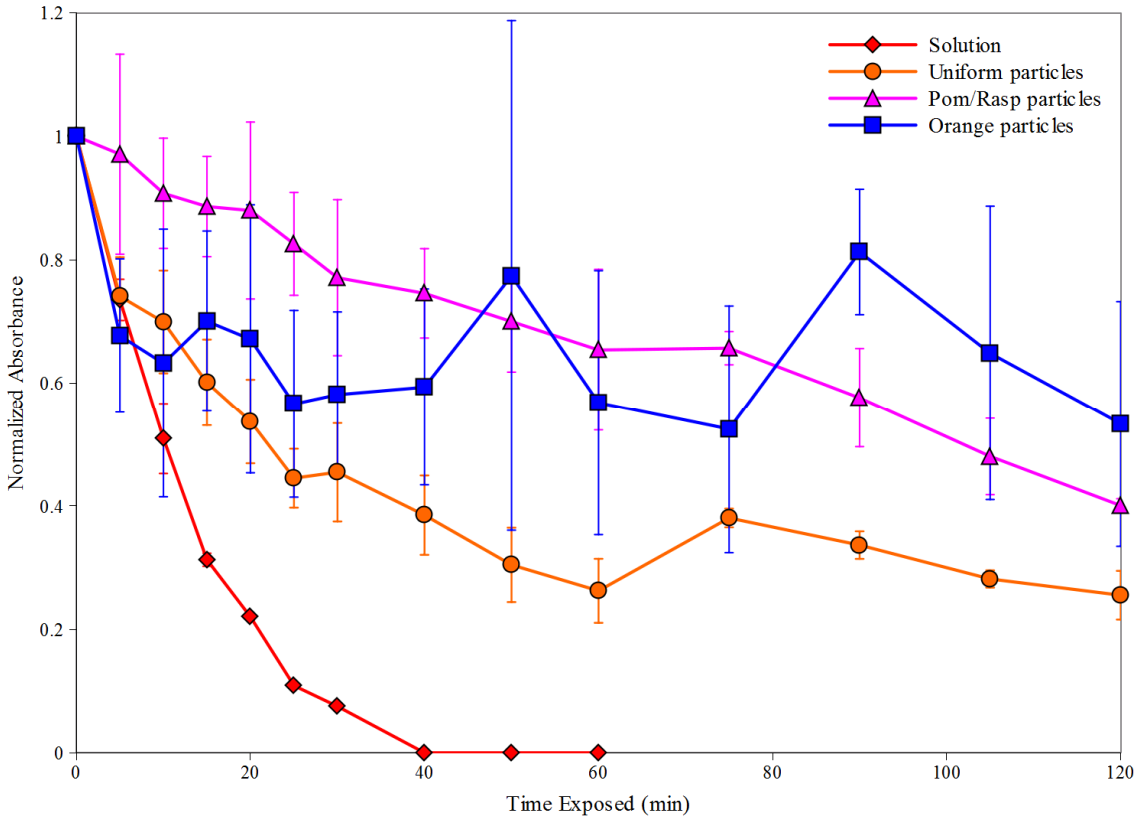

Figure 4.3: A comparison of a solution of beta-carotene with each particle geometry when no protectant was added.

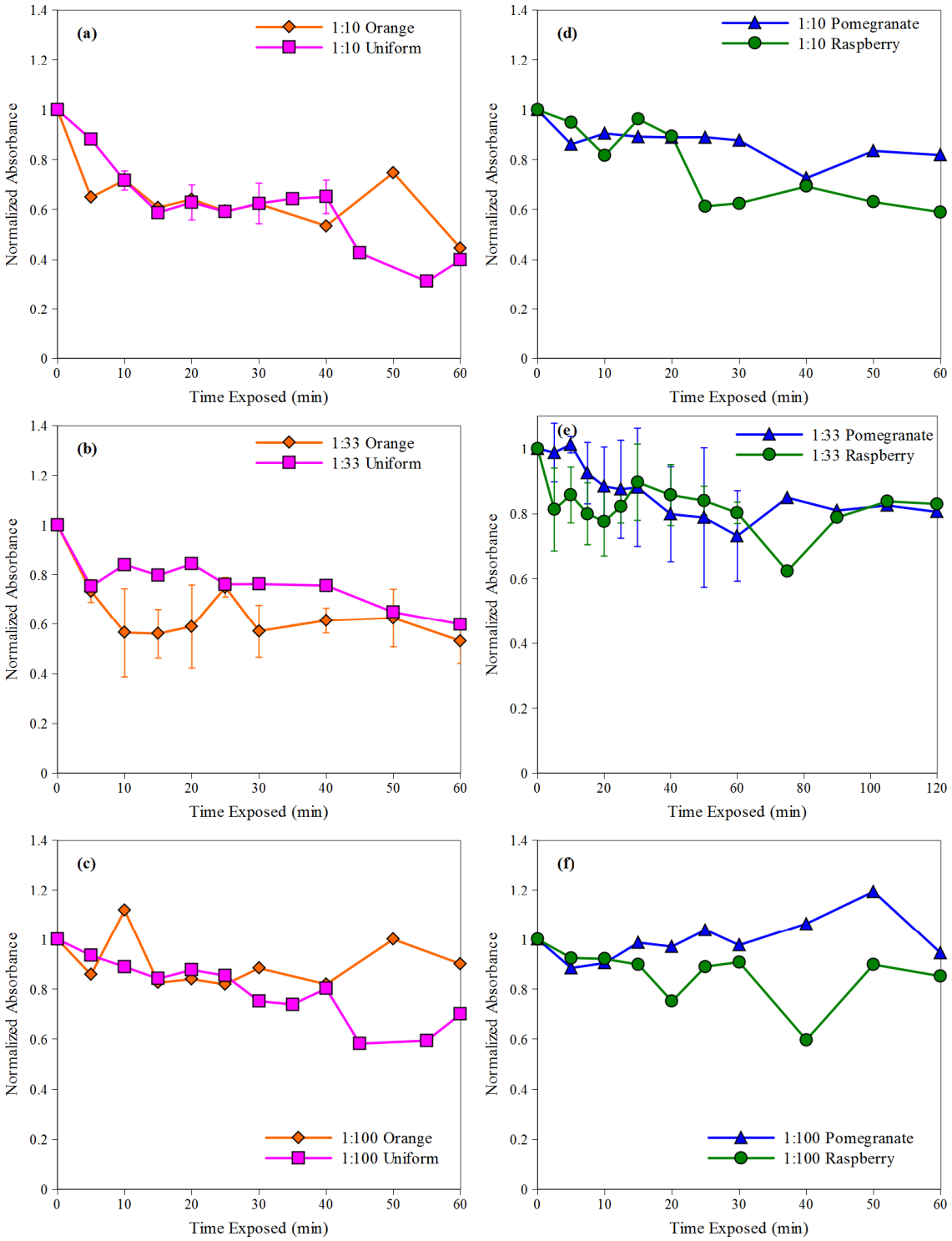

Figure 4.4: The effect of proximity when particles contain varying amounts of oxybenzone in each of the particle geometries. Figures 4.4a-c in the column on the left are for solid particles (uniform and orange) and figures 4.4d-f in the column on the right represent particles that contain smaller particles in the core (pomegranate and raspberry).

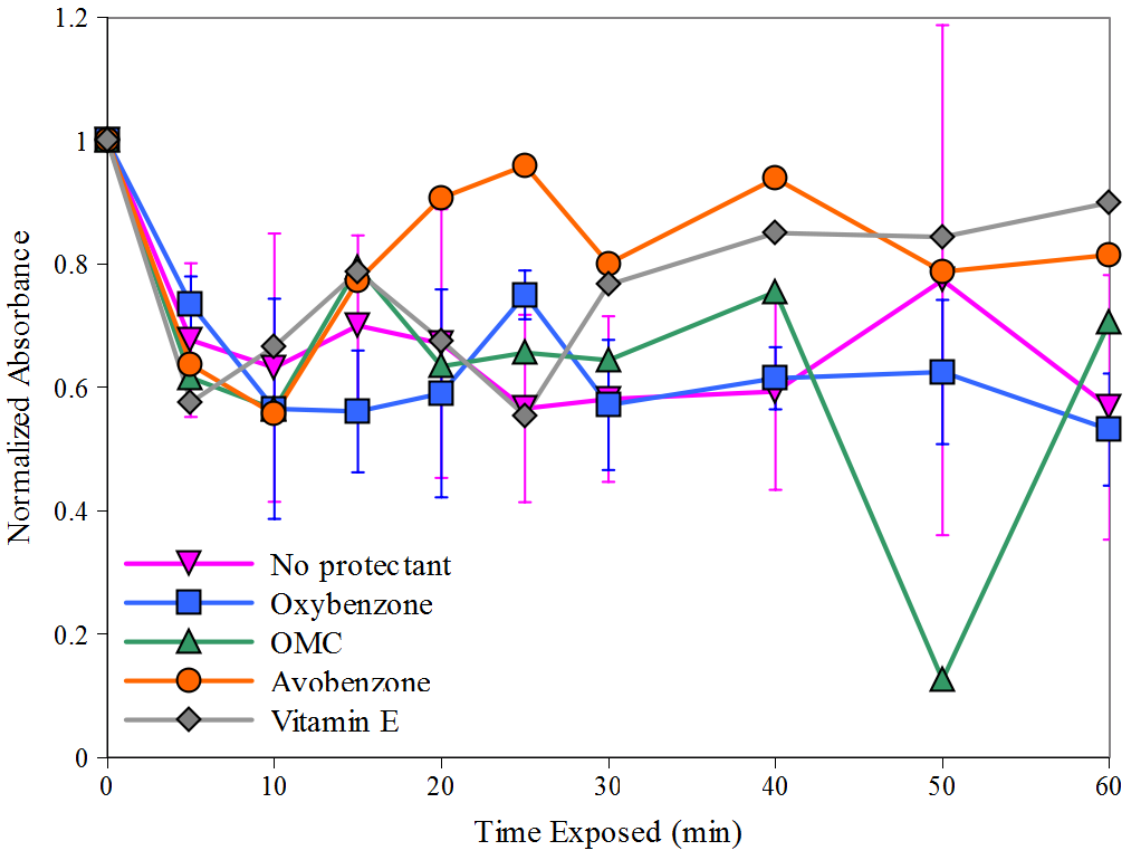

Figure 4.5: Decay curves demonstrating the effect of protectant on the protection provided by orange particles.

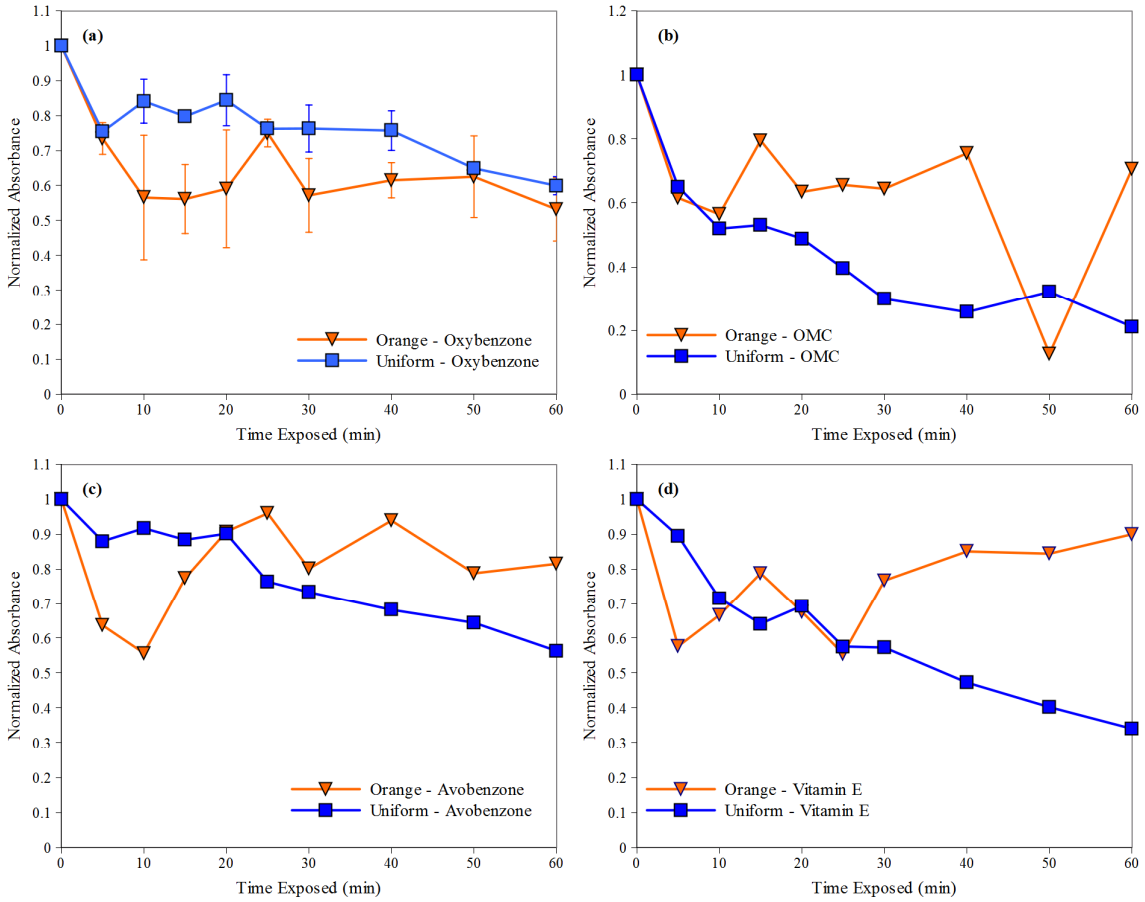

Figure 4.6: A comparison of the protection provided by (a) oxybenzone, (b) OMC, (c) avobenzone, and (d) vitamin E in the orange and uniform particles.

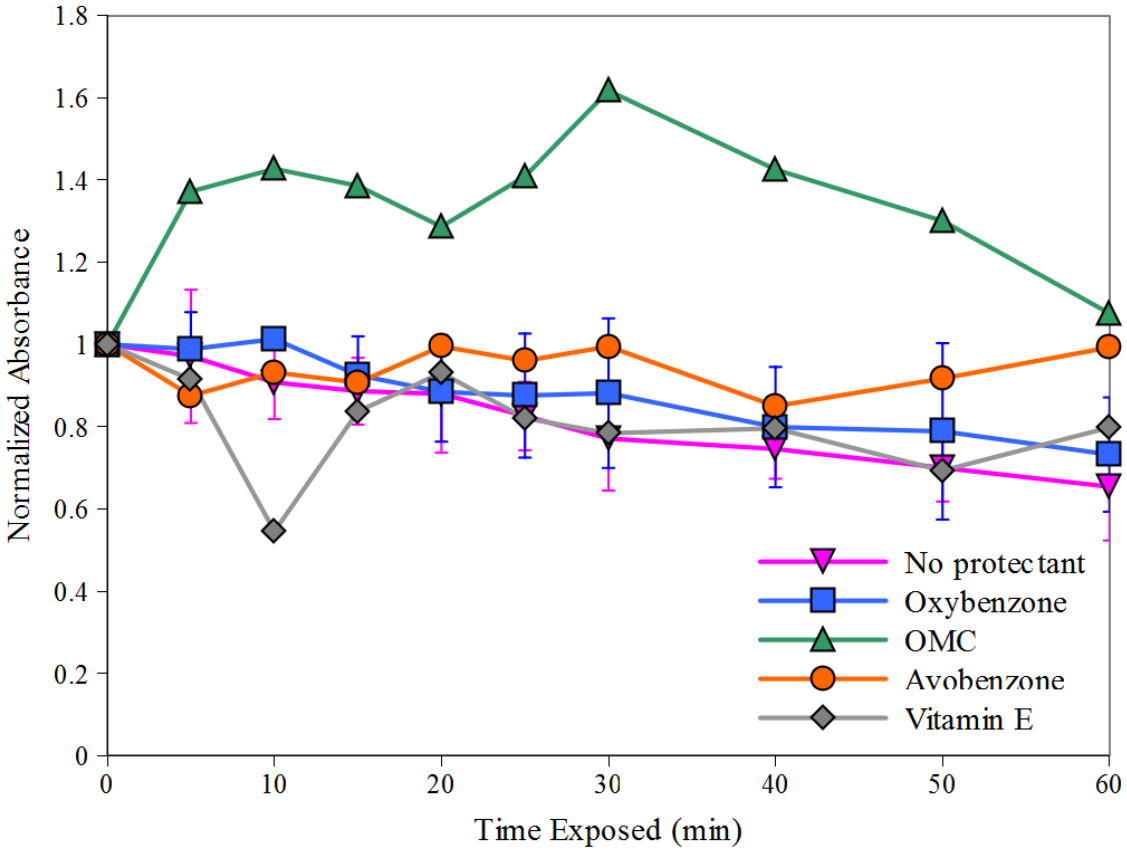

Figure 4.7: Decay curves for the pomegranate particle containing no protectant, oxybenzone, OMC, avobenzone, and vitamin E.

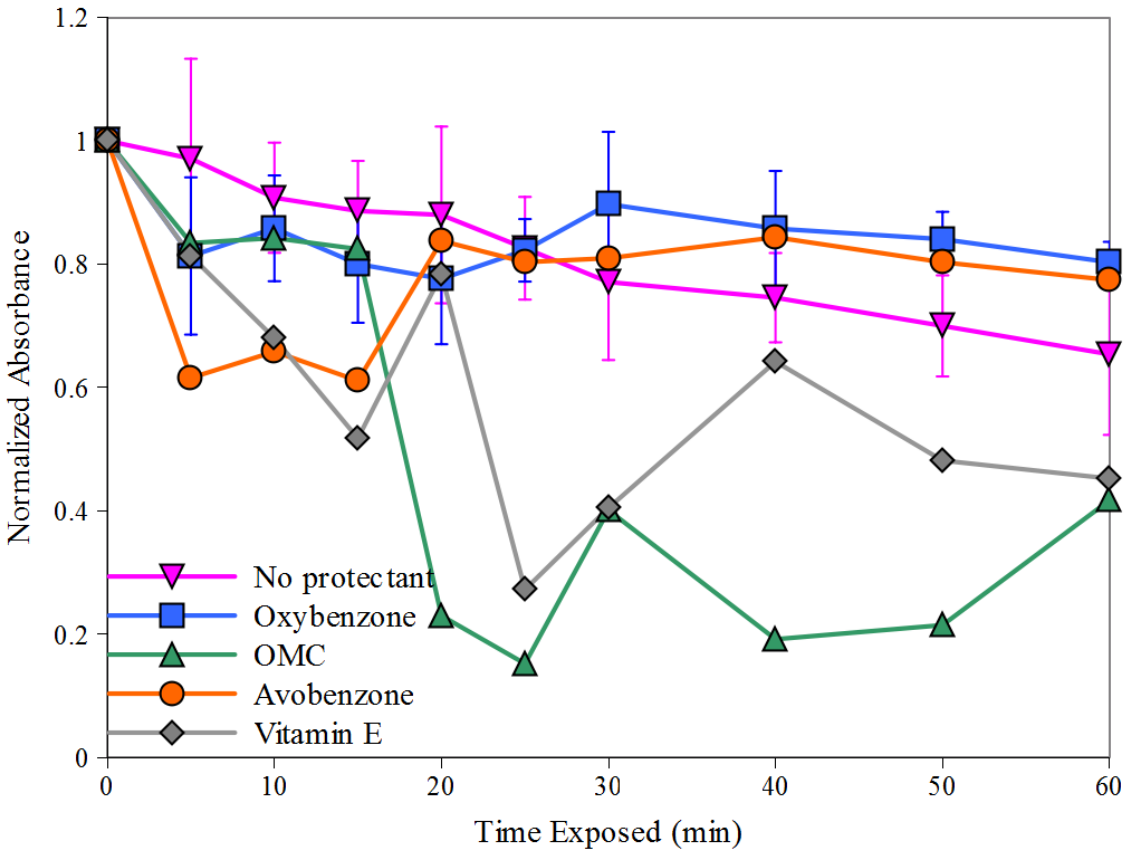

Figure 4.8: The effect of protectant on the decay curves for raspberry particles.

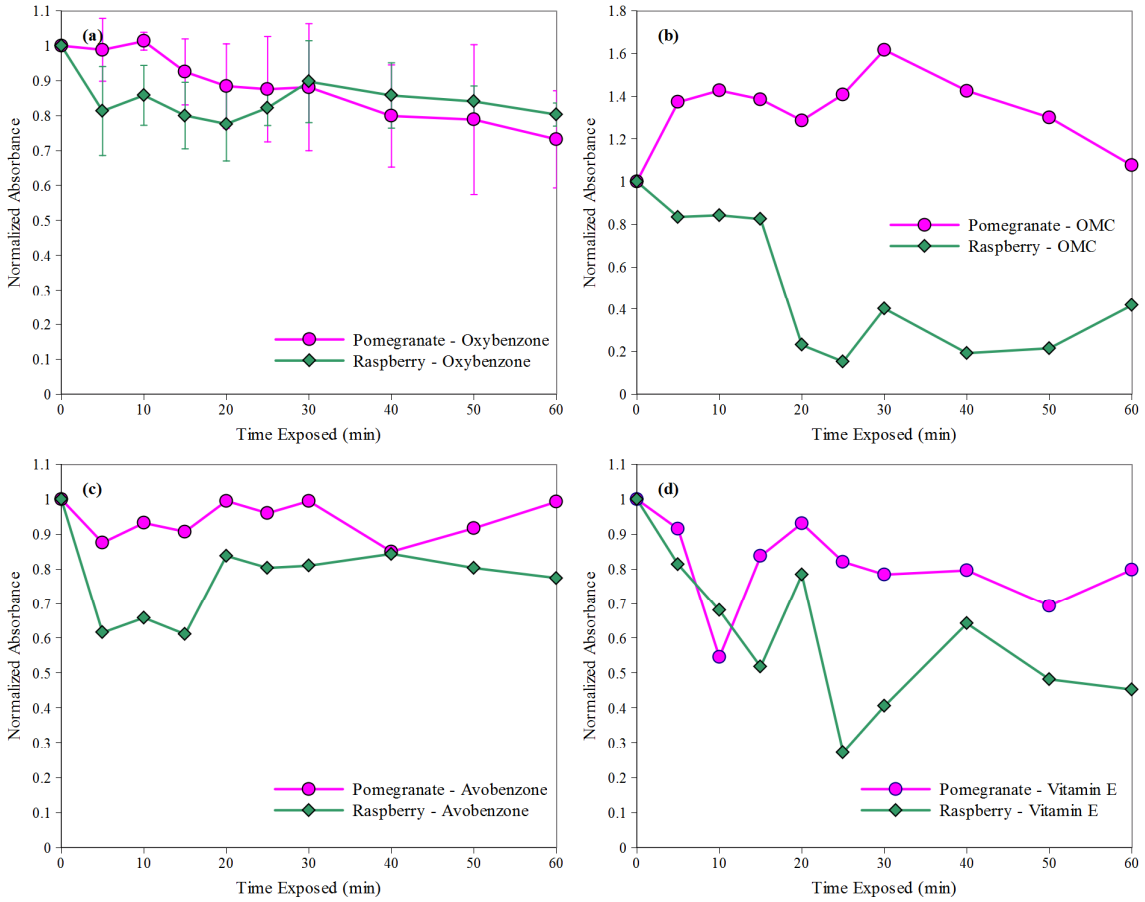

Figure 4.9: A comparison of the protection provided by (a) oxybenzone, (b) OMC, (c) avobenzone, and (d) vitamin E for the pomegranate and raspberry particles.

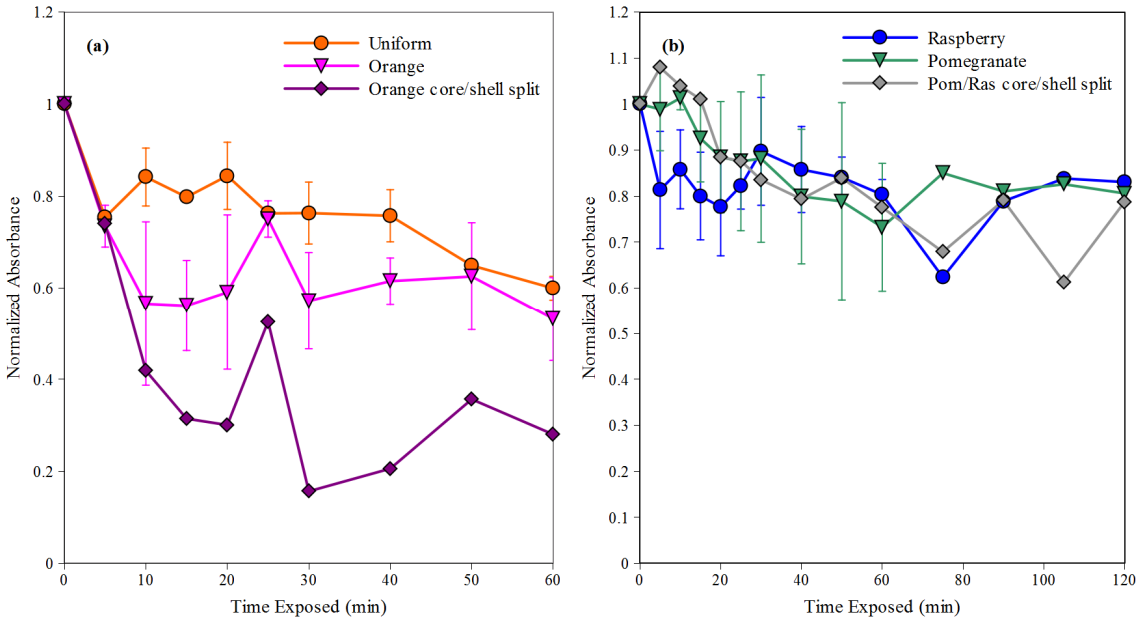

Figure 4.10: Decay curves when oxybenzone in split between the core and shell of (a) orange particles and (b) pomegranate/raspberry (pom/ras) particles.

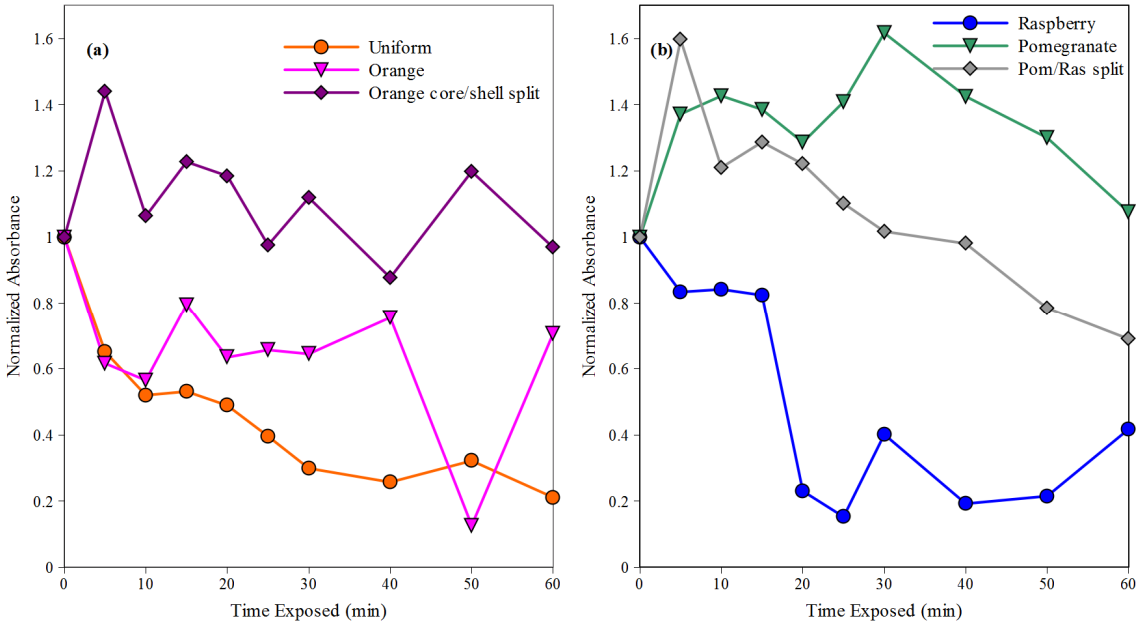

Figure 4:11: Decay curves demonstrating the effect of splitting OMC concentration between the core and shell of (a) orange particles and (b) pomegranate/raspberry (pom/ras) particles.

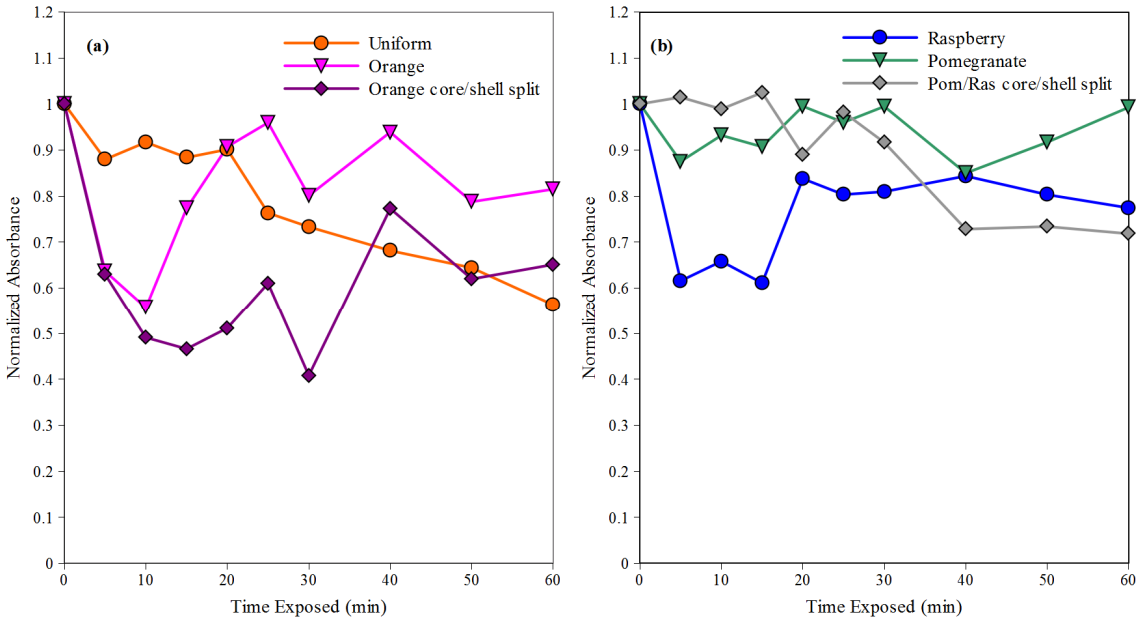

Figure 4.12: The effect of splitting avobenzone between the (a) orange and (b) pomegranate/raspberry (pom/ras) particles on beta-carotene decay curves.

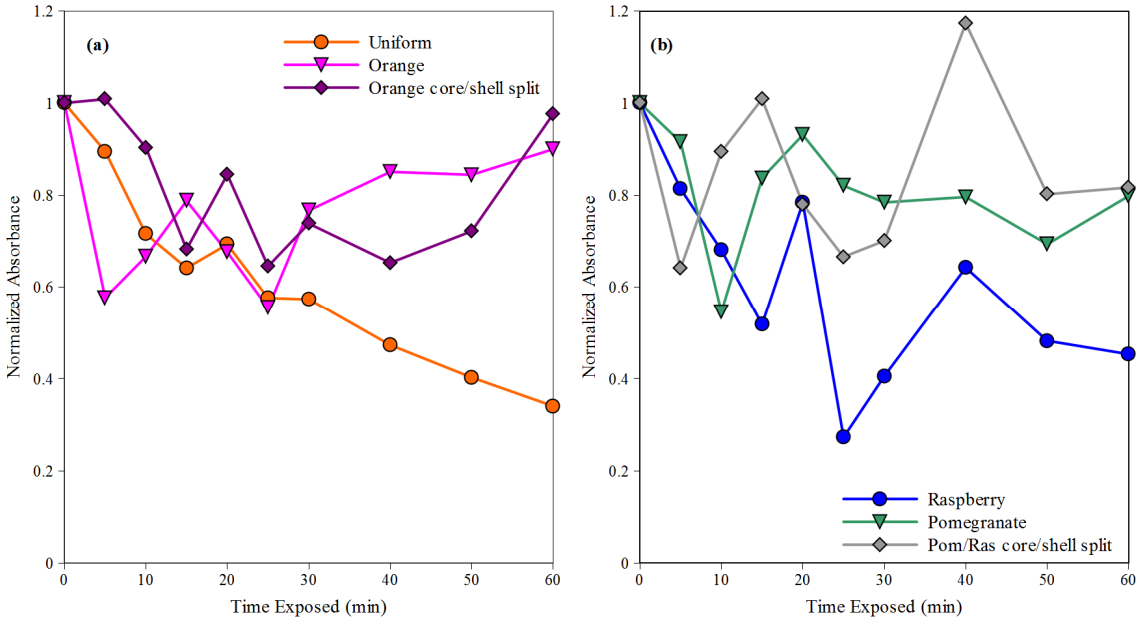

Figure 4.13: Decay curves demonstrating the effect of splitting vitamin E between the core and shell of (a) orange and (b) pomegranate/raspberry (pom/ras) particles.

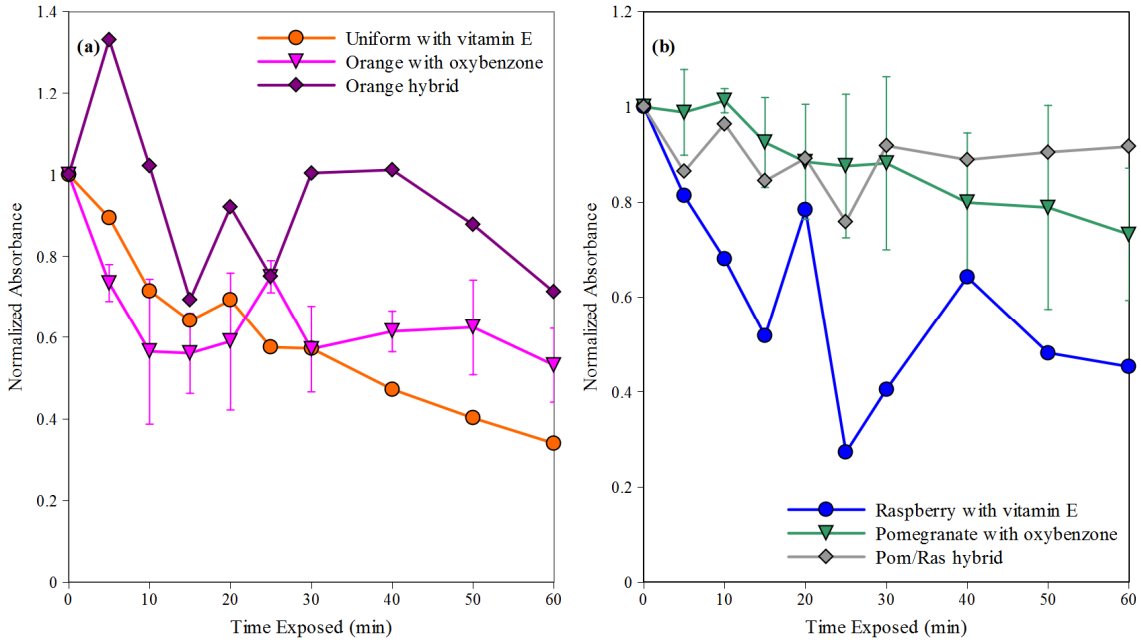

Figure 4.14: Decay curves when core-shell particles contain oxybenzone in the shell and vitamin E in the core of (a) orange and (b) pomegranate/raspberry (pom/ras) particles.

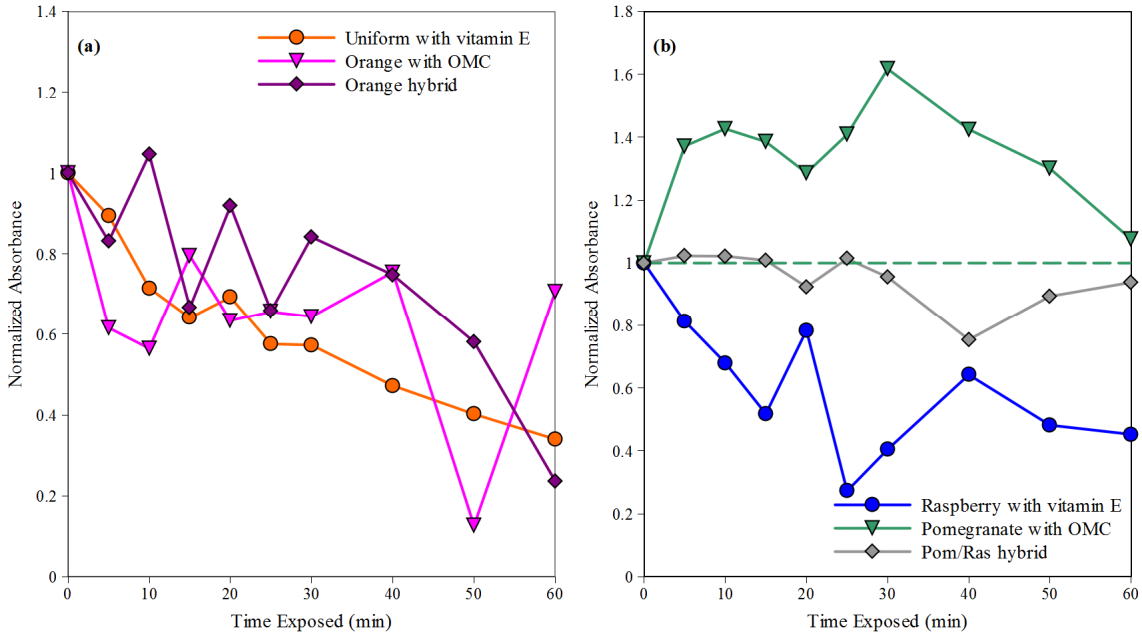

Figure 4:15: The effect of adding OMC to the particle shell and vitamin E to the particle core to decay curves of (a) orange and (b) pomegranate/raspberry (pom/ras) particles. A dashed line was added for the pomegranate particles containing OMC to assume a value of 1 since normalized absorbance cannot have a value higher than 1.

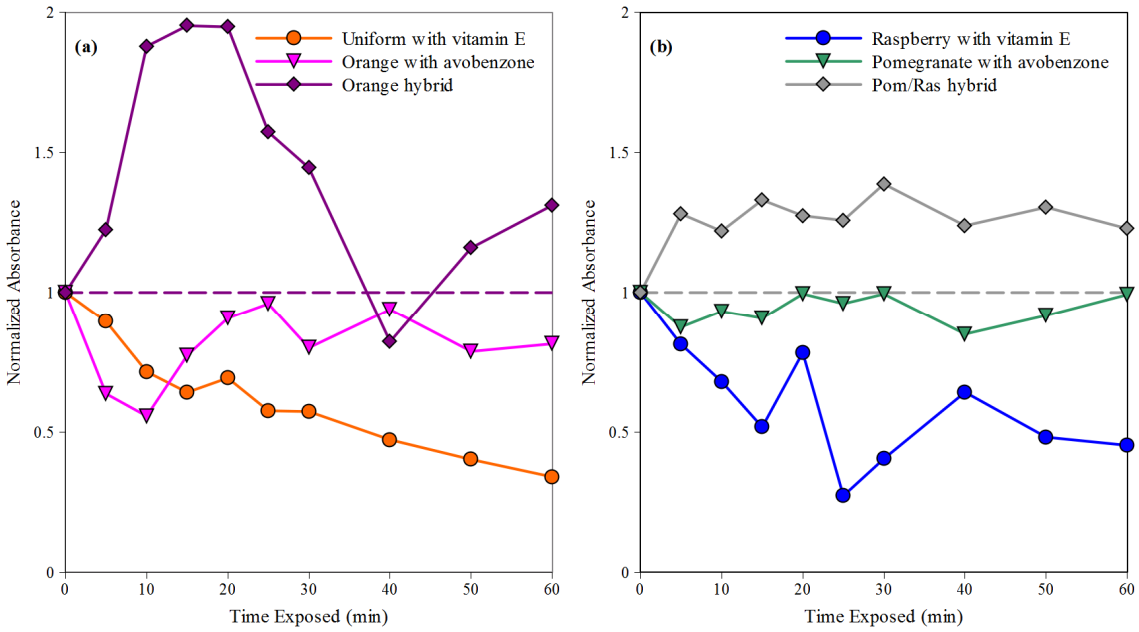

Figure 4.16: Hybrid avobenzone particles containing avobenzone in the shell and vitamin E in the core of (a) orange and (b) pomegranate/raspberry (pom/ras) particles. A dashed line was added to approximate the orange hybrid in 4.16a since normalized absorbance cannot have a value higher than 1. The same was done for the pom/ras hybrid in figure 4.16b.

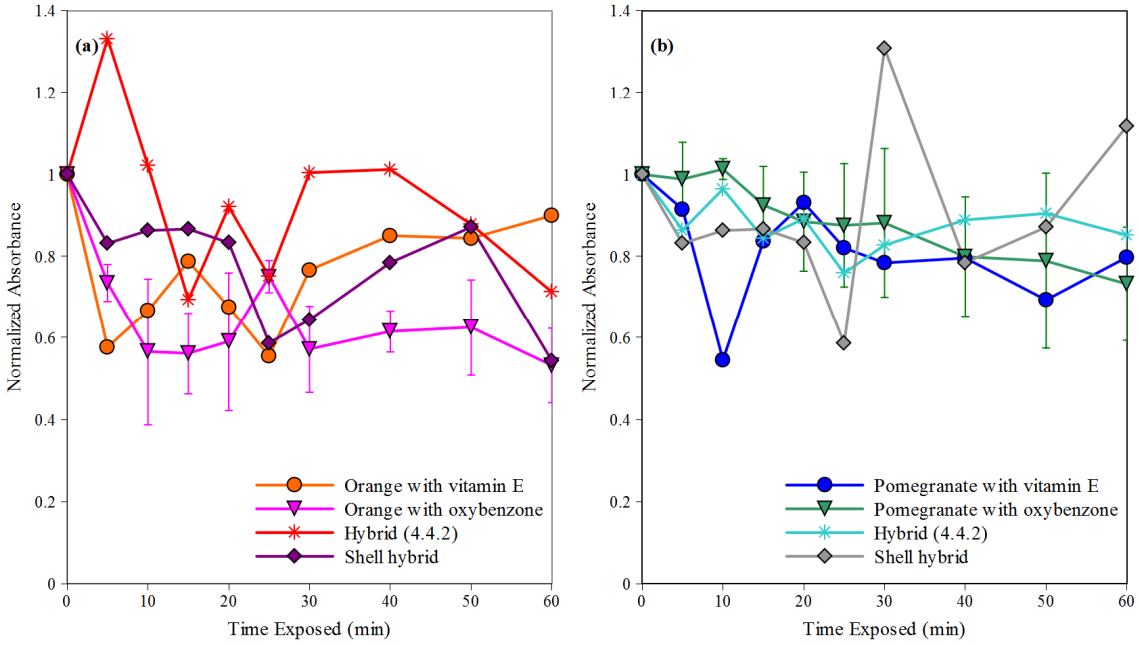

Figure 4.17: Decay curves for particles containing oxybenzone and vitamin E in the shell of (a) orange and (b) pomegranate particles.

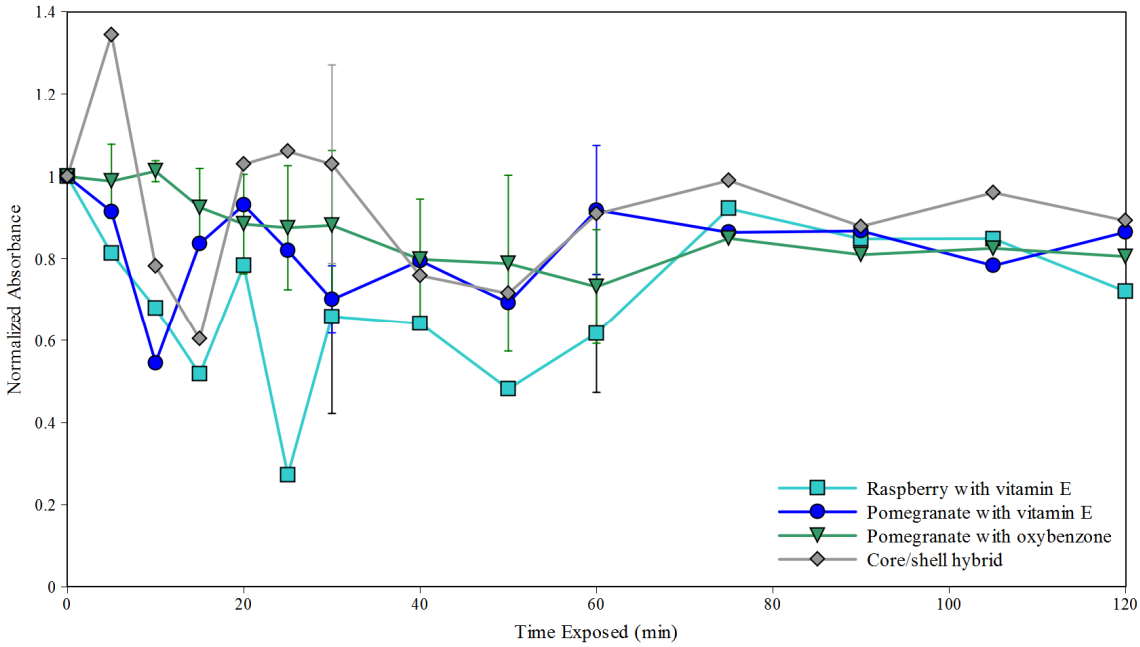

Figure 4.18: Decay curves comparing the protection provided by the pomegranate/raspberry core/shell hybrid and its constituents. The core/shell hybrid contains oxybenzone and vitamin E in the shell, along with vitamin E in the core of the particles.

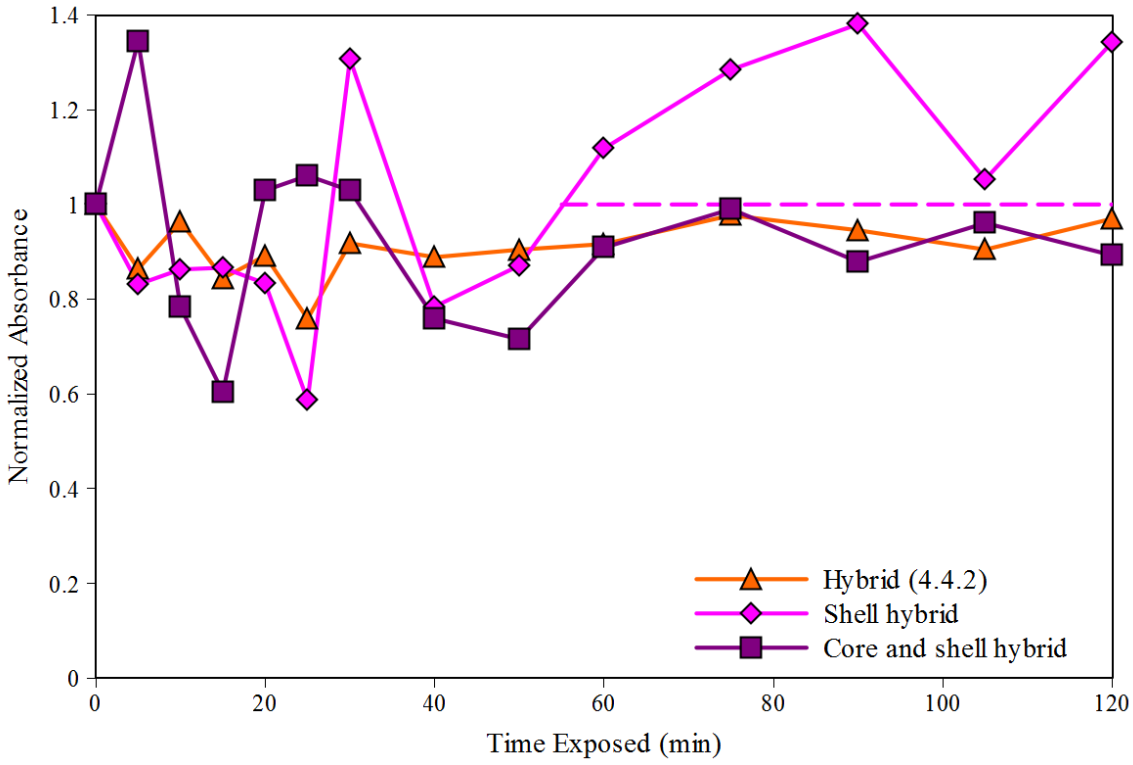

Figure 4.19: Decay curves comparing all of the pomegranate/raspberry hybrid particles. Hybrid (4.4.2) contains oxybenzone in the shell and vitamin E in the core, the shell hybrid contains oxybenzone and vitamin E in the shell, while the core and shell hybrid contains oxybenzone and vitamin E in the shell and vitamin E in the core of the particles. A dashed line was added to approximate a value of 1 for the shell hybrid when its value exceeds the highest allowable for normalized absorbance.

Chapter 5 Additional particle characteristics and their effects

5.1 Additional particle characteristics

Particle geometry, protectant, protectant amount, and placement of the protectant are some of the particle characteristics that were explored in chapters 2 and 4 due to their affect on the amount of UV protection provided. Chapter 2 discovered the ideal formulation for UV protection in a simple uniform particle environment, while chapter 4 extended these characteristics to more complex particle configurations. While these characteristics are important variables for formulations of UV protective particles, additional particle properties exist that may have an effect on UV protection.

In addition to the core-shell geometry, the particles in chapters 2 and 4 also differed quite dramatically in size. The pomegranate and orange particles also varied not just in the core contents, but in the particle size. In order to conclude that the differences in UV protection were due to geometry alone, it must be determined that the particle size must have no effect. The impact of particle size can be examined by comparing the beta-carotene decay for uniform particles of a variety of sizes.

Two configurations of core-shell particles were introduced in chapter 3. While chapter 4 investigated the effect of the solid core versus the suspension core, no changes were made to the particle shell except for the addition of protectant. The particle shell obviously plays a role in the amount of UV protection provided, as the orange and pomegranate/raspberry particles offer much better protection than the uniform particles.

The effect of the particle shell can be further examined by manipulated the shell thickness.

As the particle shell was added in chapter 4, the distance that an oxygen radical must travel to damage beta-carotene increased. The effect of this distance can be examined further by studying it in relation to the rate of reaction. The Damköhler number is a ratio of the reaction rate to the diffusion rate. Comparing the Damköhler numbers for the different particle geometries and shell thicknesses can shed light on the mechanics of UV protection in particles.

Beta-carotene was used as a model photosensitive molecule throughout this work. The decay of beta-carotene due to exposure to UV radiation is well documented, making it an ideal candidate for photosensitivity studies. Further applications of the particles can be explored by using another photosensitive molecule in place of beta-carotene, such as nifedipine, an antihypertensive medication known for its photosensitivity. The comparison of nifedipine decay in the various particle environments can display the versatility of the particles for protecting photosensitive molecules.

The effect of proximity has been studied for uniform and core-shell particles. Proximity effects can also be examined in other systems, such as solutions and polymer films, and compared to the results for particles. Collaborators at Brown University and University of Massachusetts Dartmouth have investigated both of these systems.

5.2 Particle size and shell thickness

Particle geometry was shown to have a large impact on the amount of UV protection that can be provided by particles. The methods of particle synthesis required to create the geometries produce particles of different sizes. In order to conclude that the levels of protection are due solely to geometry, a simple configuration such as the uniform particle must be studied at various sizes.

One of the geometric differences between the uniform particles and the pomegranate/raspberry and orange particles is the addition of a particle shell. The core-shell particles showed a significant increase in UV protection, as shown in figure 4.3 and discussed in chapter 4. This increase in protection was due partly to the core-shell geometry. By varying the shell thickness as described in chapter 3, it can be determined whether a change in shell thickness also changes the extent of UV protection.

5.2.1 Effect of particle size

Before particle size can be ruled out as a potential for varying UV protection, decay curves of uniform particles at various sizes must be examined. If size is not a factor, then protection is based on particle geometry, protectant location, and protectant identity. Particle size was varied by expanding upon the concept of tuning shell thickness by varying polymer[106, 107] amount in chapter 3.

Particles were synthesized using the procedure described in chapter 2, with the exception of using dichloromethane (DCM) as the solvent and varying the amount of

polymer used in the formulation. An oil phase was created consisting of 3 mg of beta-carotene, a varied amount of poly(methyl methacrylate) (PMMA) with a molecular weight of 15000, and 3 ml of DCM. No protectant was added to the particle formulations. Many repetitions have been completed in previous chapters using 0.2 g PMMA, so the amounts of polymer used in these studies were 0.3 g, 0.4 g, and 0.5 g. The aqueous phase was identical to that in chapter 2, containing 175 g of deionized water and 25 g of a stock 4% solution of poly(vinyl alcohol) (PVA). The oil phase was blended into the aqueous phase for 3 minutes at 15000 rpm using an UltraTurrax T25 basic disperser by IKA. The emulsion was stirred for approximately 4 hours to allow the DCM to evaporate. The particles were then collected via centrifugation and resuspended in 20 ml of deionized water using a sonicator. Particles were further diluted by adding 3 ml of the suspension to 30 ml of deionized water. The resulting dilute suspension was used for exposures. The method of exposing the particles to UV radiation is the same as that used in previous chapters.

As mentioned previously in the text, 0.2g PMMA uniform particles are approximately one micrometer in diameter. The additional formulations were measured using a Beckman-Coulter LS-13 320 Laser Diffraction Particle Size Analyzer. Larger particles cannot stay suspended without agitation; therefore laser diffraction had to take the place of dynamic light scattering as the method of particle size analysis. The average particle sizes were approximately 20 micrometers for the 0.3 g PMMA particles, 25 micrometers for 0.4 g PMMA particles, and 37 micrometers for 0.5 g PMMA particles. The increase in particle size with larger concentrations of polymer proves that particle size can be altered through the variation of polymer amount added to the formulation.

The results of the variance of particle size can be found in figure 5.1 as beta-carotene decay curves for each formulation. All of the curves overlap significantly for the duration of the exposures, suggesting that the size of the particle has no effect on the amount of UV protection provided. The act of encapsulation increases UV protection, but changing the amount of polymer between the UV radiation and photosensitive molecule or the curvature of the particle surface has no effect. This deduction confirms that the differences in UV protection provided by the various particle types are due to geometry alone.

5.2.2 Effect of varying shell thickness

The comparison of uniform to core-shell particles in chapter 4 suggested that the more complex geometry of the core-shell particle is an important factor in UV protection in a particle environment. The most obvious difference between the uniform and core-shell particles is the addition of a particle shell. The effect of the particle shell can be further explored by varying the shell thickness.

In chapter 2, orange particles (core-shell particles with a solid core) were synthesized with a variety of shell thicknesses. As discussed in chapter 2, the shell thickness was varied by altering the amount of polymer in the oil phase using the following amounts: 0.15, 0.175, 0.2, 0.225, 0.25, 0.3, 0.35, 0.4, 0.45, and 0.5 g of PMMA. These changes in polymer concentration yielded particles with increasing shell thickness as the polymer amount was increased. UV exposures were performed as described in chapter 4 on particles made with 0.2, 0.3, 0.4, and 0.5 g of PMMA. The

particles were analyzed both with and without oxybenzone at a 1:33 beta-carotene to oxybenzone ratio.

The effect varying shell thickness has on the amount of UV protection provided when no protectant is present can be found in figure 5.2a. Although the data exhibits a lot of variance, the four curves generally overlap for the majority of the exposures, suggesting that the change in shell thickness had no impact on the level of UV protection. This finding is not surprising following similar results in the previous chapter. Figure 5.2b shows the beta-carotene decay curves for particles with varying shell thickness when oxybenzone is present. The particles containing 0.2 g of PMMA in the particle shell exhibited the worst protection, with 50% of the beta-carotene lost after an hour of UV exposure. The formulations containing 0.3, 0.4, and 0.5 g of PMMA offer more protection, but the decay curves appear in a cluster providing approximately 90-100% protection over 60 minutes of UV exposure. The stepwise change in protection suggests a threshold of polymer needed for the oxybenzone to be adequately dispersed in the particle shell, therefore offering optimal protection. The particles without protectant did not display this step behavior because there was no protecant to disperse. Figures 5.2a and b display the tendency of core-shell particles without protectant to be unaffected by a change in shell thickness, while particles containing a protectant must pass a threshold of polymer amount that allows the protectant to be completely dispersed.

5.2.3 Particle size and shell thickness conclusions

Particle size was altered by varying the amount of polymer used in the particle formulations. Altering the particle size in this way changes the amount of polymer that UV radiation must travel through in order to reach beta-carotene not contained on the surface of the particle. The additional polymer also allows more room for the beta-carotene to distribute itself. Despite these environmental changes within the particle, figure 5.1 showed that particle size has no effect on the amount of UV protection provided by encapsulation in a simple particle.

Core-shell particles have been shown to provide much more UV protection than uniform particles. One obvious difference between the particle geometries is the addition of a shell to the core-shell particles. The shell seemed to create a large difference in particle protection, so the effect of shell thickness was explored. Shell thickness was shown to have no effect when particles contained no protectant, as in figure 5.2. When particles contained oxybenzone, a jump in protection was observed between 0.2 g and 0.3 g of PMMA, suggesting that there is a critical amount of polymer required for a protectant to disperse properly.

5.3 Diffusion/reaction analysis via dimensionless numbers

There are two steps to beta-carotene oxidation in the particles. The first step is for oxygen to diffuse through the particle in order to come into contact with a beta-carotene molecule. Once oxygen and beta-carotene molecules are in contact, they can react with

the aid of UV radiation, causing the beta-carotene to degrade. The total rate of beta-carotene decay is a combination of the rates of oxygen diffusion and its reaction with beta-carotene. In order to further study the process, the Damköhler number for each particle geometry was calculated.

The Damköhler number is a dimensionless quantity calculated as the ratio of the reaction rate to the rate of mass transport. In the particles, this ratio is the rate of reaction between beta-carotene and oxygen and the rate of diffusion of oxygen through the particle. A large Damköhler number corresponds to the rate of beta-carotene decay being dependent on diffusion, while a small Damköhler number means that the reaction is controlling the rate. Equation 5.1 shows the general equation for calculating the Damköhler number.

$$Da = \frac{kC_{A0}^{n-1}L^2}{D_{AB}} \tag{5.1}$$

The Damköhler number is dependent on the reaction rate constant (k), the initial concentration of oxygen (C_{A0}), the reaction order (n), the characteristic length (L), and the diffusion coefficient of oxygen through PMMA (D_{AB}). El-Tinay and Chichester[66] found the reaction between beta-carotene and oxygen to be a zero order reaction, causing equation 5.1 to become equation 5.2.

$$Da = \frac{k_0 L^2}{C_{A0} D_{AB}} \tag{5.2}$$

The values used for each parameter can be found in table 5.1. The characteristic length was calculated as the radius of uniform particles and the shell thickness for the orange and pomegranate/raspberry particles. An additional characteristic length was calculated by adding the shell thickness of the pomegranate/raspberry particles and the radius of the

uniform particles to account for the additional distance the oxygen would have to travel through the uniform particles after entering the particle core.

The Damköhler number was calculated for each particle geometry, and the values can be found in table 5.2. The Damköhler number in each case is large, ranging from 10 to 27640. The large Damköhler number indicates that the rate of beta-carotene decay in the particles is limited by the diffusion of oxygen through the particle to interact with beta-carotene. This would be expected since diffusion through a polymer is usually slow and photochemical reactions are rapid on a molecular level. The largest Damköhler numbers are for the pomegranate/raspberry particles, both with and without the radius of the uniform particle added. This offers some explanation as to why the pomegranate/raspberry particles provided the best protection in chapter 4. Not only do the pomegranate/raspberry particles have an additional interface for scatter, but their shell thicknesses are larger, making it more difficult for oxygen to diffuse through to the beta-carotene. The next largest Damköhler number is for the orange particles, and the uniform particles have the smallest Damköhler number. The values of the Damköhler numbers correspond with UV protection provided, with particles described by the largest Damköhler number providing the most UV protection. This suggests that the Damköhler number could be a good indicator of the quality of UV protection provided by particles to encapsulated molecules.

Because the Damköhler number revealed that the rate of beta-carotene decay in the particles is mainly controlled by the diffusion rate, the shrinking core model may be used to approximate the system.[109] The shrinking core model is based on a particle or pellet suspended in a media in which a reactant is present. As the material at the surface

of the particle begins to react, the reactant must diffuse further into the particle to reach more reactive material. This can be used to approximate the uniform particles, where it is likely that the beta-carotene at the surface of the particle is the first to decay as oxygen diffuses through the particle. The time necessary for all beta-carotene in the particle to completely decay can be calculated, but in chapter 2 it was found that approximately 10% of the beta-carotene remained after 60 minutes of exposure. The following equation can be used to approximate the amount of time it would take for 90% of the beta-carotene in the particle to decay:

$$t = \frac{\rho_{\beta-carotene} R_0^2 \phi_{\beta-carotene}}{6 D_{AB} C_{A0}} \left[1 - 3\left(\frac{R}{R_0}\right)^2 + 2\left(\frac{R}{R_0}\right)^3 \right] \tag{5.3}$$

where $\rho_{\beta\text{-carotene}}$ is the molar density of beta-carotene, $\phi_{\beta\text{-carotene}}$ is the volume fraction of beta-carotene in the particle, D_{AB} is the diffusion coefficient of oxygen through PMMA, C_{A0} is the concentration of oxygen at the surface of the particle, R is the radius of the core when 10% of the beta-carotene is remaining, and R_0 is the radius of the entire particle. The molar density and volume fraction were calculated, while the values of the diffusion coefficient and oxygen concentration were used from the Damköhler calculations. R was calculated by taking the volume of a particle that is 10% the size of a uniform particle and calculating the radius, which is 0.464 μm. Unfortunately the time calculated, 3 seconds, is much smaller than experimental observations. This is due either to an inaccurate assumption in the value of the oxygen concentration, or use of the bulk diffusion coefficient instead of the effective diffusion coefficient. The oxygen concentration at the surface of the particle could be better estimated with the use of a partition coefficient, but even so values in the literature are variable. The effective

diffusion coefficient could be calculated using the tortuosity, particle porosity, and the constriction factor. Unfortunately values for the partition coefficient, tortuosity, particle porosity, and contriction factor are not readily available.

The Damköhler number was calculated for each particle geometry to determine the limiting step of the beta-carotene decay process. The Damköhler numbers in each case were large, suggesting that diffusion of oxygen through the particle controls the rate of beta-carotene decay. It was also found that larger Damköhler numbers corresponded to better UV protection.

5.4 Pharmaceutical applications

Many active pharmaceutical ingredients contain functional groups that cause them to be prone to photodegradation.[25] The negative implications of photosensitive pharmaceuticals have been outlined in chapter one. In order to determine whether the protective effects the particle geometries have exhibited can be extrapolated to an industry such as pharmaceuticals, beta-carotene was replaced in each system with a model drug, nifedipine. Nifedipine is a photosensitive antihypertensive medication that is commonly used in photodegradation studies.[110-115]

Nifedipine was first examined in solution as a baseline to determine the effect of encapsulation. The solution contained the same amount of nifedipine by weight as the beta-carotene solution tests. As described in chapter two, each sample was exposed for the predetermined amount of time, and the amount of acetone lost to evaporation was determined by pouring the sample into a graduated cylinder. Acetone was added to

ensure that the concentration was not affected due to the evaporation. Uniform, orange, and pomegranate/raspberry particles were all synthesized using the same amount of beta-carotene that has been used in previous chapters. Uniform particles were created using 3 mg of nifedipine, and these uniform particles were also used to create the core-shell particles.

Decay curves for nifedipine in solution and in each of the particle geometries can be found in figure 5.3. Nifedipine does not seem to benefit from encapsulation in a uniform particle as beta-carotene did, possibly because the decay rate in solution was already slower than that of beta-carotene. Beta-carotene in solution decayed completely by 40 minutes of exposure, and encapsulating beta-carotene resulted in 20% beta-carotene left after 60 minutes of exposure. Nifedipine in solution retained 40% of the original concentration after 60 minutes of exposure, greater than both beta-carotene in solution and encapsulated. This suggests that a threshold exists, where if a molecule is photosensitive enough to be below the threshold, such as beta-carotene, that encapsulation is beneficial. If a molecule is stable enough to stay above the threshold when exposed to UV radiation, then the additional scatter created by encapsulation it not necessary and does not offer improvement.

Unlike the uniform particles, the core-shell particles did increase the photostability of nifedipine. The orange particles provided additional protection for times greater than 30 minutes of exposure, while the pomegranate/raspberry particles protected better than the solution for exposure times greater than 15 minutes. While the initial interface created by encapsulation in a uniform particle did not offer benefit, the additional interfaces created by core-shell particles propagated enough scatter to offer

protection to the nifedipine molecule. The particle shell may also play a role in protecting nifedipine as the molecule has no interaction with the surrounding aqueous environment. As with beta-carotene, the amount of decay after 60 minutes of exposure was similar for the orange and pomegranate/raspberry particles, although the pomegranate/raspberry particles did display less variability. This suggests that, as with beta-carotene, the pomegranate/raspberry particles are the optimal geometry for UV protection of nifedipine.

Protection from ultraviolet radiation via encapsulation in various particle geometries has been extended to pharmaceuticals by encapsulating a known photosensitive active pharmaceutical ingredient – nifedipine. While encapsulation in a uniform particle did not yield additional UV protection, encapsulation in a core-shell particle increased nifedipine remaining after 60 minutes of exposure from approximately 40% to 70%. The increase in photostability when encapsulating in a core-shell particle suggests that the core-shell particle systems studied in chapter 4 can be extrapolated for use in the pharmaceutical industry.

5.5 Proximity effect in solutions and films

The effect of proximity on UV protection has been examined in chapters 2 and 4. The distance between a beta-carotene molecule and a protectant molecule was calculated and compared to the UV protective performance of the system. This methodology can be extended to determine the effect of proximity in other systems. Collaborators at Brown

University and University of Massachusetts Dartmouth have explored UV protection in systems of solutions and polymer films.

Solutions have been created by Kenneth Morabito and Anubhav Tripathi from Brown University to simulate some of the particles discussed in chapters 2 and 4.[49] A normal cuvette was used, along with a divided cuvette with two wells. Figure 5.4 displays how these cuvettes were used to create three configurations of solutions known as homogeneous, core/shell, and hybrid. The homogeneous solution contains beta-carotene and OMC throughout, simulating uniform or raspberry particles. The core-shell solution contains a beta-carotene solution in the well furthest from the light source, and an OMC solution closest to the light source to model the pomegranate and orange particles. The hybrid solutions mimic the split particles from chapter 4 by containing OMC both in a well by itself, and in the well containing beta-carotene. Like the particles, the solutions offered more protection as the concentration of OMC was increased. A comparison of decay curves for each geometry in solutions and particles is in figure 5.5. The homogeneous solution offered the most protection, followed by the hybrid configuration, and the core/shell solutions offered the least protection. From figure 5.5 it can be concluded that in solution OMC offers the best protection when in close proximity to beta-carotene. This is much different than what was observed for the particles, where particles simulated by the homoegenous solution (uniform and raspberry) offered the least protection, while the particles modeled by the core/shell and hybrid solutions (orange, pomegranate, and split) offered considerable protection. The complete difference in protection is likely due to the ability of the molecules to move freely in solutions, as well as the lack of interfaces to produce scatter.

Polymer films simulating uniform particles and orange particles have been analyzed by Dapeng Li and Paul Calvert at University of Massachusetts Dartmouth. The films were examined using multiple combinations of photosensitive dyes and antioxidants.[103] In unpublished work, single layer and dual layer films containing beta-carotene, polymer, and butylated hydroxytoluene (BHT) were studied. Single layer films were created with poly(methyl methacrylate) (PMMA), and the second layer with polyvinylpyrrolidone (PVP). Beta-carotene decayed quickly in single layer films without BHT. Single layer films with BHT showed slower beta-carotene decay, with protection increasing as the BHT concentration was increased. Adding a second film to the beta-carotene film increased protection, this could be further increased by the addition of BHT to the PVP film. These results more closely resemble the results from the particles, with a large increase in protection occurring with the addition of a second film or particle shell.

Two additional systems were discussed to examine the effect of proximity between beta-carotene and a protectant. Solutions behave very differently than the particles they were meant to simulate, with increased proximity leading to increased protection. Films more closely resembled particles, as protection was increased with the addition of a second film, which mimics the shell of a core-shell particle. Addition of protectant to the beta-carotene film increased protection, but a greater increase was observed when the protectant was added to the second film. Proximity had a significant effect in each system, although the optimum proximity between beta-carotene and a protectant was different in each system.

5.6 Conclusions

The effects of particle characteristics such as particle geometry, the choice protectants in the formulation, the placement of the protectant, and protectant amount, have been examined in previous chapters. Additional characteristics were studied in this chapter to increase understanding of UV protection in the particle system. It was found that particle size had no impact on the amount of UV protection provided by uniform particles. The shell thickness of core-shell particles also had no effect on UV protection when no protectant was present. An increase in UV protection was found when oxybenzone was present in the shell and the amount of polymer used to create the shell was increased from 0.2 g to 0.3 g, but no increase in protection was observed with additional polymer. This suggests that there is a critical amount of polymer, 0.3 g, needed to adequately disperse the protectant. The Damköhler number was calculated for each particle geometry, and the large value indicated that the rate of beta-carotene decay was controlled by diffusion. The value of the Damköhler number also corresponded to the degree of UV protection, with a large number signifying good UV protection. Nifedipine, an active pharmaceutical ingredient, replaced beta-carotene in particle formulations. Uniform particles did not offer protection to nifedipine, probably because its decay was much slower than that of beta-carotene. Orange and pomegranate/raspberry particles, however, did offer protection to nifedipine. Solutions and polymer films were also studied with respect to proximity. Solutions required close proximity between beta-carotene and OMC to adequately protect, while films protected better when the two molecules were separated, similar to the particles.

5.7 Figures for Chapter 5

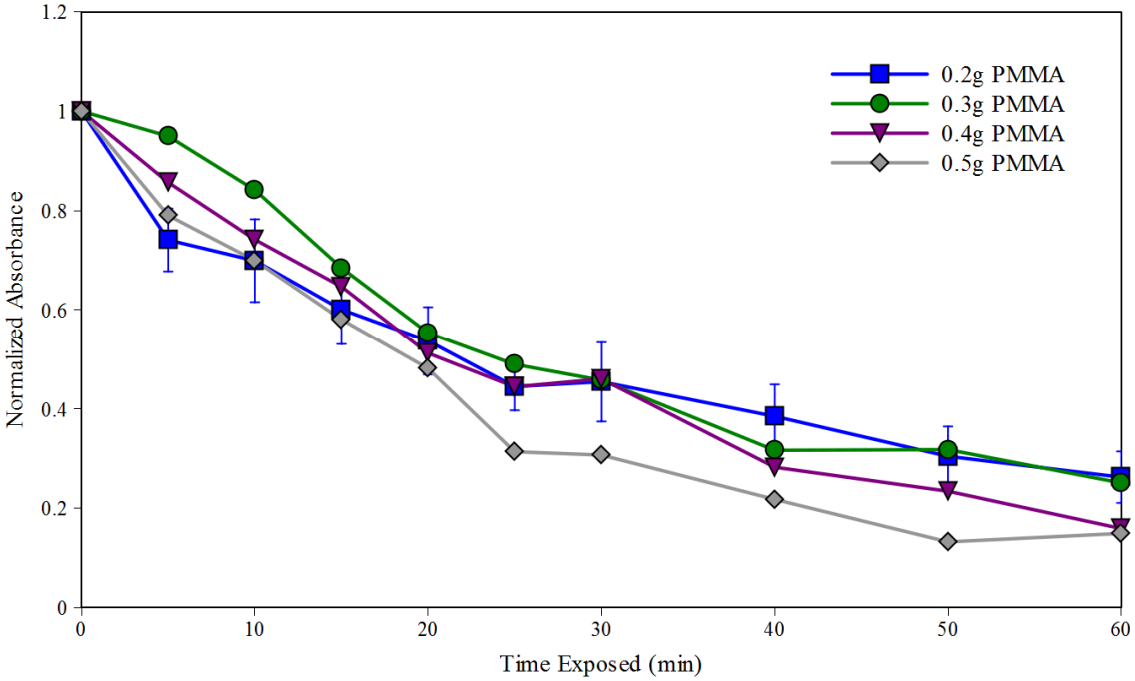

Figure 5.1: Beta-carotene decay curves for uniform particles synthesized using four different amounts of PMMA to alter the particle size.

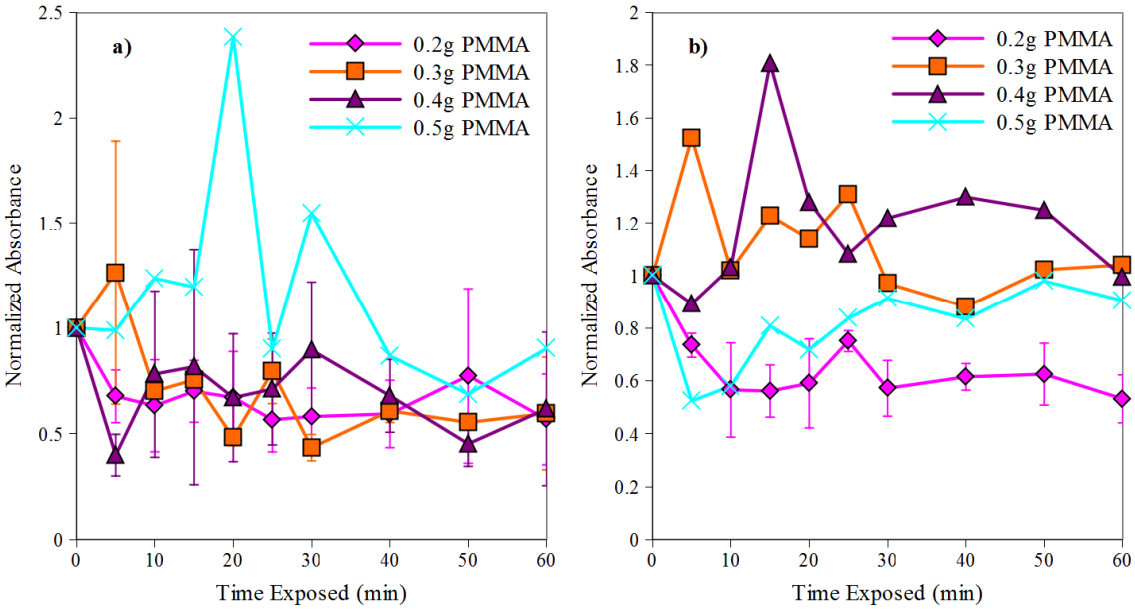

Figure 5.2: Beta-carotene decay curves comparing shell thickness controlled by the amount of PMMA used to create the particle shell when (a) the particles contain no protectant and (b) the particles contain the 1:33 ratio of beta-carotene to oxybenzone.

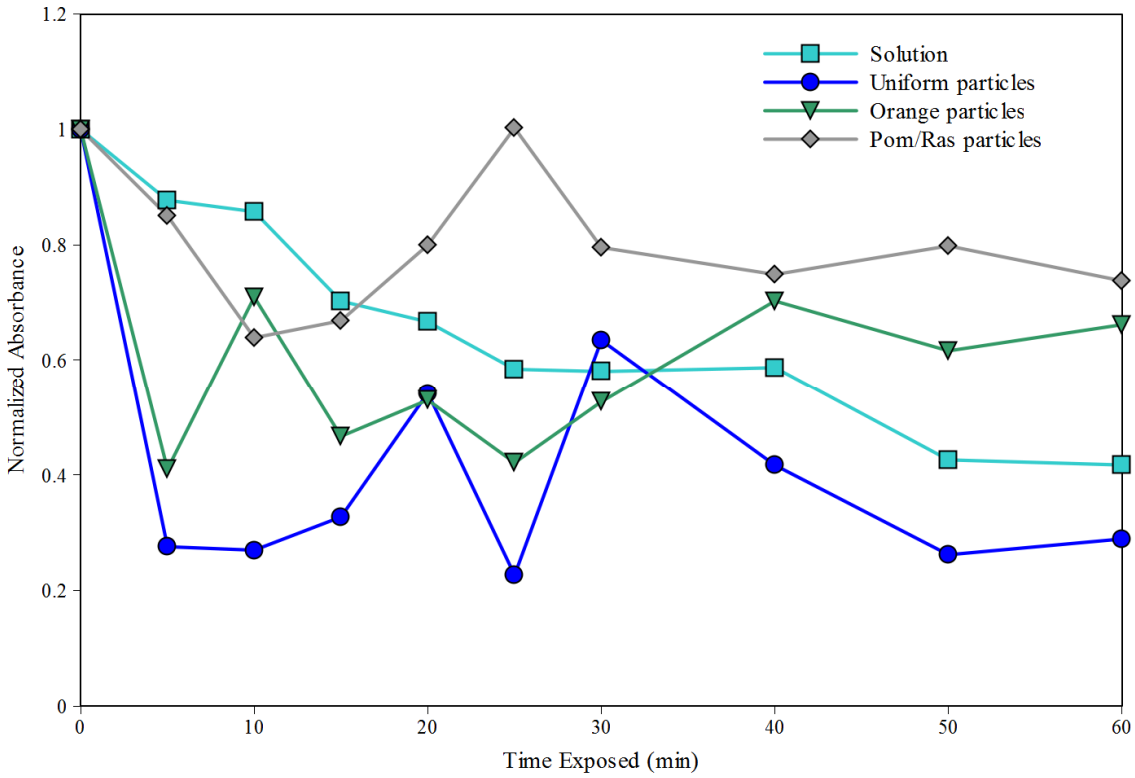

Figure 5.3: Nifedipine decay curves for nifedipine in solution, uniform particles, orange particles, and pomegranate/raspberry particles to show the effect of geometry on UV protection of nifedipine

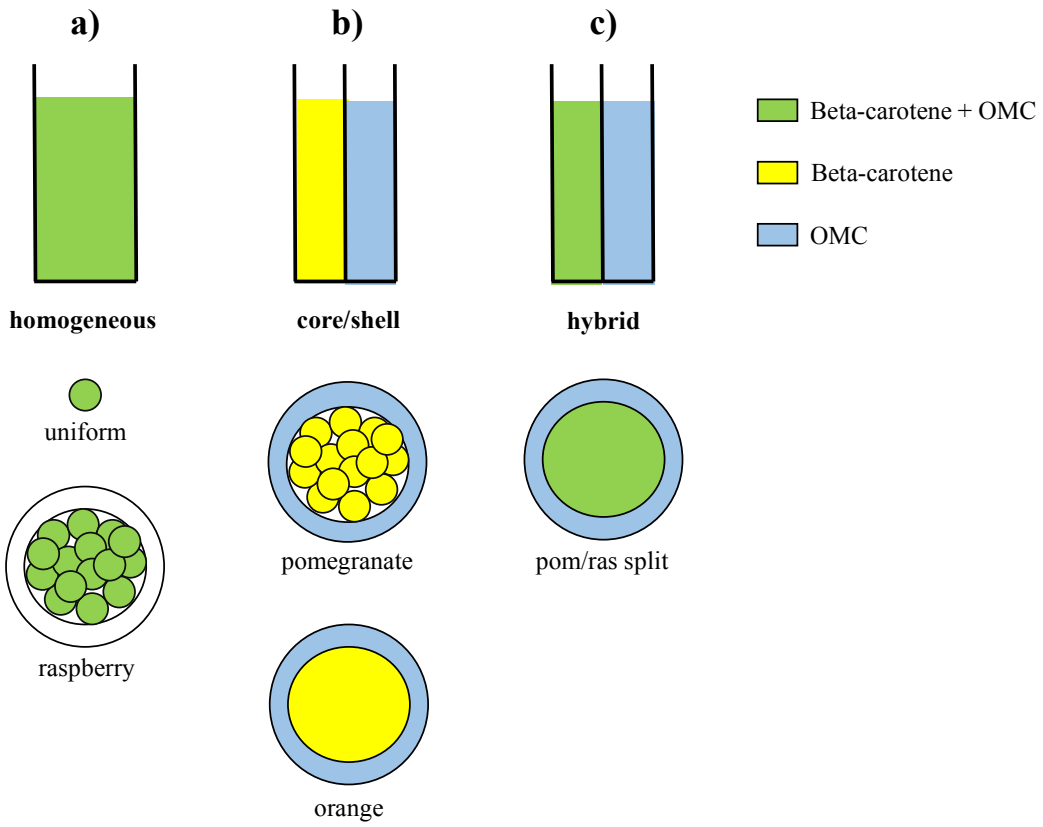

Figure 5.4: Diagrams displaying how the single and double cuvettes were used along with the solutions to mimic the particle geometries.

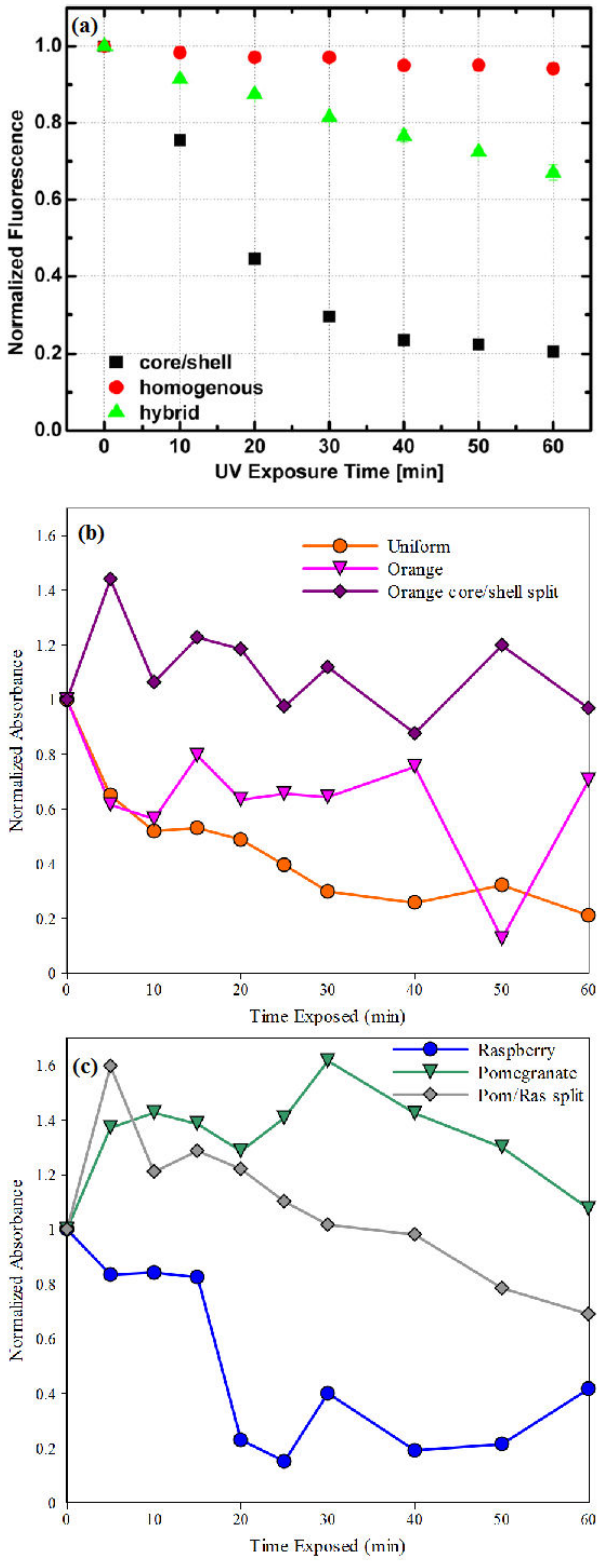

Figure 5.5: Comparison of the three configurations of (a) solutions from Morabito *et al.,*[49] (b) solid particles, and (c) encapsulation suspensions.

5.8 Tables for Chapter 5

Table 5.1: Parameter values for Damköhler number calculations		
Parameter	**Value**	**Units**
k_1	0.0393*	L/mol·s
C_{A0}	2.637E-04†	mol/L
D_{AB}	3.4E-08‡	cm^2/s
L (uniform particle radius)	5E-05	cm
L (pom/ras shell thickness)	2.461E-03	cm
L (orange shell thickness)	1.6E-03	cm
L (uniform + pom/ras)	2.511E-03	cm
Parameter value sources: *El-Tinay and Chichester (1970)[66] †Calculated with solubility value from Carpenter (1966)[116] ‡Kaptan *et al.*(1989)[117]		

Table 5.2: Damköhler numbers for each particle geometry	
Particle geometry	**Damköhler number**
Uniform particles	10.96
Pomegranate/raspberry particles (shell only)	2.655E+04
Orange particles	1.122E+04
Pomegranate/raspberry particles (shell + uniform)	2.764E+04

Chapter 6 Conclusions and future work

Ultraviolet radiation causes damage to many materials such as human skin, dyes, pharmaceuticals, and automotive coatings. The wide array of photosensitive materials is motivation to develop innovative ways to protect materials from damaging UV radiation. This work investigated particles as a UV protection system and developed core-shell particle geometries as novel protection systems.

Uniform particles were synthesized to confirm that encapsulation offers protection as well as provide a baseline for comparison to core-shell particles. Encapsulation did provide UV protection to beta-carotene, and the protection was enhanced by the addition of oxybenzone, avobenzone, or vitamin E. OMC provided no additional protection. UV protection was dependent on concentration of protectant, except when using OMC. Using oxybenzone in combination with another UV absorber did not increase protective capabilities of the particle, while vitamin E and UV absorber combinations offered superior protection. Changing the polymer used or the concentration of particles did not affect the amount of protection provided. The concentrations providing the best protection correspond to a spacing of 5nm or less between beta-carotene and protectant molecules.

Designs of experiments were created to determine processes for synthesizing the core-shell particle geometries. The double emulsion solvent evaporation method was implemented and various parameters were examined. The experimental designs resulted in two particle geometries, one with a solid polymer core containing beta-carotene and

one whose core consisted of a suspension of polymer and beta-carotene particles. These particles were used to further examine particles as a vehicle for UV protection.

The core-shell particle geometries proved to offer better UV protection than the uniform particles when protectant was not added to the formulation. Increasing the concentration of a protectant in the formulation resulted in an increase in protection for all particles except the pomegranate particles, which already provided substantial protection. In most cases it was more beneficial to have the protectant in the shell of the particle (orange and pomegranate particles) than in the core (uniform and raspberry particles). Splitting the protectant between the core and shell had a minimal effect. The particles offering the best protection were made with vitamin E in the core and a UV absorber, such as oxybenzone, in the shell of the particle.

Additional particle characteristics that may have an affect on the particles' ability to protect from UV radiation were also explored. The size of uniform particles and the shell thickness of core-shell particles did not affect the level of UV protection provided. When a protectant was added to the shell, a threshold was observed that greater than 0.2 g of polymer must be used in order for the protectant to adequately disperse. The Damköhler number was found to be large for all particle geometries, and the value was larger for the particles offering the best protection. Nifedipine was used as a model pharmaceutical to assess how the particles would protect a molecule other than beta-carotene. The uniform particles offered no additional protection compared to nifedipine in solution, but the core-shell particles did increase stability. The particles were also compared to similar solutions and films. The solutions offered the best protection when

beta-carotene and the protectant were in close proximity, while the particles and films benefitted from a separation between the molecules.

Many particle geometries and formulations were examined to determine the parameters that affected UV protection and find an optimal particle to protect beta-carotene. The particles offering the most UV protection were core-shell particles with a UV absorber in the shell and a suspension of uniform particles containing vitamin E in the core. While only beta-carotene and nifedipine were examined, the particles have applications in many industries.

The core-shell particles were designed to have either a solid core or a core filled with a suspension of uniform particles. Other than the shell thickness, no other attributes were optimized. For future work, additional designs of experiments should be undertaken to explore how to manipulate particle characteristics such as particle size, core size, and number of cores in a single particle. Once a deeper understanding of the process is attained, particles can be tailored to any application.

Future work should also include examining the particles for other applications. Other photosensitive pharmaceutical molecules could be studied to gain a more general understanding of how active pharmaceutical molecules behave when encapsulated in a UV protective environment. Additional experiments could also be designed to tailor particles for products such as sunscreens and automotive coatings.

References

1. Urbach, F., *The historical aspects of sunscreens.* Journal of Photochemistry and Photobiology B: Biology, 2001. **64**(2–3): p. 99-104.
2. Donaldson, M.R. and B.M. Coldiron, *No End in Sight: The Skin Cancer Epidemic Continues.* Seminars in Cutaneous Medicine and Surgery, 2011. **30**(1): p. 3-5.
3. Shindo, Y., et al., *Enzymic and Non-Enzymic Antioxidants in Epidermis and Dermis of Human Skin.* J Investig Dermatol, 1994. **102**(1): p. 122-124.
4. Brash, D.E., et al., *A role for sunlight in skin cancer: UV-induced p53 mutations in squamous cell carcinoma.* Proceedings of the National Academy of Sciences, 1991. **88**(22): p. 10124-10128.
5. Armstrong, B.K. and A. Kricker, *The epidemiology of UV induced skin cancer.* Journal of Photochemistry and Photobiology B: Biology, 2001. **63**(1-3): p. 8-18.
6. Sambandan, D.R. and D. Ratner, *Sunscreens: An overview and update.* Journal of the American Academy of Dermatology, 2011. **64**(4): p. 748-758.
7. Hoeijmakers, J.H.J., *DNA Damage, Aging, and Cancer.* New England Journal of Medicine, 2009. **361**(15): p. 1475-1485.
8. Pitts, D.G. and T.J. Tredici, *EFFECTS OF ULTRAVIOLET ON THE EYE.* Journal Name: Amer. Ind. Hyg. Ass. J. 32: 235-46(Apr 1971).; Other Information: Orig. Receipt Date: 31-DEC-71, 1971: p. Medium: X.
9. Cullen, A.P., *Photokeratitis and Other Phototoxic Effects on the Cornea and Conjunctiva.* International Journal of Toxicology (Taylor & Francis), 2002. **21**(6): p. 455-464.
10. Sliney, D.H., *Photoprotection of the eye – UV radiation and sunglasses.* Journal of Photochemistry and Photobiology B: Biology, 2001. **64**(2–3): p. 166-175.
11. Feng, X., et al., *New insights into solar UV-protective properties of natural dye.* Journal of Cleaner Production, 2007. **15**(4): p. 366-372.
12. Tragoonwichian, S., E.A. O'Rear, and N. Yanumet, *Admicellar polymerization of 2-hydroxy-4-acryloyloxybenzophenone: The production of UV-protective cotton.* Colloids and Surfaces A: Physicochemical and Engineering Aspects, 2008. **329**(1-2): p. 87-94.
13. Czajkowski, W., et al., *Synthesis of reactive UV absorbers, derivatives of monochlorotriazine, for improvement in protecting properties of cellulose fabrics.* Dyes and Pigments, 2006. **71**(3): p. 224-230.
14. Damiani, E., et al., *Synthesis and application of a novel sunscreen-antioxidant.* Free Radical Research, 2006. **40**(5): p. 485-494.
15. Wissing, S.A. and R.H. Müller, *A novel sunscreen system based on tocopherol acetate incorporated into solid lipid nanoparticles.* International Journal of Cosmetic Science, 2001. **23**(4): p. 233-243.
16. Gallardo, A., et al., *Dose-dependent progressive sunscreens. A new strategy for photoprotection?* Photochemical & Photobiological Sciences, 2010. **9**(4): p. 530-534.
17. Zarkogianni, M., et al., *Colour and fastness of natural dyes: revival of traditional dyeing techniques.* Coloration Technology, 2011. **127**(1): p. 18-27.
18. Cristea, D. and G. Vilarem, *Improving light fastness of natural dyes on cotton yarn.* Dyes and Pigments, 2006. **70**(3): p. 238-245.

19. Bechtold, T., et al., *Natural dyes in modern textile dyehouses — how to combine experiences of two centuries to meet the demands of the future?* Journal of Cleaner Production, 2003. **11**(5): p. 499-509.
20. Gerlock, J.L., et al., *18O- time-of-flight secondary ion mass spectrometry technique to map the relative photooxidation resistance of automotive paint systems.* Polymer Degradation and Stability, 1999. **65**(1): p. 37-45.
21. Smith, C.A., J.L. Gerlock, and R.O. Carter, *Determination of ultraviolet light absorber longevity and distribution in automotive paint systems using ultraviolet micro-spectroscopy.* Polymer Degradation and Stability, 2001. **72**(1): p. 89-97.
22. Iyengar, R. and B. Schellenberg, *Loss rate of UV absorbers in automotive coatings.* Polymer Degradation and Stability, 1998. **61**(1): p. 151-159.
23. Bauer, D.R., *Interpreting weathering acceleration factors for automotive coatings using exposure models.* Polymer Degradation and Stability, 2000. **69**(3): p. 307-316.
24. Mirabedini, S.M., et al., *Weathering performance of the polyurethane nanocomposite coatings containing silane treated TiO2 nanoparticles.* Applied Surface Science, 2011. **257**(9): p. 4196-4203.
25. Albini, A. and E. Fasani, *Photochemistry of drugs: An overview and practical problems.* 1998: p. 1-73.
26. Kawabe, Y., et al., *Photochemical stabilities of some dihydropyridine calcium-channel blockers in powdered pharmaceutical tablets.* Journal of Pharmaceutical and Biomedical Analysis, 2008. **47**(3): p. 618-24.
27. Baertschi, S.W., K.M. Alsante, and H.H. Tonnesen, *A critical assessment of the ICH guideline on photostability testing of new drug substances and products (Q1B): Recommendation for revision.* Journal of pharmaceutical sciences, 2010. **99**(7): p. 2934-40.
28. Maggi, L., *Photostability of extended-release matrix formulations.* European Journal of Pharmaceutics and Biopharmaceutics, 2003. **55**(1): p. 99-105.
29. Aman, W. and K. Thoma, *The influence of formulation and manufacturing process on the photostability of tablets.* International journal of pharmaceutics, 2002. **243**(1-2): p. 33-41.
30. Zhan, X., et al., *Cumulative illuminometer and shelf life of drugs in daylight indoors.* International journal of pharmaceutics, 1998. **167**(1-2): p. 7-11.
31. Henry, B., C. Foti, and K. Alsante, *Can light absorption and photostability data be used to assess the photosafety risks in patients for a new drug molecule?* Journal of photochemistry and photobiology. B, Biology, 2009. **96**(1): p. 57-62.
32. Onoue, S., et al., *High-throughput reactive oxygen species (ROS) assay: An enabling technology for screening the phototoxic potential of pharmaceutical substances.* Journal of Pharmaceutical and Biomedical Analysis, 2008. **46**(1): p. 187-193.
33. Onoue, S. and Y. Tsuda, *Analytical Studies on the Prediction of Photosensitive/Phototoxic Potential of Pharmaceutical Substances.* Pharmaceutical Research, 2006. **23**(1): p. 156-164.
34. Piechocki, J.T. and K. Thoma, eds. *Pharmaceutical Photostability and Stabilization Technology*. Drugs and the Pharmaceutical Sciences, ed. J. Swarbrick. Vol. 163. 2007, Informa Healthcare USA, Inc.: New York, NY. 445.

35. Béchard, S.R., O. Quraishi, and E. Kwong, *Film coating: effect of titanium dioxide concentration and film thickness on the photostability of nifedipine.* International journal of pharmaceutics, 1992. **87**(1–3): p. 133-139.
36. Templeton, A.C., et al., *Implications of Photostability on the Manufacturing, Packaging, Storage, and Testing.* Pharmaceutical Technology, 2005. **29**(3): p. 68-86.
37. Murphy, G.M., *Sunblocks: Mechanisms of action.* Photodermatology, Photoimmunology & Photomedicine, 1999. **15**(1): p. 34-36.
38. Dransfield, G.P., *Inorganic Sunscreens.* Radiation Protection Dosimetry, 2000. **91**(1-3): p. 271-273.
39. Zohdy, M.H., et al., *Novel UV-protective formulations for cotton, PET fabrics and their blend utilizing irradiation technique.* European Polymer Journal, 2009. **45**(10): p. 2926-2934.
40. Gasparro, F.P., ed. *Sunscreen photobiology: molecular, cellular and physiological aspects*. 1997, Springer-Verlag: Georgetown, Texas. 194.
41. Lowe, N.J., N.A. Shaath, and M.A. Pathak, eds. *Sunscreens: Development, Evaluation, and Regulatory Aspects*. Second ed. Cosmetic Science and Technology, ed. E. Jungermann1997, Marcel Dekker, Inc.: New York, New York. 792.
42. Buettner, G.R., *The Pecking Order of Free Radicals and Antioxidants: Lipid Peroxidation, α-Tocopherol, and Ascorbate.* Archives of Biochemistry and Biophysics, 1993. **300**(2): p. 535-543.
43. Ingold, K.U., *Inhibition of the Autoxidation of Organic Substances in the Liquid Phase.* Chemical Reviews, 1961. **61**(6): p. 563-589.
44. Burton, G.W. and K.U. Ingold, *Vitamin E: application of the principles of physical organic chemistry to the exploration of its structure and function.* Accounts of Chemical Research, 1986. **19**(7): p. 194-201.
45. Eklund, P.C., et al., *Chemical studies on antioxidant mechanisms and free radical scavenging properties of lignans.* Organic & Biomolecular Chemistry, 2005. **3**(18): p. 3336-3347.
46. Perugini, P., et al., *Effect of nanoparticle encapsulation on the photostability of the sunscreen agent, 2-ethylhexyl-p-methoxycinnamate.* International journal of pharmaceutics, 2002. **246**(1-2): p. 37-45.
47. Weiss-Angeli, V., et al., *Nanocapsules of Octyl Methoxycinnamate Containing Quercetin Delayed the Photodegradation of Both Components Under Ultraviolet A Radiation.* Journal of Biomedical Nanotechnology, 2008. **4**(1): p. 80-89.
48. Carlotti, M., et al., *Study on the Photostability of Octyl ‐p ‐Methoxy Cinnamate in SLN.* Journal of Dispersion Science and Technology, 2005. **26**(6): p. 809-816.
49. Morabito, K., et al., *Proximal effects of ultraviolet light absorbers and polymer matrix in the photostability of β-carotene.* Dyes and Pigments, 2012. **92**(1): p. 509-516.
50. O'Donnell, P.B. and J.W. McGinity, *Preparation of microspheres by the solvent evaporation technique.* Advanced Drug Delivery Reviews, 1997. **28**(1): p. 25-42.
51. Freitas, S., H.P. Merkle, and B. Gander, *Microencapsulation by solvent extraction/evaporation: reviewing the state of the art of microsphere preparation*

process technology. Journal of controlled release : official journal of the Controlled Release Society, 2005. **102**(2): p. 313-32.
52. Li, M., O. Rouaud, and D. Poncelet, *Microencapsulation by solvent evaporation: state of the art for process engineering approaches.* International journal of pharmaceutics, 2008. **363**(1-2): p. 26-39.
53. Desgouilles, S., et al., *The Design of Nanoparticles Obtained by Solvent Evaporation: A Comprehensive Study.* Langmuir, 2003. **19**(22): p. 9504-9510.
54. Yang, Y.-Y., T.-S. Chung, and N. Ping Ng, *Morphology, drug distribution, and in vitro release profiles of biodegradable polymeric microspheres containing protein fabricated by double-emulsion solvent extraction/evaporation method.* Biomaterials, 2001. **22**(3): p. 231-241.
55. Mao, S., et al., *Effects of process and formulation parameters on characteristics and internal morphology of poly(d,l-lactide-co-glycolide) microspheres formed by the solvent evaporation method.* European Journal of Pharmaceutics and Biopharmaceutics, 2008. **68**(2): p. 214-223.
56. Rosca, I.D., F. Watari, and M. Uo, *Microparticle formation and its mechanism in single and double emulsion solvent evaporation.* Journal of Controlled Release, 2004. **99**(2): p. 271-280.
57. Conti, B., et al., *Investigation on Process Parameters Involved in Polylactide-Co-Glycolide Microspheres Preparation.* Drug Development and Industrial Pharmacy, 1995. **21**(5): p. 615-622.
58. Anselmi, C., et al., *New microencapsulated sunscreens: technology and comparative evaluation.* International journal of pharmaceutics, 2002. **242**(1-2): p. 207-211.
59. Mu, L. and S.S. Feng, *A novel controlled release formulation for the anticancer drug paclitaxel (Taxol®): PLGA nanoparticles containing vitamin E TPGS.* Journal of Controlled Release, 2003. **86**(1): p. 33-48.
60. Bodmeier, R. and J.W. McGinity, *The Preparation and Evaluation of Drug-Containing Poly(<i>dl</i>-lactide) Microspheres Formed by the Solvent Evaporation Method.* Pharmaceutical Research, 1987. **4**(6): p. 465-471.
61. Kader, A. and R. Jalil, *Formulation Factors Affecting Drug Release from Poly(Lactic Acid) (PLA) Microcapsule Tablets.* Drug Development and Industrial Pharmacy, 1999. **25**(2): p. 141-151.
62. Bodmeier, R. and J.W. McGinity, *Solvent selection in the preparation of poly(dl-lactide) microspheres prepared by the solvent evaporation method.* International journal of pharmaceutics, 1988. **43**(1–2): p. 179-186.
63. Herrmann, J. and R. Bodmeier, *Somatostatin containing biodegradable microspheres prepared by a modified solvent evaporation method based on W/O/W-multiple emulsions.* International journal of pharmaceutics, 1995. **126**(1–2): p. 129-138.
64. Sansdrap, P. and A.J. Moës, *Influence of manufacturing parameters on the size characteristics and the release profiles of nifedipine from poly(DL-lactide-co-glycolide) microspheres.* International journal of pharmaceutics, 1993. **98**(1–3): p. 157-164.
65. Burton, G.W., *Antioxidant Action of Carotenoids.* The Journal of Nutrition, 1989. **119**: p. 109-111.

66. El-Tinay, A.H. and C.O. Chichester, *Oxidation of .beta.-carotene. Site of initial attack.* The Journal of Organic Chemistry, 1970. **35**(7): p. 2290-2293.
67. Kennedy, T.A. and D.C. Liebler, *Peroxyl radical oxidation of .beta.-carotene: formation of .beta.-carotene epoxides.* Chemical Research in Toxicology, 1991. **4**(3): p. 290-295.
68. Stratton, S.P., W.H. Schaefer, and D.C. Liebler, *Isolation and identification of singlet oxygen oxidation products of .beta.-carotene.* Chemical Research in Toxicology, 1993. **6**(4): p. 542-547.
69. Yamauchi, R., et al., *Products formed by peroxyl radical oxidation of .beta.-carotene.* Journal of Agricultural and Food Chemistry, 1993. **41**(5): p. 708-713.
70. Foote, C.S. and R.W. Denny, *Chemistry of singlet oxygen. VII. Quenching by .beta.-carotene.* Journal of the American Chemical Society, 1968. **90**(22): p. 6233-6235.
71. Yeo, Y. and K. Park, *Control of encapsulation efficiency and initial burst in polymeric microparticle systems.* Archives of Pharmacal Research, 2004. **27**(1): p. 1-12.
72. Castro, G., S. Blanco, and O. Giordano, *UV Spectral Properties of Benzophenone. Influence of Solvents and Substituents.* Molecules, 2000. **5**(3): p. 424-425.
73. Szczurko, C., et al., *Photocontact allergy to oxybenzone: ten years of experience.* Photodermatology, Photoimmunology & Photomedicine, 1994. **10**(4): p. 144-147.
74. Wissing, S.A. and R.H. Müller, *Solid lipid nanoparticles as carrier for sunscreens: in vitro release and in vivo skin penetration.* Journal of Controlled Release, 2002. **81**(3): p. 225-233.
75. Schlumpf, M., et al., *<italic>In Vitro</italic> and <italic>in Vivo</italic> Estrogenicity of UV Screens.* Environ Health Perspect, 2001. **109**(3).
76. Wang Sq, B.M.E.L.H.W., *Safety of oxybenzone: Putting numbers into perspective.* Archives of Dermatology, 2011. **147**(7): p. 865-866.
77. Darvay, A., et al., *Photoallergic contact dermatitis is uncommon.* British Journal of Dermatology, 2001. **145**(4): p. 597-601.
78. Wolf, R., B. Tüzün, and Y. Tüzün, *Sunscreens.* Dermatologic Therapy, 2001. **14**(3): p. 208-214.
79. McVean, M. and D.C. Liebler, *Inhibition of UVB induced DNA photodamage in mouse epidermis by topically applied alpha-tocopherol.* Carcinogenesis, 1997. **18**(8): p. 1617-1622.
80. Mestiri, M., F. Puisieux, and J.P. Benoit, *Preparation and characterization of cisplatin-loaded polymethyl methacrylate microspheres.* International journal of pharmaceutics, 1993. **89**(3): p. 229-234.
81. Sivakumar, M. and K.P. Rao, *Synthesis and characterization of poly(methyl methacrylate) functional microspheres.* Reactive and Functional Polymers, 2000. **46**(1): p. 29-37.
82. Sprockel, O.L. and J.C. Price, *Development of an Emulsion-Solvent Evaporation Technique for Microencapsulation of Drus-Resin complexes.* Drug Development and Industrial Pharmacy, 1990. **16**(2): p. 361-376.
83. Bodmeier, R., et al., *Microencapsulation of Antimicrobial Ceftiofur Drugs.* Pharmaceutical Development and Technology, 1997. **2**(4): p. 323-334.

84. Morello, A.P., R. Burrill, and E. Mathiowitz, *Preparation and characterization of poly(methyl methacrylate)—iron (III) oxide microparticles using a modified solvent evaporation method.* Journal of Microencapsulation, 2007. **24**(5): p. 476-491.
85. Maa, Y.F. and C.C. Hsu, *Effect of primary emulsions on microsphere size and protein-loading in the double emulsion process.* Journal of Microencapsulation, 1997. **14**(2): p. 225-241.
86. Nordstierna, L., et al., *Comparison of release behaviour from microcapsules and microspheres.* Progress in Organic Coatings, 2010. **69**(1): p. 49-51.
87. Gogna, D., et al., *Microsphere Based Improved Sunscreen Formulation of Ethylhexyl Methoxycinnamate.* Current Drug Delivery, 2007. **4**(2): p. 153-159.
88. Yuksel, N., et al., *Investigation of triacetin effect on indomethacin release from poly(methyl methacrylate) microspheres: Evaluation of interactions using FT-IR and NMR spectroscopies.* International journal of pharmaceutics, 2011. **404**(1–2): p. 102-109.
89. Hollick, E.J., et al., *Biocompatibility of poly(methyl methacrylate), silicone, and AcrySof intraocular lenses: randomized comparison of the cellular reaction on the anterior lens surface.* Journal of cataract and refractive surgery, 1998. **24**(3): p. 361-366.
90. Jäger, M. and A. Wilke, *Comprehensive biocompatibility testing of a new PMMA-HA bone cement versus conventional PMMA cement in vitro.* Journal of Biomaterials Science, Polymer Edition, 2003. **14**(11): p. 1283-1298.
91. Frazer, R.Q., et al., *PMMA: an essential material in medicine and dentistry.* Journal of long-term effects of medical implants, 2005. **15**(6): p. 629-639.
92. Jayakrishnan, A., et al., *Hydrogel microspheres from crosslinked poly(methyl methacrylate): synthesis and biocompatibility studies.* Bulletin of Materials Science, 1989. **12**(1): p. 17-25.
93. Nagai, N., T. Matsunobe, and T. Imai, *Infrared analysis of depth profiles in UV-photochemical degradation of polymers.* Polymer Degradation and Stability, 2005. **88**(2): p. 224-233.
94. Ito, F., et al., *Study of types and mixture ratio of organic solvent used to dissolve polymers for preparation of drug-containing PLGA microspheres.* European Polymer Journal, 2009. **45**(3): p. 658-667.
95. Chiellini, E., et al., *Biodegradation of poly (vinyl alcohol) based materials.* Progress in Polymer Science, 2003. **28**(6): p. 963-1014.
96. Lee, S.C., et al., *Quantitative analysis of polyvinyl alcohol on the surface of poly(d,l-lactide-co-glycolide) microparticles prepared by solvent evaporation method: effect of particle size and PVA concentration.* Journal of Controlled Release, 1999. **59**(2): p. 123-132.
97. Sahoo, S.K., et al., *Residual polyvinyl alcohol associated with poly (d,l-lactide-co-glycolide) nanoparticles affects their physical properties and cellular uptake.* Journal of Controlled Release, 2002. **82**(1): p. 105-114.
98. Boury, F., et al., *Dynamic Properties of Poly(DL-lactide) and Polyvinyl Alcohol Monolayers at the Air/Water and Dichloromethane/Water Interfaces.* Journal of Colloid and Interface Science, 1995. **169**(2): p. 380-392.

99. Koo, B.-M., et al., *Encapsulation and Stabilization of Photo-Sensitive Antioxidants by Using Polymer Microcapsules with Controlled Phase Heterogeneity.* Macromolecular Rapid Communications, 2008. **29**(6): p. 498-502.
100. Lee, J.-S., et al., *Photochemical properties of UV-absorbing chemicals in phase-controlled polymer microspheres.* Colloid and Polymer Science, 2004. **283**(2): p. 194-199.
101. Naito, T., K. Horie, and I. Mita, *Photochemistry in polymer solids. 11. The effects of the size of reaction groups and the mode of photoisomerization on photochromic reactions in polycarbonate film.* Macromolecules, 1991. **24**(10): p. 2907-2911.
102. Tarras-Wahlberg, N., et al., *Changes in Ultraviolet Absorption of Sunscreens After Ultraviolet Irradiation.* 1999. **113**(4): p. 547-553.
103. Li, D., et al., *Stabilization of Natural Dyes by High Levels of Antioxidants.* Advanced Materials Research, 2012. **441**: p. 192-199.
104. Nihant, N., et al., *Polylactide Microparticles Prepared by Double Emulsion/Evaporation Technique. I. Effect of Primary Emulsion Stability.* Pharmaceutical Research, 1994. **11**(10): p. 1479-1484.
105. Uchida, T., et al., *Optimization of Preparative Conditions for Polylactide (PLA) Microspheres Containing Ovalbumin.* CHEMICAL & PHARMACEUTICAL BULLETIN, 1995. **43**(9): p. 1569-1573.
106. Dowding, P.J., et al., *Oil Core−Polymer Shell Microcapsules Prepared by Internal Phase Separation from Emulsion Droplets. I. Characterization and Release Rates for Microcapsules with Polystyrene Shells.* Langmuir, 2004. **20**(26): p. 11374-11379.
107. Loxley, A. and B. Vincent, *Preparation of Poly(methylmethacrylate) Microcapsules with Liquid Cores.* Journal of Colloid and Interface Science, 1998. **208**(1): p. 49-62.
108. Gao, F., et al., *Double Emulsion Templated Microcapsules with Single Hollow Cavities and Thickness-Controllable Shells.* Langmuir, 2009. **25**(6): p. 3832-3838.
109. Fogler, H.S., *Elements of Chemical Reaction Engineering*. 4th ed2006, Upper Saddle River, NJ: Pearson Education, Inc.
110. Shamsipur, M., *A study of the photo-degradation kinetics of nifedipine by multivariate curve resolution analysis.* Journal of Pharmaceutical and Biomedical Analysis, 2003. **31**(5): p. 1013-1019.
111. Grundy, J.S., R. Kherani, and R.T. Foster, *Photostability determination of commercially available nifedipine oral dosage formulations.* Journal of Pharmaceutical and Biomedical Analysis, 1994. **12**(12): p. 1529-1535.
112. Hayase, N., S. Inagaki, and Y. Abiko, *Effects of photodegradation products of nifedipine: the nitroso-derivative relaxes contractions of the rat aortic strip induced by norepinephrine and other agonists.* Journal of Pharmacology and Experimental Therapeutics, 1995. **275**(2): p. 813-821.
113. Hayase, N., et al., *Newly discovered photodegradation products of nifedipine in hospital prescriptions.* Journal of pharmaceutical sciences, 1994. **83**(4): p. 532-538.

114. Vries, H.d. and G.M.J.B.v. Henegouwen, *PHOTODEGRADATION OF NIFEDIPINE UNDER in vivo-RELATED CIRCUMSTANCES.* Photochemistry and Photobiology, 1995. **62**(6): p. 959-963.
115. Vries, H.d. and G.M.J. Beijersbergen van Henegouwen, *Photoreactivity of nifedipine in vitro and in vivo.* Journal of Photochemistry and Photobiology B: Biology, 1998. **43**(3): p. 217-221.
116. Carpenter, J.H., *New Measurements of Oxygen Solubility in Pure and Natural Water.* Limnology and Oceanography, 1966. **11**(2): p. 264-277.
117. Kaptan, Y., et al., *Determination of diffusion coefficient of oxygen into polymers by using electron spin resonance spectroscopy. I. Poly(methyl methacrylate).* Journal of Applied Polymer Science, 1989. **37**(9): p. 2577-2585.